156784

VOL. I.

Jan 1977

CTS COMMUNICATIONS LINK CHARACTERIZATION EXPERIMENT

TECHNICAL DATA REPORT

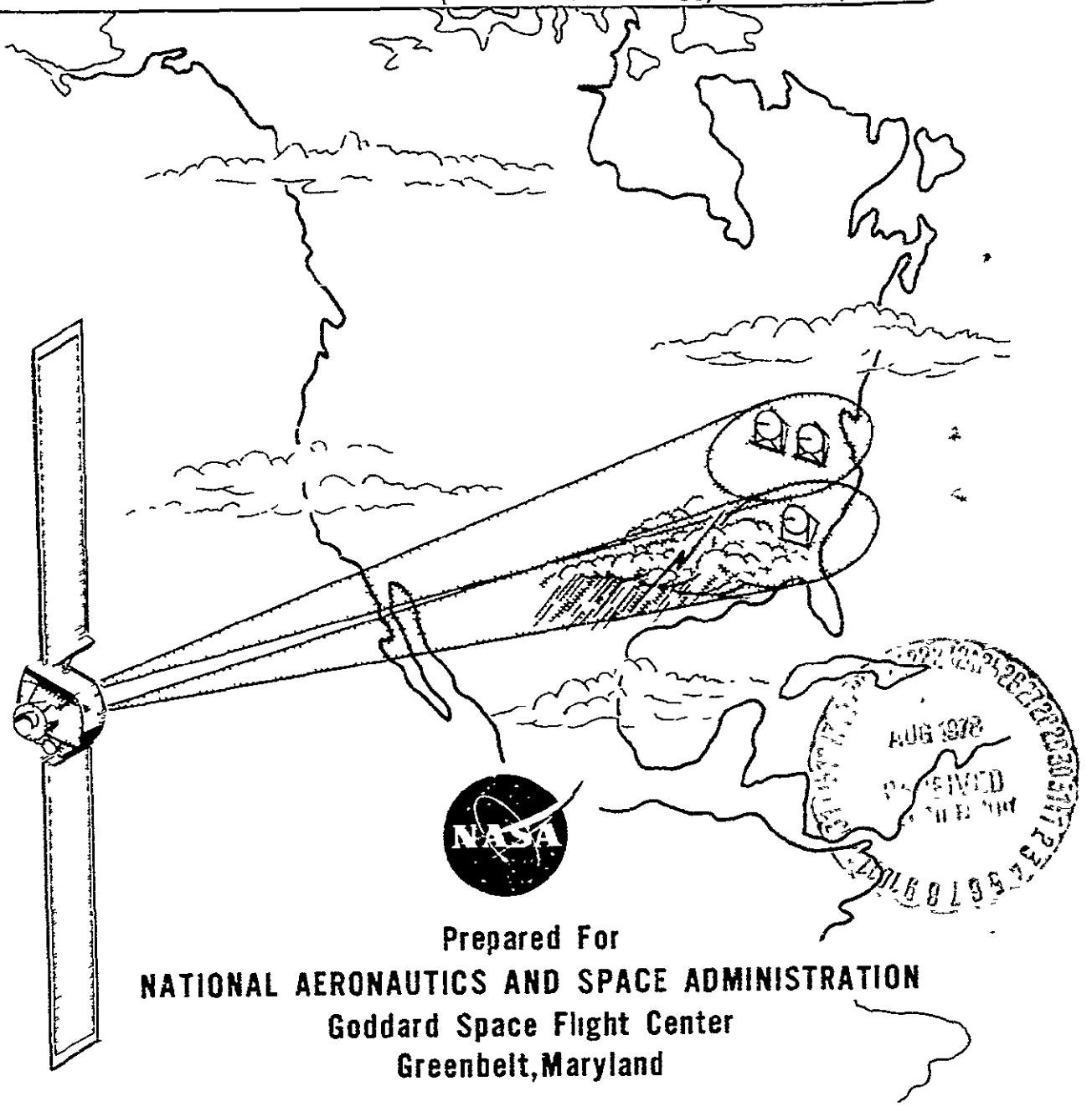

Prepared For

NATIONAL AERONAUTICS AND SPACE ADMINISTRATION

Goddard Space Flight Center

Greenbelt, Maryland

FIS-76-4039A

Data analyzed up to Oct 31, 1976

COMMUNICATIONS LINK CHARACTERIZATION EXPERIMENT (CLCE)

TECHNICAL DATA REPORT

CONTRACT NAS 5-20729

JANUARY 1977

ORIGINAL CONTAINS COLOR ILLUSTRATIONS

WESTINGHOUSE ELECTRIC CORPORATION
Defense and Electronic Systems Center
P.O. Box 1693
Baltimore, Maryland 21203

TABLE OF CONTENTS

TABLE OF CONTENTS (Continued)

LIST OF ILLUSTRATIONS

LIST OF ILLUSTRATIONS (Continued)

LIST OF ILLUSTRATIONS (Continued)

LIST OF TABLES

SECTION 1
INTRODUCTION

The purpose of this report is to present the results of the data which has been acquired, reduced, and analyzed as of October 31, 1976 from the Communications Link Characterization Experiment (CLCE) while utilizing the CTS satellite. An exception to the end date is made for interesting signal scintillation data that was recorded on November 29. Data presented in this report was acquired from the NASA Goddard CTS station and the NASA Rosman station located in Rosman, North Carolina. The CTS satellite was launched on January 17, 1976 and the omnipresent 11.7 GHz beacon CW signal was first received by the Goddard station on February 2, 1976. The initial "lock-on" of the beacon signal by this station occurred on May 17, 1976. Because of the labor dispute at the Rosman station, the various units were not operationally checked until June 1, 1976. On this date various check out procedures were initiated to determine the operating status of the equipment.

The test data obtained from both stations consisted of the results of various TV tests, attenuation (δ) and rain rate data. An additional meteorological parameter is measured at the Rosman station and it consists of the back-scatter returns of the multi-frequency weather radar. In addition, the personnel at the Rosman station conducted an Electro-Magnetic Interference (EMI) experiment. Test results and analysis of most of the above tests will be presented for the test period between June 1, 1976 to October 31, 1976. Also, long term rain rate statistics will be presented from January 1, 1976 to October 31, 1976 for the Goddard station. Because the spacecraft transmitter and beacon were turned off during the eclipse period which lasted from September 1 to October 16 no attenuation measurements were available for this period. However, rain rate and radar data was taken during this time.

The Rosman station was able to obtain a more definitive description of the meteorological environment because on-beam measurements were obtained from the dual frequency weather radar and rain rate measurements were obtained from 10 tipping buckets rather than one as is the case for the Goddard station. Also a finer resolution of the attenuation data is obtained from Rosman because the on-site computer

records the data at secondly average values. The Goddard station reduces the data manually from a strip chart; hence, a minutely average value is the shortest averaging time that is practical for data reduction.

In section 2 of the report all of the data obtained from the Goddard station and the corresponding analysis will be presented along with a functional description of the station. In section 3 the same factors will be covered for the Rosman station. Examples of signal scintillations that were measured on the CTS beacon link at the Goddard stations will also be presented. This will include measured frequency spectra of the received signals obtained from the Ubiquitous Spectrum Analyzer. In addition, the results of the analysis of attempting to fit the measured attenuation obtained from the Goddard data to the Weibull distribution utilizing the Chi-Square test criterion will be presented. A summary and conclusion section will be presented in section 4.

SECTION 2
GODDARD CTS STATION

2.1 STATION DESCRIPTION

The CTS station at Goddard Space Flight Center is located at the Propagation Test Facility (PTF). The station has full duplex video capability through CTS, and also has two c.w. receivers for recording propagation data. Figure 2-1 shows an overall basic block diagram of the Goddard CTS millimeter wave facility. As shown, the uplink video signal is fed to a 70 MHz FM modulator and upconverted to the uplink RF frequency. Two successive power amplifiers boost the signal power to 80 watts into the antenna feed. The uplink antenna is a 10 foot Cassagrain feed parabolic antenna.

On the receive side, the downlink signal is received on a separate antenna. This is a 15 foot Cassagrain feed parabolic antenna, as shown in figure 2-1. The composite RF signal is amplified and downconverted in a low noise front end. The resultant signal is the first IF band centered on 2.4 GHz. This signal, entering the trailer via coax cable, is split by a hybrid inside the trailer. One side is routed to a distribution network, where the appropriate beacon signal is selected and mixed down to the propagation receiver input frequency. The other side is routed to the video racks where, after amplification, the signal is fed to a 2.6 GHz receiver.

Figure 2-1 shows the station configuration existing during the data acquisition given in this report. During the time the satellite was turned off because of eclipse, an overall receiver calibration system was installed. This will be used during future data acquisition. The transmitter shown in figure 2-1 is a temporary arrangement and will be replaced by a higher powered unit, capable of saturating the CTS and thus obtaining maximum output power. It will also be capable of transmitting either of the propagation tones, or video carriers.

As presently configured, the transmitter-receiver leakage is excessive because of inadequate RF filtering. This increases the interference on the propagation signal and decreases the C/N value of the video signal, during transmission times. This will be alleviated when the permanent transmitter is installed. Also, the present

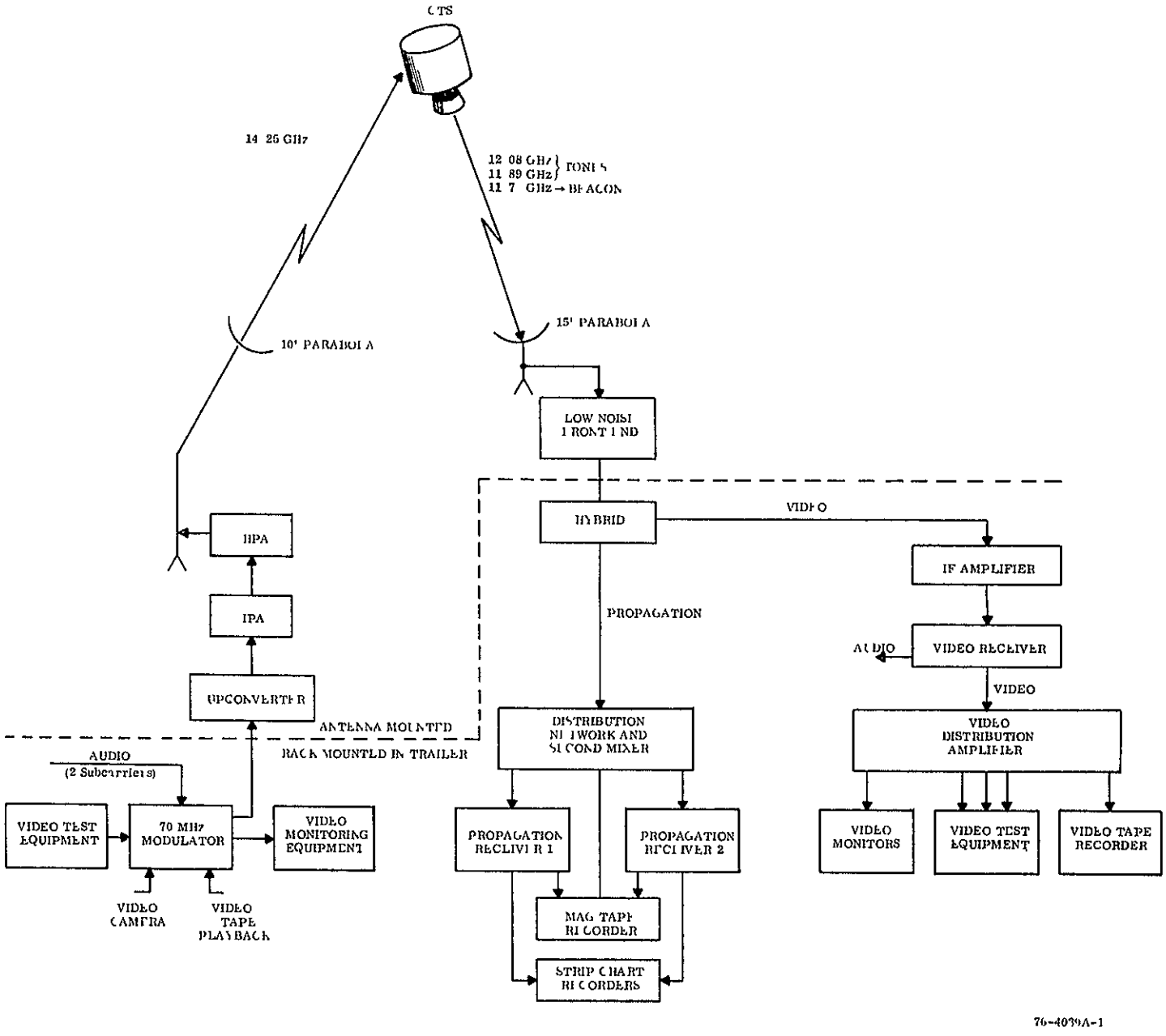

Figure 2-1. Functional Description of Goddard CTS Station

HPA is incapable of capturing the full satellite transmitter power, which will not be the case with the permanent transmitter.

Problems arose before the present configuration was instrumented. Before June, the permanent front end had not been installed and a temporary installation involving a Gunn diode L.O. was used. The resultant IF signal was too unstable for the narrowband propagation receiver to lock to. As a result, no propagation data could be acquired. Later, after a stable permanent front end was installed, a test signal generator had to be used in the signal distribution drawer as the second mixer L.O. The resultant IF signal was both frequency and level unstable, making the propagation data unreliable. However, over three months of propagation data have been acquired using the system shown in figure 2-1.

The anticipated performance of the receiver system can be determined through the link calculations. The following calculations are based on the CTS 11.7 GHz beacon signal, received with the system shown in figure 2-1. As shown, the anticipated margin on the beacon is 30.7 dB.

THEORETICAL PERFORMANCE OF GODDARD CTS STATION

Beacon Signal:

Satellite EIRP		+41.5 dBm
Path loss (31° elev angle)	-205.5	
Clear Sky Atten.	-0.3	-208.8
Polarization loss	-3.0	
Receive ant. gain		52.4
Line loss (est.)		-1.5
Signal power at front end input		-116.4 dBm
Front end gain		30.0
Cable loss		-10.0
First hybrid		-3.0
IF amp. gain		+30.0
Signal dist. & mixer conv. loss		-16.0
Max level at PLL input		-85.4 dBm

Noise

Clear sky noise temp	30°K
Eff sky temp ref to preamp input	21.2°K
Eff line loss ref to preamp input	84.7°K
Eff preamp noise ref to its input	288.6°K
Eff line loss noise temp ref to preamp input	5.5°K
Eff IF amp noise temp ref to preamp input	8.7°K
Total eff noise temp ref to preamp input	408.7°K

THEORETICAL PERFORMANCE OF GODDARD CTS STATION (Continued)

Noise: (Continued)

N_o at preamp input	-172.5 dBm
C/N_o = 172.5 - 116.4 =	56.1 dB
C/N in 100 Hz PLL BW	36.1 dB
Anticipated margin for beacon = 36.1 - 5.4 =	30.7 dB

2.2 TV EXPERIMENT

The temporary transmitter setup at the Goddard CTS Station has been used for all TV demonstrations and tests. During the period June - August, numerous demonstrations were conducted in support of various teleconferences, such as ICC '76 in Philadelphia and several other occasions. These events have demonstrated the highly satisfactory television relay at K band through CTS, during fair weather. During the overall test period a total of 65 hours of test time was utilized in various system performance tests. As a general rule the Goddard station transmitted and received its own transmission. Occasionally the Goddard station acted as the transmitting station for video tests being conducted at the Rosman station. During the 65 hours of test time no precipitation was encountered to determine the possible picture degradation due to rain attenuation. As a result, the resulting attenuation condition was simulated by antenna movement. Measurements of the overall system performance utilizing standard video tests were performed. These include C/N, TT/N, differential phase and differential gain. The results for a clear weather condition are given in Table 2-1.

TABLE 2-1

VIDEO SYSTEM MEASUREMENTS AUGUST 26, 1976
AUDIO SUBCARRIERS OFF

Measurement	Value, dB	Conditions of Noise Measurement
C/N	20.4 (P_{ts}=131W)	Gnd T_x off. Rec. ant. 10° off S/C
	16.0 (P_{ts}=131W)	Gnd T_x on. Rec. ant. 10° off S/C
	15.0 (P_{ts}=131W)	Gnd T_x off. Rec. ant. peaked on S/C
TT/N	35 (P_{ts}=131W)	Noise measured with carrier being transmitted. Value represents RMS TT to RMS noise at the output of the 4.2 MHz video filter.

TABLE 2-1

VIDEO SYSTEM MEASUREMENTS AUGUST 26, 1976
AUDIO SUBCARRIERS OFF (Continued)

Measurement	Value	Conditions of Measurement
Differential gain	3 - 4%	GSFC transmitting. P_{ts} = 92 watts.
Differential phase	5°	P_{ts} = 92 watts.

C/N - RMS Carrier to RMS Noise defined in the 30 MHz IF Noise Bandwidth

TT/N - Test tone to noise ratio defined in a 4.2 MHz bandwidth

P_{ts} - Spacecraft Transmit Power

Comparison of the C/N values in Table 2-1 shows the degradation due to direct $T_x - R_x$ leakage to be some 4.4 dB. The degradation due to earth noise relayed through the satellite is some 5.4 dB.

The above C/N measurement should improve substantially when the permanent ground transmitter is installed.

In addition to the above measurements, the LNR receiver passband frequency response was measured, after alignment.

An objective of the TV experiment is to determine picture quality as a function of the rain rate parameter. To accomplish this objective, some measure of picture quality must be employed during different periods and types of precipitation. Two different experiments were performed for assessing picture quality as a function of the resulting ratio of peak-to-peak video signal to rms noise (S/N) defined in a 4.2 MHz bandwidth. The first was reported in the literature in June of 1960. The tests[1] were conducted by the Television Allocation Study Organization (TASO). This organization utilized a standard commercial TV system which is a special form of an AM system called a vestigial sideband system. In the test, 38 men and 38 women viewed selected still pictures as the S/N (defined as the RMS signal during sync peak to RMS noise in a 6 MHz bandwidth channel) was varied. The various picture categories along with the S/N value that was required by 50% of the viewers are listed in Table 2-2. A similar experiment was repeated at a later time and the results reported in the CCIR Reference 215-3 section 4.2. The corresponding values for 50% of the viewers are also listed in Table 2-2. The data reported in the CCIR reference requires a higher S/N value than

TABLE 2-2

TASO QUALITY PICTURES

PICTURE GRADE	PICTURE CATEGORIES	REQUIRED $\frac{S}{N}$ PK TO PK VIDEO TO RMS NOISE IN 4.2 MHZ BW FOR 50% OF VIEWERS	
		TASO	CCIR
1	EXCELLENT	>40 DB	
1.5			>37 5 DB
2	FINE	>31 DB	>33.2 DB
3	PASSABLE	>26 DB	>28.0 DB
4	MARGINAL	>20.5 DB	>23.6 DB
5	INFERIOR	>14.5 DB	>18.4 DB

SEE NOTE

FOR NASA GODDARD STATION

COMPUTED (DB)	(DB)	CCIR	TASO	
C/N=16.1	S/N=42 1	EXCELLENT	EXCELLENT	
C/N=11.3	S/N=37.3	FINE	FINE	
C/N=8.2	S/N=34.2	FINE	FINE	
C/N=6.2	S/N=31.7	PASSABLE	FINE	THRESHOLD CONDITION IMPULSE
C/N=1.5	S/N=20.5	INFERIOR	INFERIOR	NOISE IS PRESENT THAT WILL DEGRADE PICTURE QUALITY FURTHER

NOTE: FM S/N AM S/N

$$\left.\frac{\text{Peak to Peak Video}}{\text{RMS Noise}}\right|_{4.2\ \text{MHz}} = \left.\frac{\text{RMS Signal During Peak Sync.}}{\text{RMS Noise}}\right|_{6\ \text{MHz}} - 2\ \text{dB}$$

the earlier test. Since there are subjective tests, the results could indicate that viewers are more discriminating as to picture quality due to the continuous viewing of TV over the time period between tests.

For the test period under consideration no precipitation occurred to test the effect of rain on picture quality. Therefore, it was decided to simulate the rain fades by varying the ground station EIRP. For this test a color bar generator was employed as the transmission standard. The EIRP was varied which in turn simulated an uplink fade and also a downlink fade since the magnitude of the spacecraft transmit power (P_{ts}) is a function of the spacecraft received power. The EIRP was reduced in convenient steps and the received C/N (defined in an IF noise bandwidth of 30 MHz) was measured and a photograph was taken of the resulting color bar pattern as it was displayed on a monitor.

The results of the test for 5 measured C/N values is shown in Figure 2-2. The corresponding S/N values and the picture grades are shown in Table 2-2.

The clear weather reference is defined at a measured overall link C/N of 16.1 dB. As shown in the link performance calculations, (page 2-11) the overall link C/N is 16.6 dB with the system being uplink limited by the uplink C/N of 16.8 dB. Varying the ground EIRP resulted in a simulated fade condition on both the up and the downlink paths. However, the effects of the simulated uplink fade was the limiting factor from the standpoint of picture fidelity. The slope of the CTS transfer characteristics defined as $\Delta P_{ts}/\Delta P_{rs}$ is constant in the measured P_{ts} region of 128 watts to 11.3 watts obtained in the test. Therefore, the dB change in P_{ts} is a direct measure of the simulated fade on the uplink. The dB difference between C/N and P_{ts} does track down to a C/N of 8.2 dB as shown in the following listing:

Photo Number	Measured Overall Link C/N (dB)	dB Difference	Measured P_{ts} (watts)	dB Difference
1	16.1		128	
2	11.3	4.8	50	4.1
3	8.2	3.1	25	3
5	6.2	2	18.5	1.3
4	1.5	4.7	11.3	2.1

Lack of correspondence between C/N and P_{ts} below 8.2 dB is probably due to the measurement errors in both C/N and P_{ts}.

From empirically derived data, relating the measured post detection S/N with the predetection C/N taken on the video FM system that operated with ATS-1 and ATS-3, it was determined that the FM threshold occurred at a C/N of about 7 dB. This is lower than the normally accepted value of about 10 dB. Actually, the threshold value varies directly with the modulation index (M). For this system the M value is equal to $2.4\ (\frac{10\ \text{MHz}}{4.2\ \text{MHz}})$. Because of this low value, a corresponding low value for the threshold level should be expected. An empirically derived expression that relates the threshold value $(C/N)_T$ to M can be employed to obtain a qualitative measure of a system threshold value. It is as follows.

$$\left(\frac{C}{N}\right)_T = 6.3\sqrt[3]{M}$$

For an M of 2.4 the corresponding $(C/N)_T$ is 8.4 dB. The calculated S/N values given in Table 2-2 for a measured C/N were obtained assuming a threshold of 8 dB and an emphasis improvement of 2.5 dB. Below threshold values were obtained from performance curves of actual measured values of S/N versus C/N. As expected the unusable and inferior classifications characterize below threshold operation.

Because the system is uplink limited the simulated fades correspond to the 14 GHz uplink frequency. As shown in Figure 2-2 and Table 2-2 degradations in the color fidelity starts to occur when the C/N value decreases below 8 dB. This corresponds to an uplink fade of 8 dB. For the system under consideration, it follows that rain will degrade picture fidelity for the time that the fade level exceeds 8 dB at 14 GHz. A measure of this time can be obtained from the 11.7 GHz attenuation statistics given in figure 2-3 if the equivalent fade level at 14 GHz can be determined. It has been shown by Ippolito[2] that the following relationship between the attenuation at 11.7 GHz ($\delta_{11.7}$) and at 14 GHz (δ_{14}) is related to rain rate (R) by the following expression·

$$\frac{\delta_{14}}{\delta_{11.7}} = 1.58R^{-0.06}$$

FIGURE 2-2
EIA COLOR BAR PRESENTATION
FOR VARIOUS CARRIER-TO-NOISE RATIOS

14 GHz FADE LEVELS			TASO / CCIR
0 dB	C/N=16.1 dB Pts =128 W	S/N= 42.1 dB	EXCELLENT / EXCELLENT
4.8 dB	C/N =11.3 dB Pts =50 W	S/N= 37.3 dB	FINE / FINE
7.9 dB	C/N =8.2 dB Pts =25 W	S/N= 34.2 dB	FINE / FINE
9.9 dB	C/N =6.2 dB Pts =18.5 W	S/N= 31.7 dB	FINE / PASSABLE
14.6 dB	C/N =1.5 dB Pts =11.3 W	S/N= 20.5 dB	INFERIOR / INFERIOR

2-9/2-10

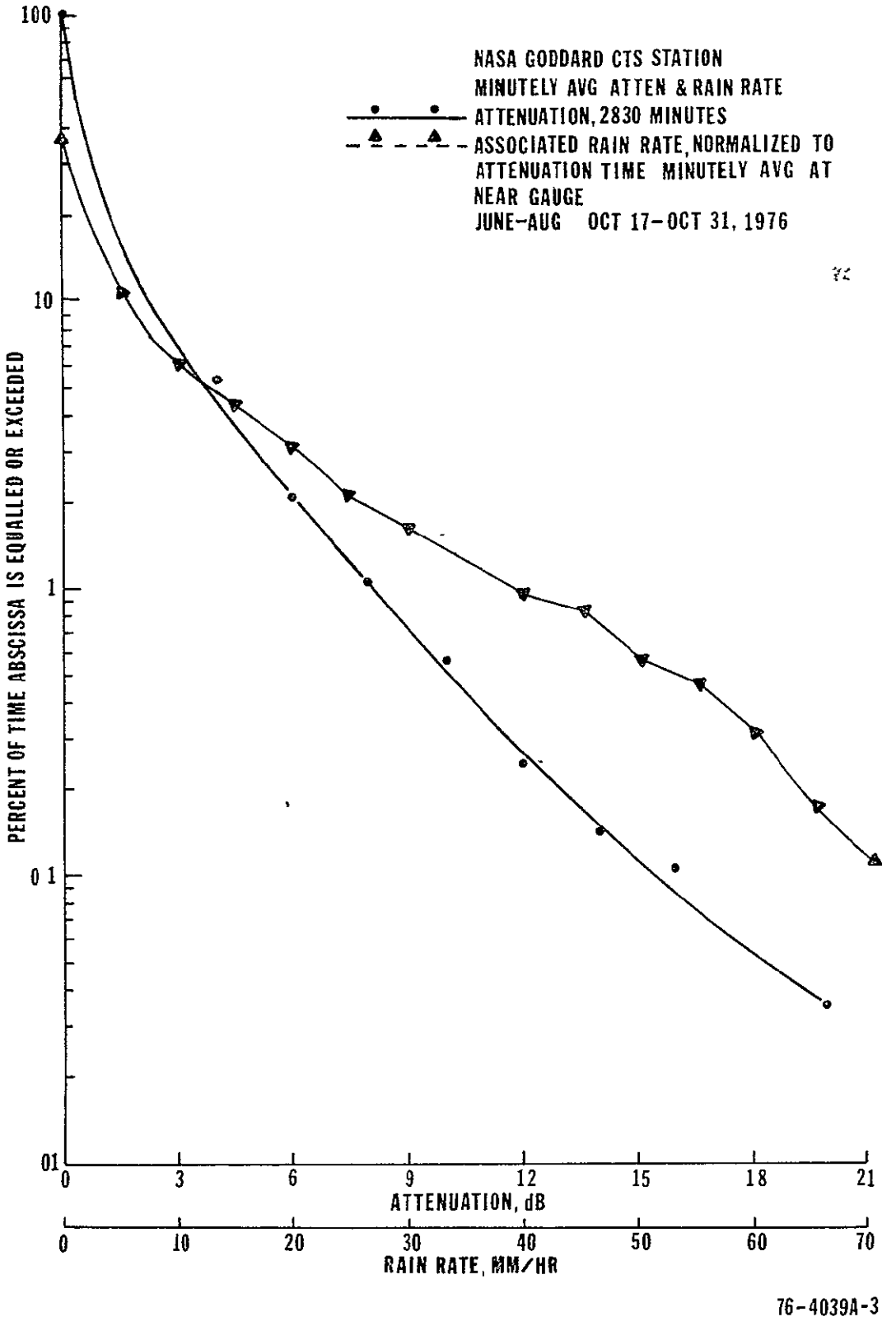

Figure 2-3. NASA Goddard CTS Station, Minutely Average Attenuation and Rain Rate

For the general levels of $\delta_{11.7}$, the R range of interest would be 20 to 40 MM/Hr and for this range the average value of $R^{-0.06}$ is 0.82. Therefore,

$$\frac{\delta_{14}}{\delta_{11.7}} = 1.29$$

In comparison to the above ratio value previous measurements of attenuation[3] at 30 GHz and 20 GHz resulted in a ratio value of 2. For an 8 dB fade at 14 GHz the corresponding fade at 11.7 GHz is 6.2 dB. This fade level corresponds to a time percentage of 2%. Therefore for a total test time of 2830 minutes, fidelity of the color picture will be effected by rain for 56.6 minutes of that period, for the system under consideration over an overall time period of June through October.

SIMPLEX VIDEO LINK CALCULATIONS

UPLINK (14 GHz)		DOWNLINK (12 GHz)	
P_{tg} = 50 watts	= 47 dBm	P_{ts} = 128 watts	51 dBm
G_{tg} (10' Antenna)	= 48.1 dB	G_{ts}	36.9 dB
EIRP	95.1 dBm	S/C EIRP	87.9 dBm
Free Space Loss	-206.8 dB	Free Space Loss	-205.5 dB
Other Losses	-2.0 dB	Other Losses	-2.0 dB
Total Losses	-208.8 dB	Total Losses	-207.5 dB
G_{rs} (S/C Rec. Ant. Gain)	37.9 dB	G_{rg} (15' Antenna)	52.4 dB
P_{rs}	= -75.8 dBm	P_{rg}	= -67.2 dBm
T_s = 1315°K		T_s = 409°K	
N_o	= -167.4 dBm/Hz	N_o	= -172.5 dBm/Hz
$\frac{C}{N_o}$	= 91.6 dB Hz	$\frac{C}{N_o}$	= 105.3 dB Hz
B_{IF}	= 30 MHz	B_{IF}	= 30 MHz
$U_u = \frac{C}{N}$	= 16.8 dB	$U_{dt} = \frac{C}{N}$	= 30.5 dB

Overall Link $\frac{C}{N} = \frac{U_u U_{dt}}{U_{dt} + (U_u + 1)} = 16.6$

Measured $\frac{C}{N}$ = 16.1 dB.

2.3 PROPAGATION MEASUREMENTS

At the Goddard station, rain rate measurements were started in January of 1976. Measurements of clear weather scintillations and rain attenuation was started in June of 1976. The date and time of these measurements are listed in Table 2-3. These measurements consists of a total of 35,947 minutes of data in the test period. A certain portion of this time only involved periods of precipitation. As shown in the table, each test is defined by a given weather class (WC) designation of 1 to 7. The definition of each WC is given in Appendix A. A WC designation of 1 to 4 signifies a period of non-precipitation as determined by the station personnel. The period in which a WC of 5 to 7 was present at the station was 2830 minutes. In this period a measurement of attenuation was attempted.

Figure 2-4 shows the rain rate cumulative distributions for the period January - October, 1976, and during the period wherein satellite beacon data was acquired. The curves in this figure represent the average rain rate between tips of a tipping bucket rain gauge near the receive antenna. Each curve is normalized to the time period given in the legend.

The similarity of the two curves in figure 2-4 points out that the distribution of rates during the time period encompassing attenuation data acquisition is similar to that of the year so far.

So that data from the Rosman and Goddard stations can be compared, the attenuation and associated rain rate cumulative distributions are shown in figure 2-3. As shown, both curves are based on 2830 minutes of attenuation and associated rain rate. This corresponds to the total time that attenuation measurements were attempted.

The highest minutely average rain rate during the test period was 75 MM/HR. The highest minutely average attenuation was nearly 21 dB. So that the effect of averaging can be seen, figure 2-5 is a plot of instantaneous and minutely average rain rate during the total observed precipitation time of 2830 minutes. As shown, the average curve lies below the instantaneous and deviates markedly from the instantaneous in the high rain rate region.

TABLE 2-3

BEACON DATA ACQUISITION TIMES, GODDARD CTS STATION
JUNE - OCTOBER, 1976

Date	Time	No. Hours & Min.		WC
June 8, 76	1800Z - 2000Z	2		4
June 9, 76	1320Z - 1400Z		40	1
June 9, 76	1800Z - 2000Z	2		1
June 10, 76	1400Z - 1517Z			1
June 11, 76	1215Z - 1614Z	3	59	1
June 14, 76	1507Z - 2149Z	6	42	4
June 15, 76	1400Z - 2400Z	10		1, 2, 3
June 16, 76	0000Z - 1400Z	14		1, 2, 3
June 16, 76	1757Z - 1930Z	1	33	4
June 17, 76	2000Z - 2400Z	4		2
June 18, 76	0000Z - 1300Z	13		2
June 20, 76	0200Z - 2400Z	22		4, 6, 7
June 21, 76	0000Z - 1245Z	12	45	4, 6, 7
June 21, 76	1435Z - 2400Z	9	35	4, 6
June 22, 76	0000Z - 1230Z	12	30	4, 6
June 30, 76	1930Z - 2240Z	3	10	4, 6, 7
July 2, 76	1320Z - 1458Z	1	38	1
July 6, 76	1239Z - 2400Z	11	21	1, 4, 6
July 7, 76	0000Z - 1230Z	12	30	1, 4, 6
July 7, 76	1330Z - 1900Z	5	30	4
July 8, 76	1800Z - 2400Z	6		4
July 9, 76	0000Z - 0400Z	4		4
July 11, 76	1800Z - 2400Z	6		4, 6, 7
July 12, 76	0000Z - 1230Z	12	30	3, 4, 6
July 12, 76	1400Z - 2400Z	10		3, 4, 6
July 13, 76	0000Z - 0600Z	6		3, 4, 6
July 15, 76	1916Z - 2400Z	4	44	4
July 16, 76	0000Z - 0700Z	7		4
July 16, 76	1430Z - 2400Z	9	30	1, 4, 6, 7
July 17, 76	0000Z - 2400Z	24		1, 4, 6, 7
July 18, 76	0000Z - 1430Z	14	30	1, 4, 6, 7
July 21, 76	2030Z - 2400Z	3	30	4
July 22, 76	0000Z - 1230Z	12	30	4
July 23, 76	2030Z - 2400Z	3	30	1, 3, 4
July 24, 76	0000Z - 2400Z	24		1, 3, 4
July 25, 76	0000Z - 1230Z	12	30	1, 3, 4

TABLE 2-3

BEACON DATA ACQUISITION TIMES, GODDARD CTS STATION
JUNE - OCTOBER, 1976 (Continued)

Date	Time	No. Hours & Min.		WC
July 27, 76	1632Z - 2400Z	7	28	4
July 28, 76	0000Z - 1704Z	17	4	4
July 28, 76	2030Z - 2400Z	3	30	4
July 29, 76	0000Z - 1430Z	14	30	4
July 29, 76	2030Z - 2400Z	3	30	4
July 30, 76	0000Z - 1230Z	12	30	4
July 30, 76	2030Z - 2400Z	3	30	4
Aug. 1, 76	0000Z - 0100Z	1		
Aug. 6, 76	2000Z - 2400Z	4		4
Aug. 7, 76	0000Z - 2300Z	23		4
Aug. 8, 76	0000Z - 1230Z	12	30	4, 6, 7
Aug. 9, 76	1230Z - 2400Z	11	30	6
Aug. 10, 76	0000Z - 1230Z	12	30	6
Aug. 14, 76	2150Z - 2400Z			4, 6, 7
Aug. 15, 76	0000Z - 2400Z	24		4, 6, 7
Aug. 16, 76	0000Z - 1230Z	12	30	4, 6, 7
Aug. 27, 76	1300Z - 1510Z	2	10	4
Aug. 27, 76	1700Z - 2400Z	7		4
Aug. 28, 76	0000Z - 2400Z	24		4, 6
Aug. 29, 76	0000Z - 1630Z	16	30	4, 6
Oct. 18, 76	1300Z - 2000Z	7		1
Oct. 20, 21, 76	1230Z - 1230Z	24		4, 6
Oct. 24, 25, 76	2000Z - 1230Z	16	30	4, 6
Oct. 25, 26, 76	1230Z - 1230Z	24		4, 6
Oct. 26, 76	1230Z - 1818Z	5	48	3, 4

It is of interest to see how some of the fading events comprising figure 2-3 looked in real time. Three of these have been plotted and are shown in figures 2-6, 2-7, and 2-8. Figures 2-6 and 2-7 show typical time plots of instantaneous (average between tips) rain rate and attenuation. Rain typically fell a number of minutes after the peak attenuation was reached. Dark, moisture-laden clouds usually intersected the beam from the South, causing significant attenuation, after which rainfall was measured. As the rain rate increased, the attenuation decreased, often becoming insignificant by the time the peak rain rate was measured. This is seen in both figures 2-6 and 2-7. Figure 2-8 shows the less frequent case of peak attenuation being measured after the peak rain rate.

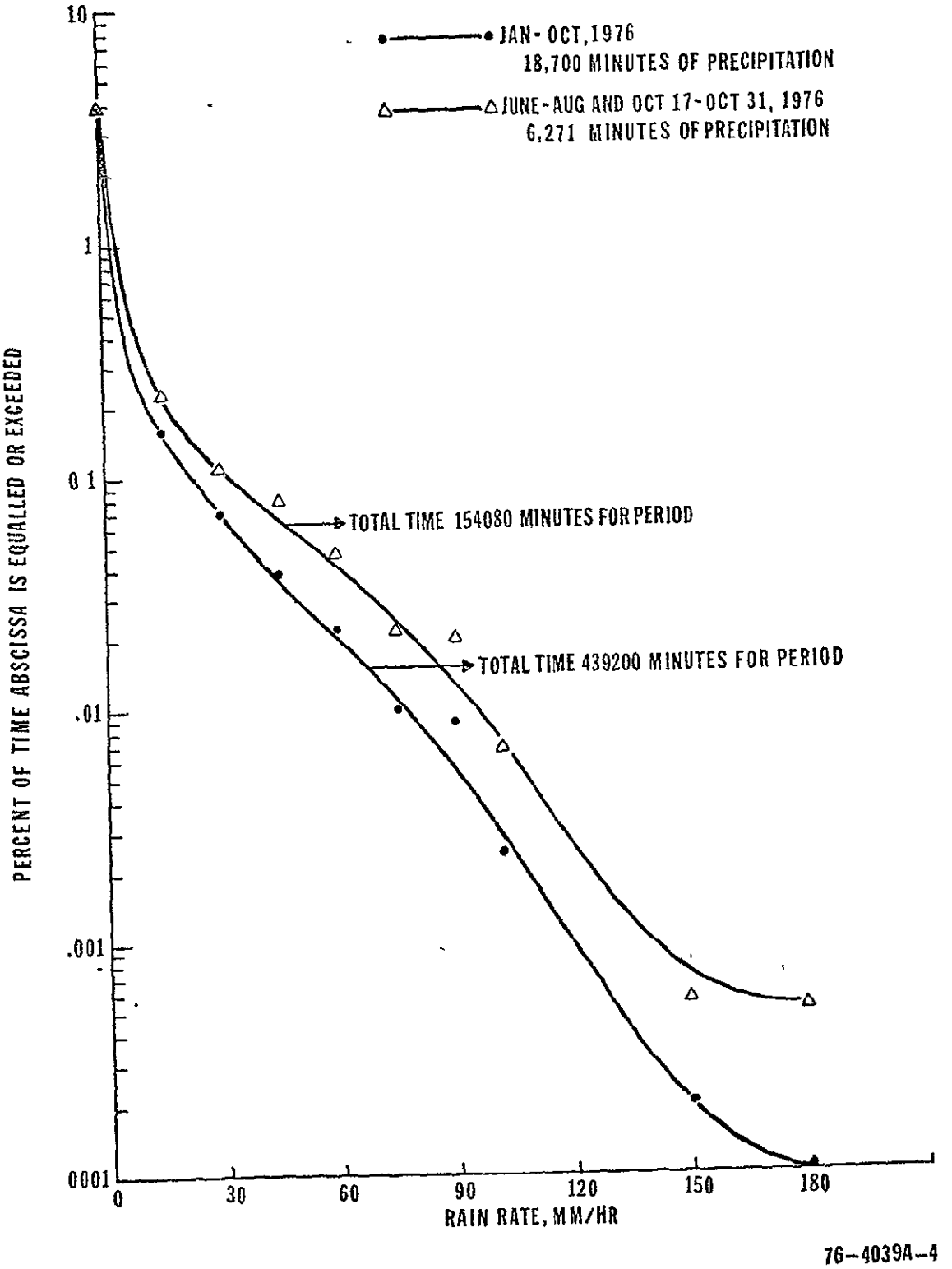

Figure 2-4. NASA Goddard CTS Station, Instantaneous Rain Rate, Near Gauge

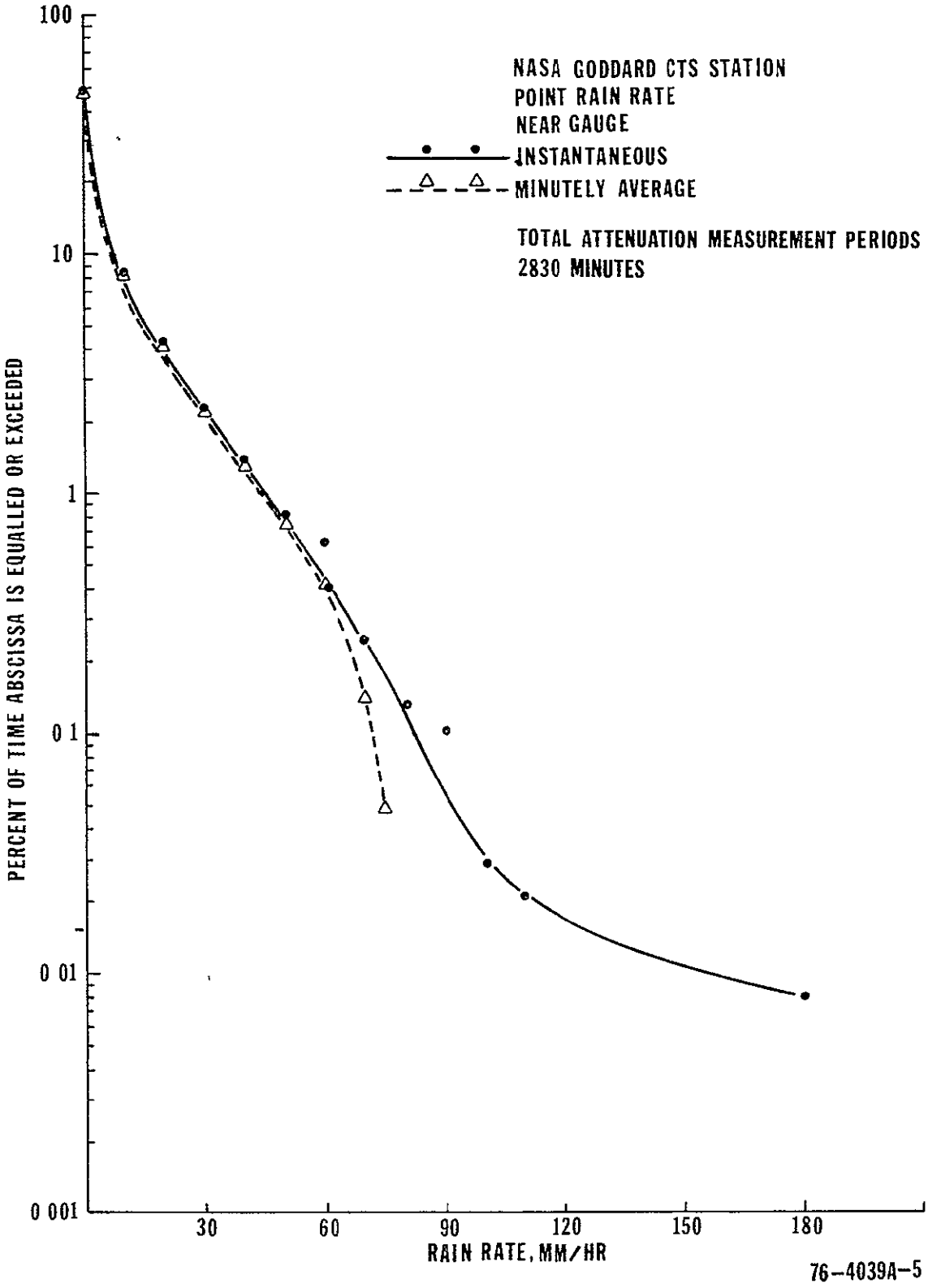

Figure 2-5. NASA Goddard CTS Station, Rain Rate During Attenuation Measurement, June-October, 1976, Near Gauge

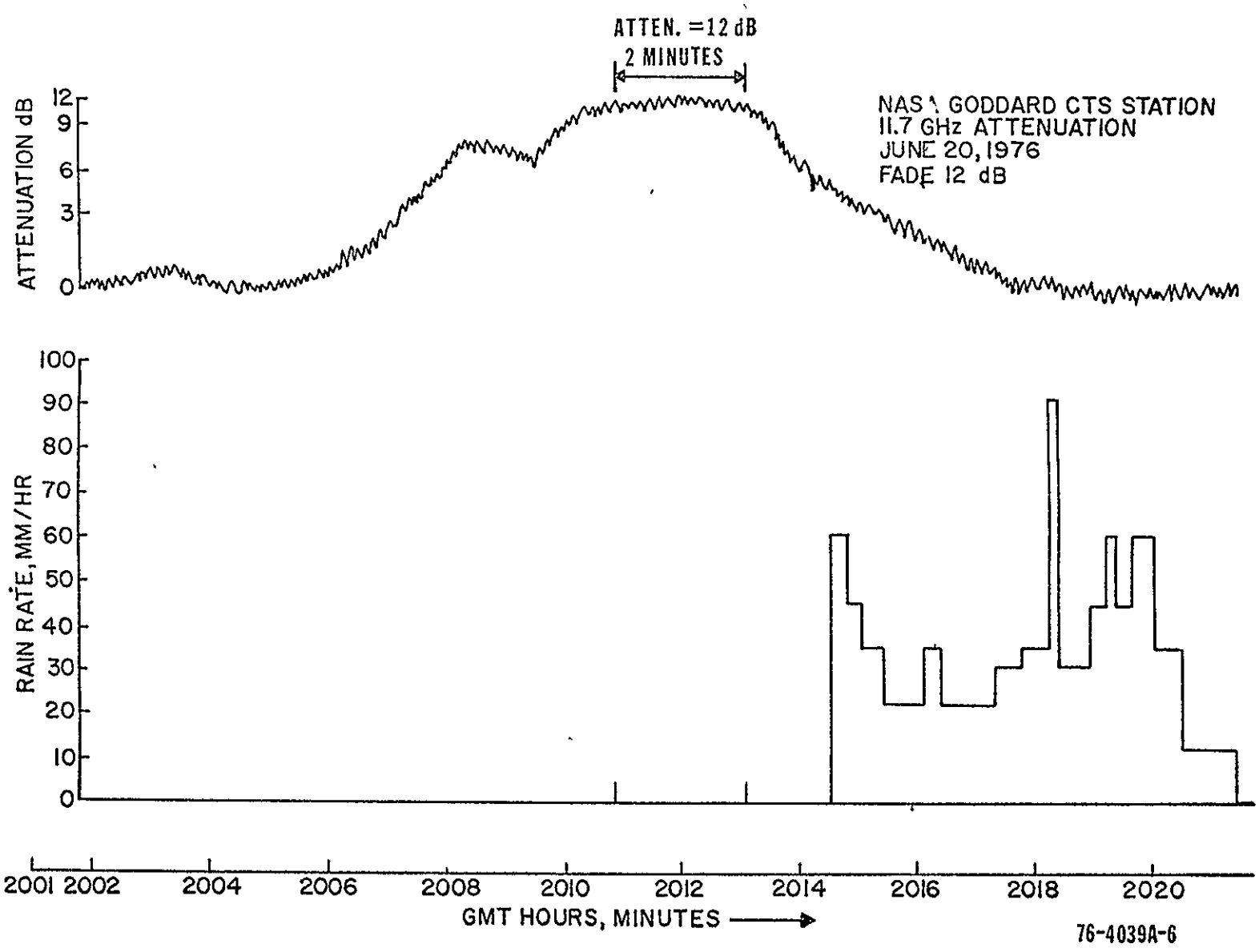

Figure 2-6. NASA Goddard CTS Station, 11.7 GHz Attenuation, June 20, 1976, Fade 12 dB

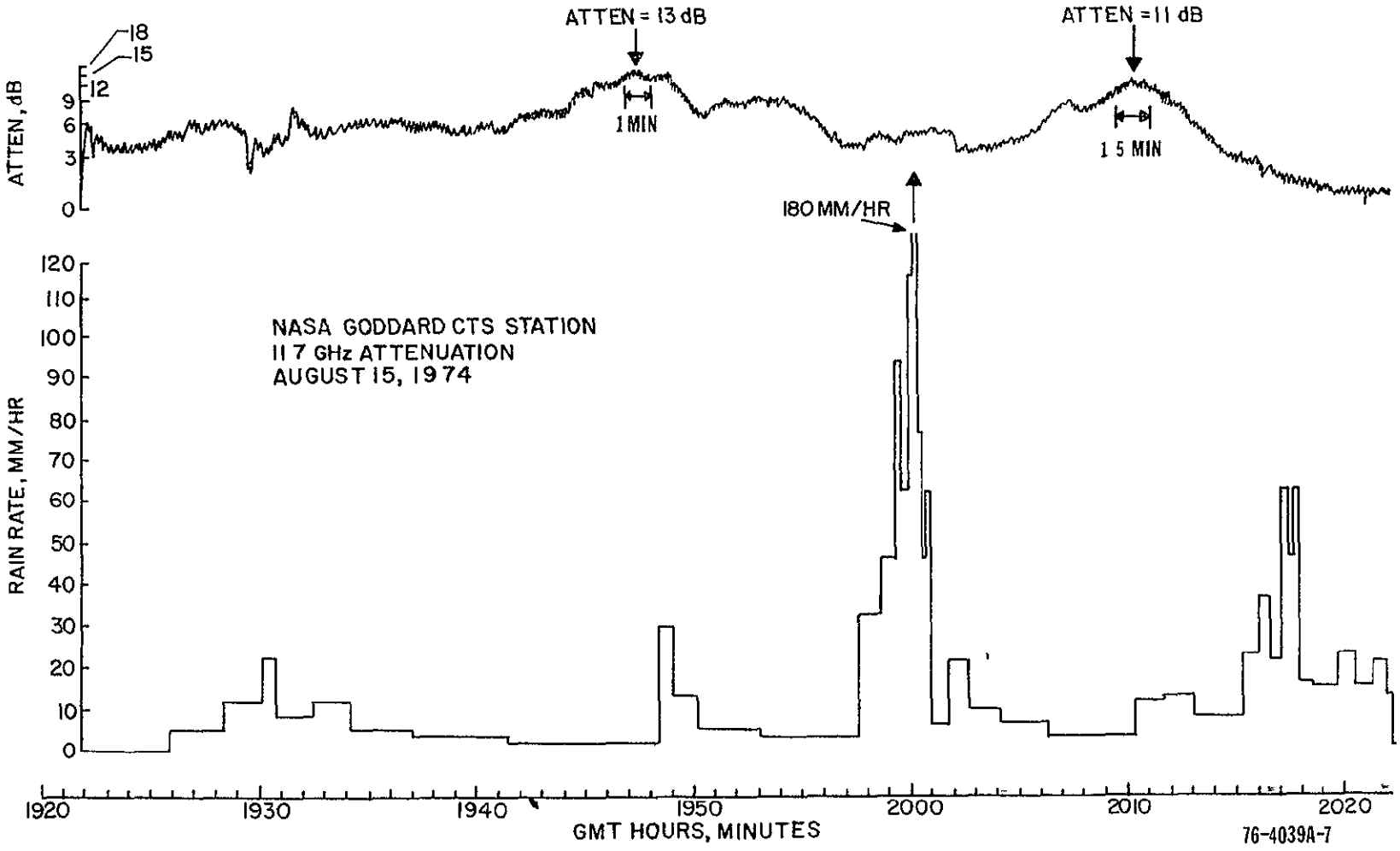

Figure 2-7. NASA Goddard CTS Station, 11.7 GHz Attenuation, August 15, 1974

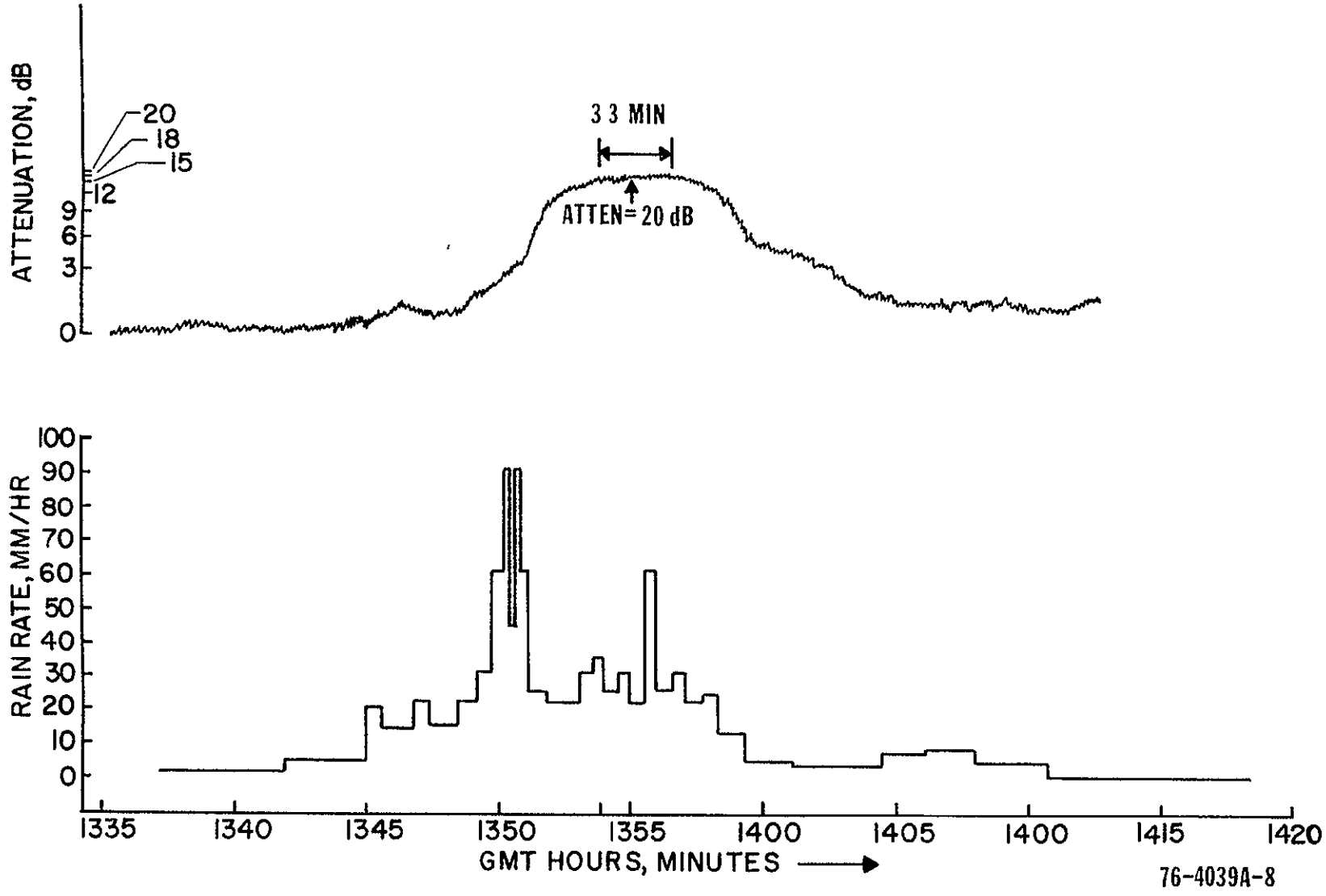

Figure 2-8. NASA Goddard CTS Station, 20 dB Fade, August 8, 1976, CTS 11.7 GHz Beacon

In addition to the total time the signal exceeded a certain dB value seen in the attenuation distribution in figure 2-3, it is of interest to know how many times the signal, having undergone a fade below a certain level, remains below that level for a given time. Figures 2-9 through 2-11 show this for the June - August attenuation measurements. Figure 2-9 shows the 3 dB level. This figure shows, for instance, that twice during the 1680 minute data acquisition interval the signal, having faded below the 3 dB level remained below that level for 3 minutes. Figure 2-10 shows a similar graph for the 6 dB fade level and figure 2-11 shows the 9, 12, 15, and 18 dB levels.

If it is of interest to know the time of day fading occurred, figures 2-12 through 2-15 show this. Figure 2-12, for instance, shows that the data contained two fades which exceeded 3 dB during GMT hours 1500 and 1600. Similarly, figures 2-13 through 2-15 are for the 6, 9, and 12-18 dB levels.

A functional relationship between rain rate (R) and attenuation (δ) is discussed in section 3.4. From a empirically derived relationship, the values of δ versus R for constant path lengths of 1 km, 5 km, 7 km and 10 km are plotted in figure 2-16. For widespread rain, an estimate of the path length for the Goddard station can be obtained from the height value of the melting layer. For the months of June, July, and August this height relative to sea level is 3.5 km. For an elevation angle of 29.5° and an effective height above sea level of 42 meters the corresponding slant range to the melting layer is 7 km. As shown in figure 2-16, the measured δ and peak rain rate pairs are superimposed on the constant path length curves. The 7 km calculation assumes a widespread rain condition that should be present for relatively low values of R. For measured values of R less than about 30 mm/hr an assumed path length of 7 km would have resulted in a reasonable estimate of the δ value. The disadvantage of employing a point rain rate value for an estimate of the precipitation within the elevated beam is shown for the cases where an attenuation did, in fact, exist, however, the tipping bucket did not record the precipitation.

The curve marked "DATA" was produced by a least mean square fit of the measured δ-R pairs to an aR^b function. The prediction curve was determined from measured 15.3 GHz δ and R pairs obtained from the propagation experiment conducted on the ATS-5 satellite. The δ data was translated to the 11.7 GHz test frequency by the method developed in section 2.2. Both curves show that as R increases the dependence of δ on path length decreases. This follows from the fact that high values of R are characterized by intense rain cells of limited extent.

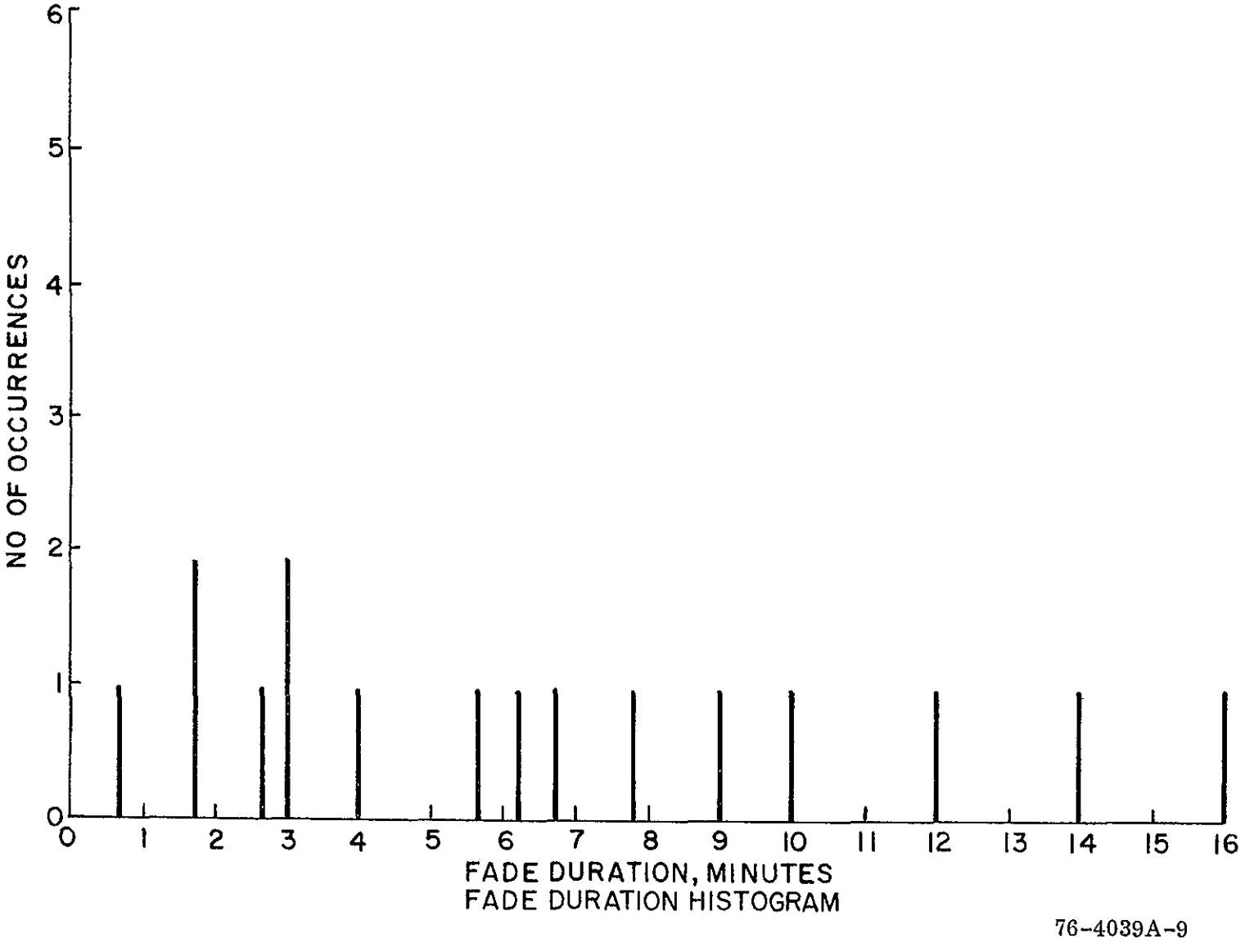

Figure 2-9. NASA Goddard CTS Station, 11.7 GHz, Fades > 3 dB, June, July, August, 1976
Total Test Time = 668 Minutes

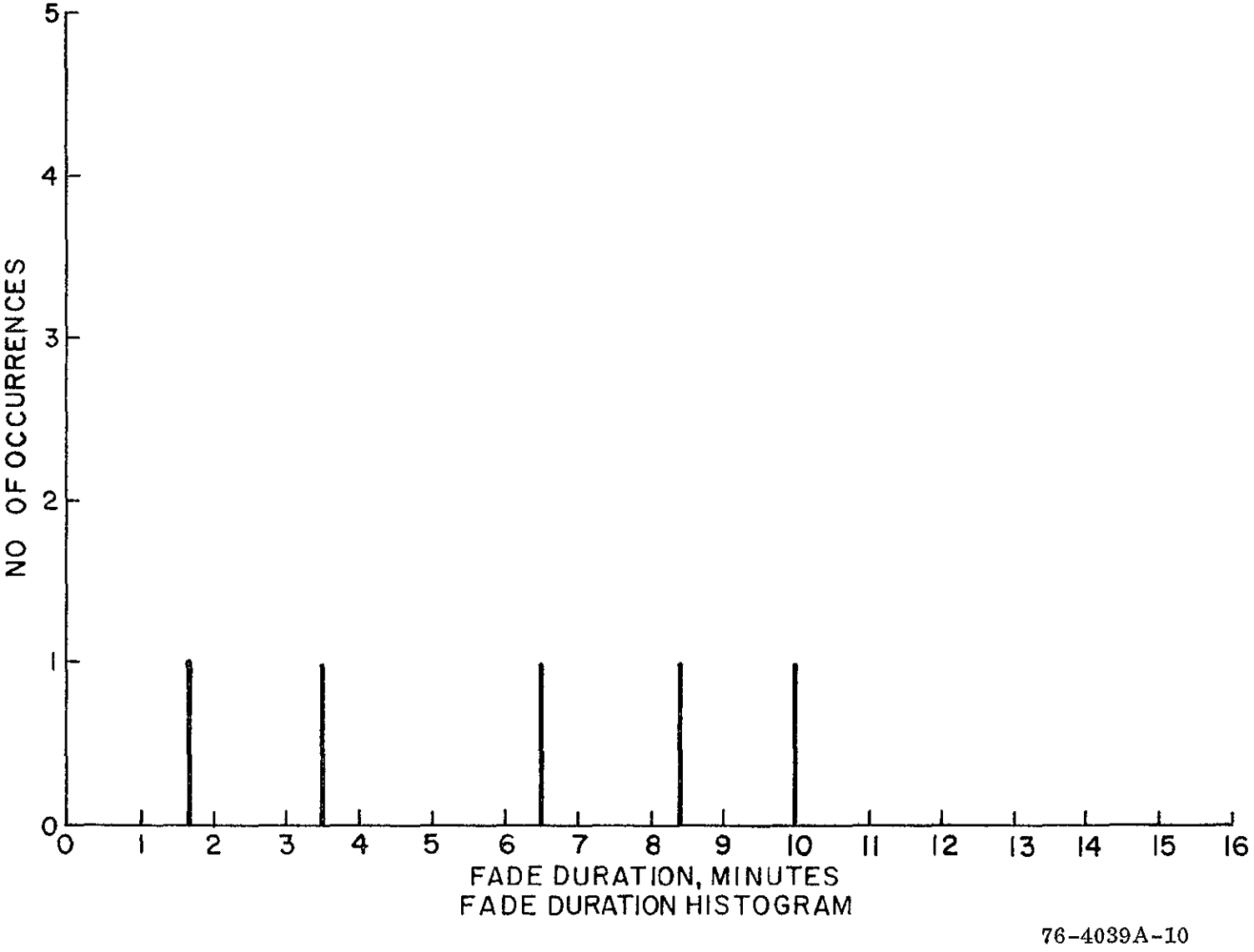

Figure 2-10. NASA Goddard CTS Station, 11.7 GHz, Fades > 6 dB, June, July, August, 1976
Total Test Time = 668 Minutes

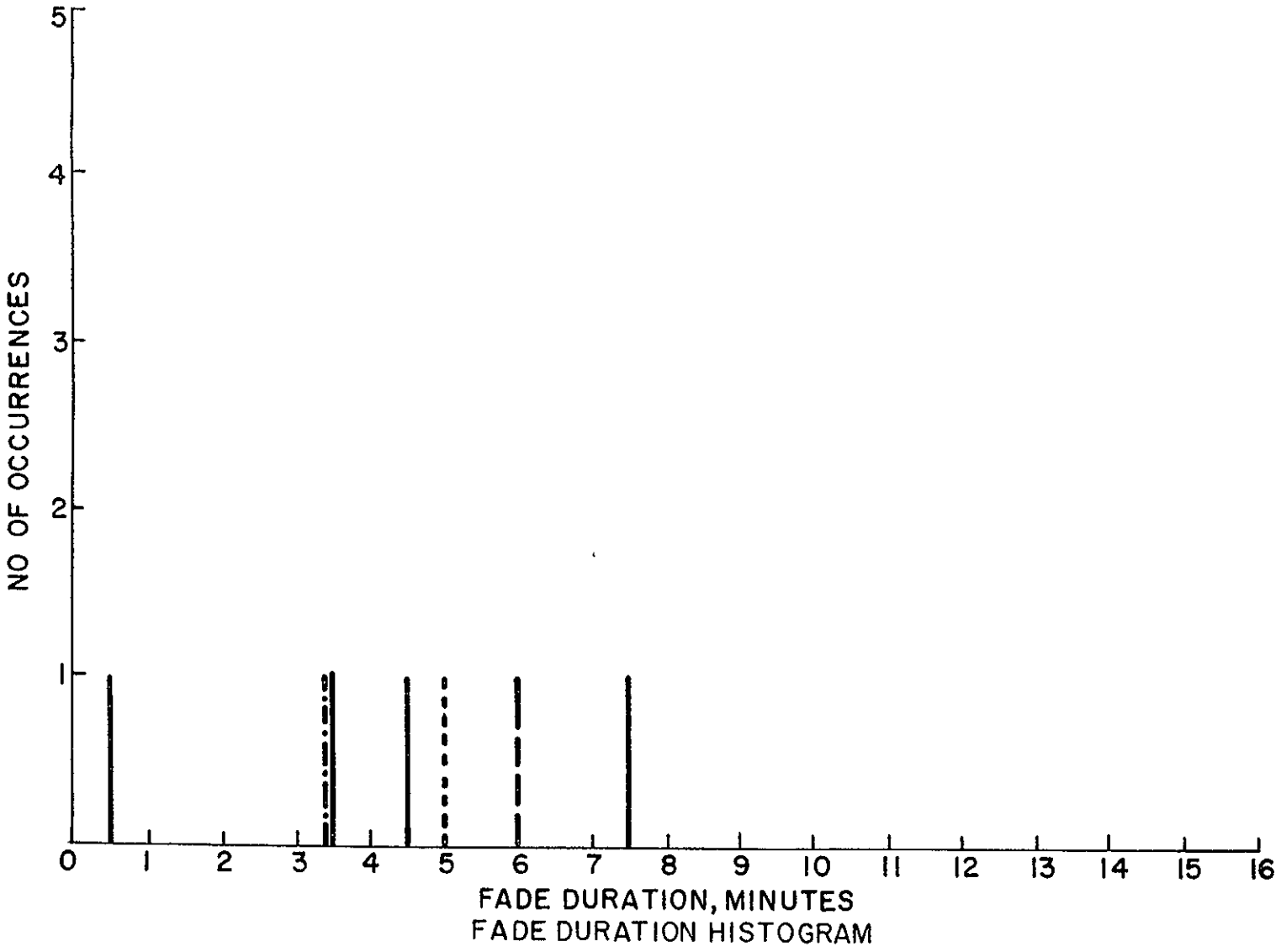

Figure 2-11. NASA Goddard CTS Station, 11.7 GHz,
Fades > 9 dB ——— > 12 dB — — — — > 15 dB ------ > 18 dB — - —
June, July, August, 1976, Total Test Time = 668 Minutes

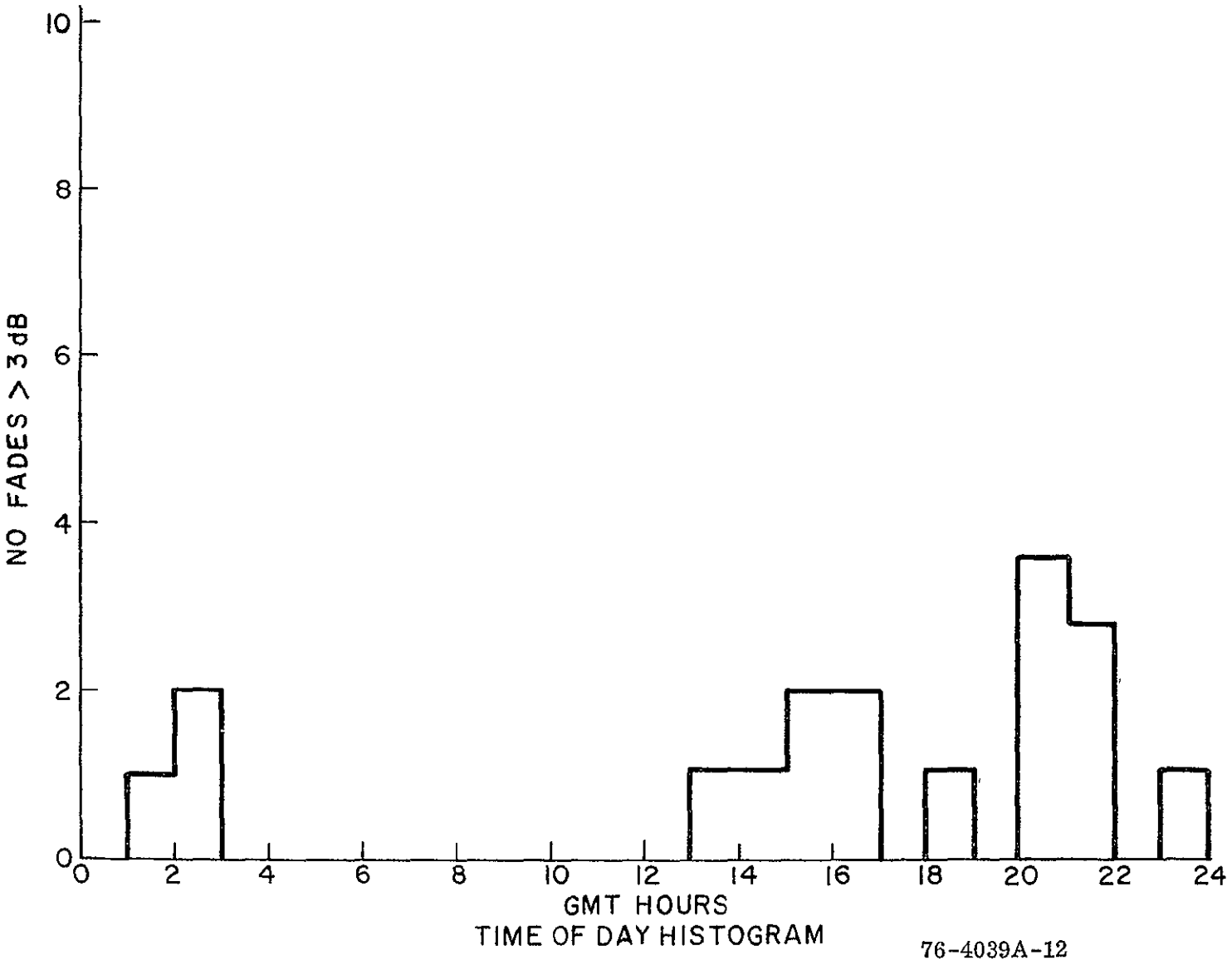

Figure 2-12. NASA Goddard CTS Station, Fades > 3 dB, June, July, August, 1976, Total Test Time = 668 Minutes

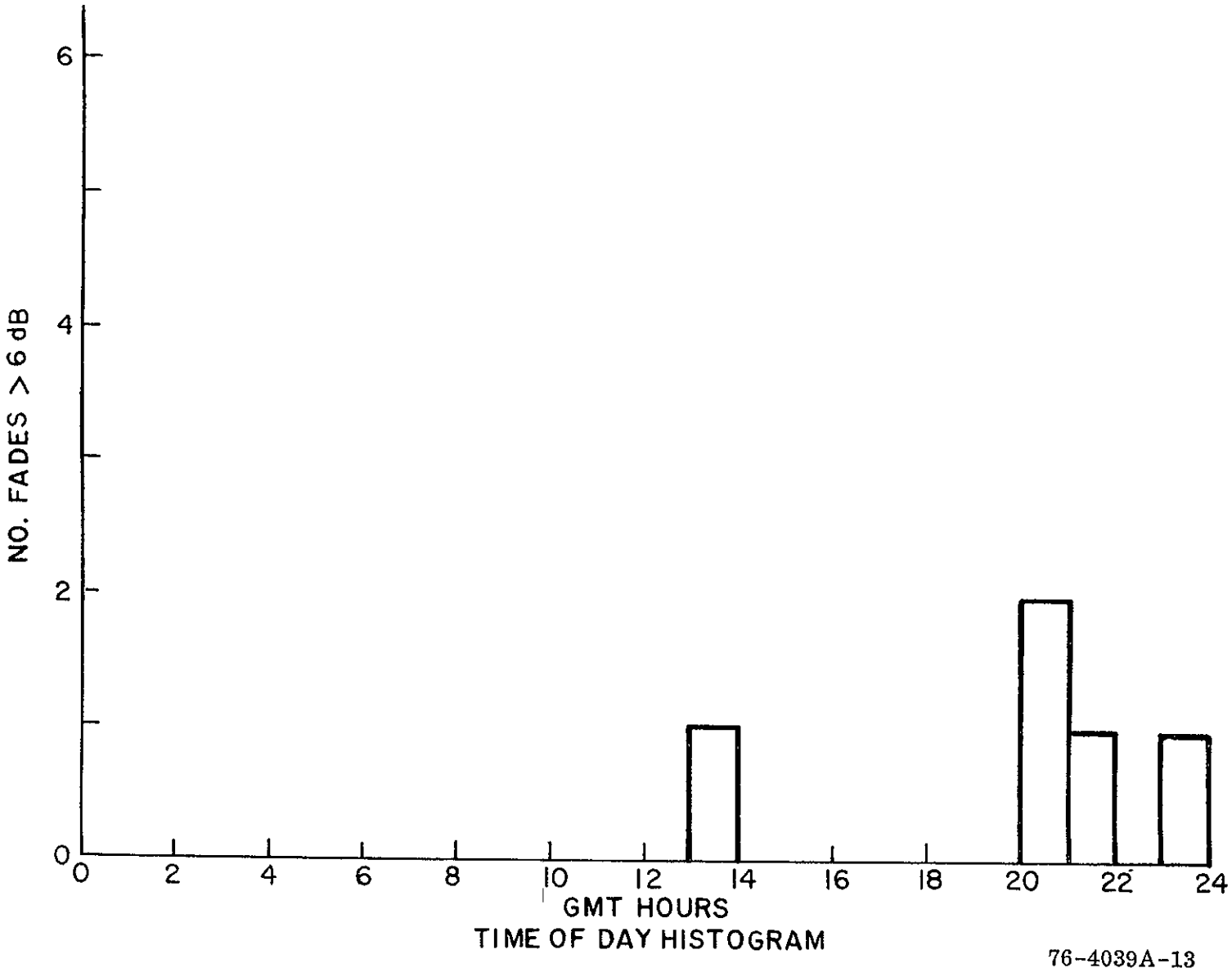

Figure 2-13. NASA Goddard CTS Station, Fades > 6 dB, 11.7 GHz, Total Test Time = 668 Minutes, June, July, August, 1976

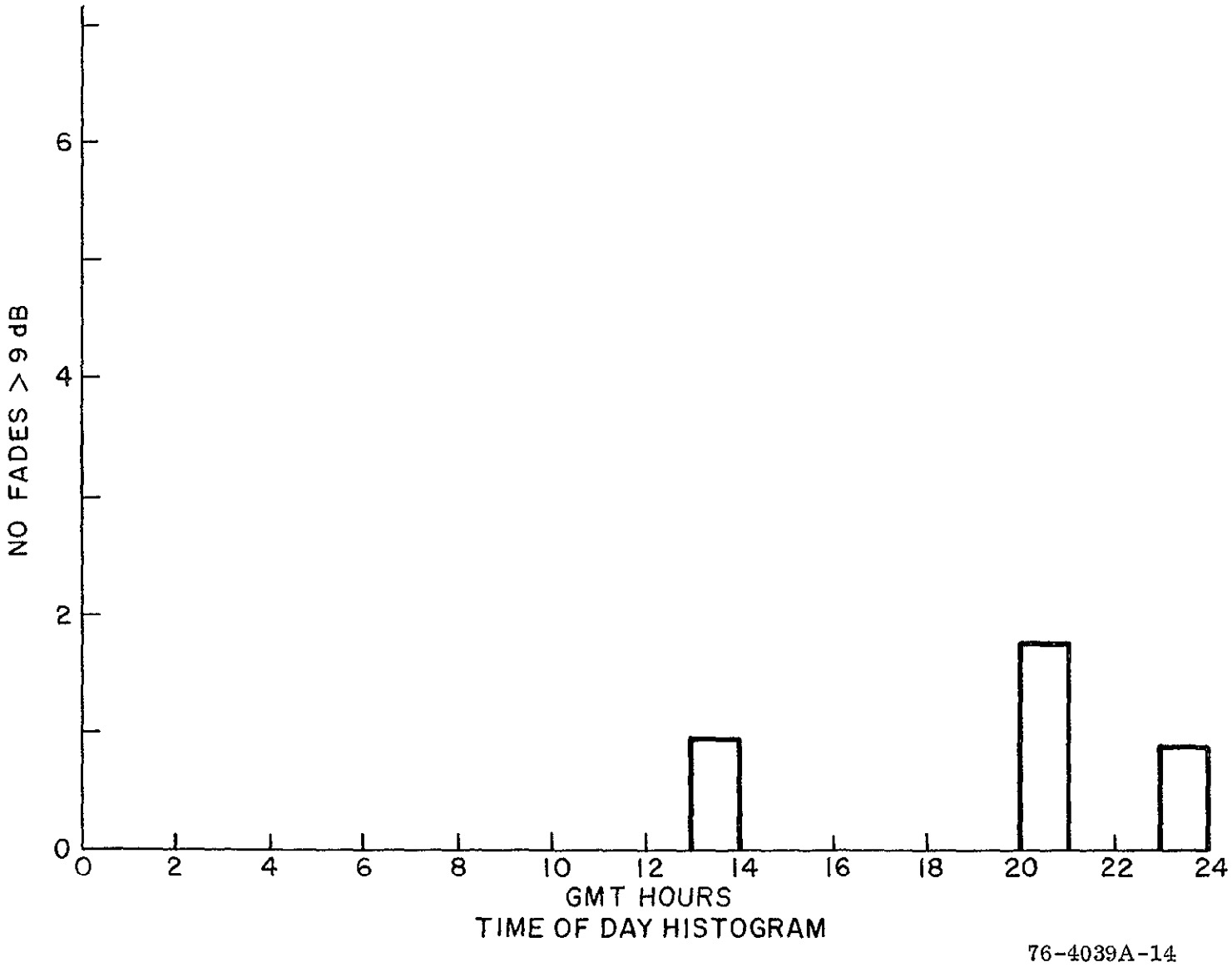

Figure 2-14. NASA Goddard CTS Station, Fades > 9 dB, 11.7 GHz, June, July, August, 1976, Total Test Time = 668 Minutes

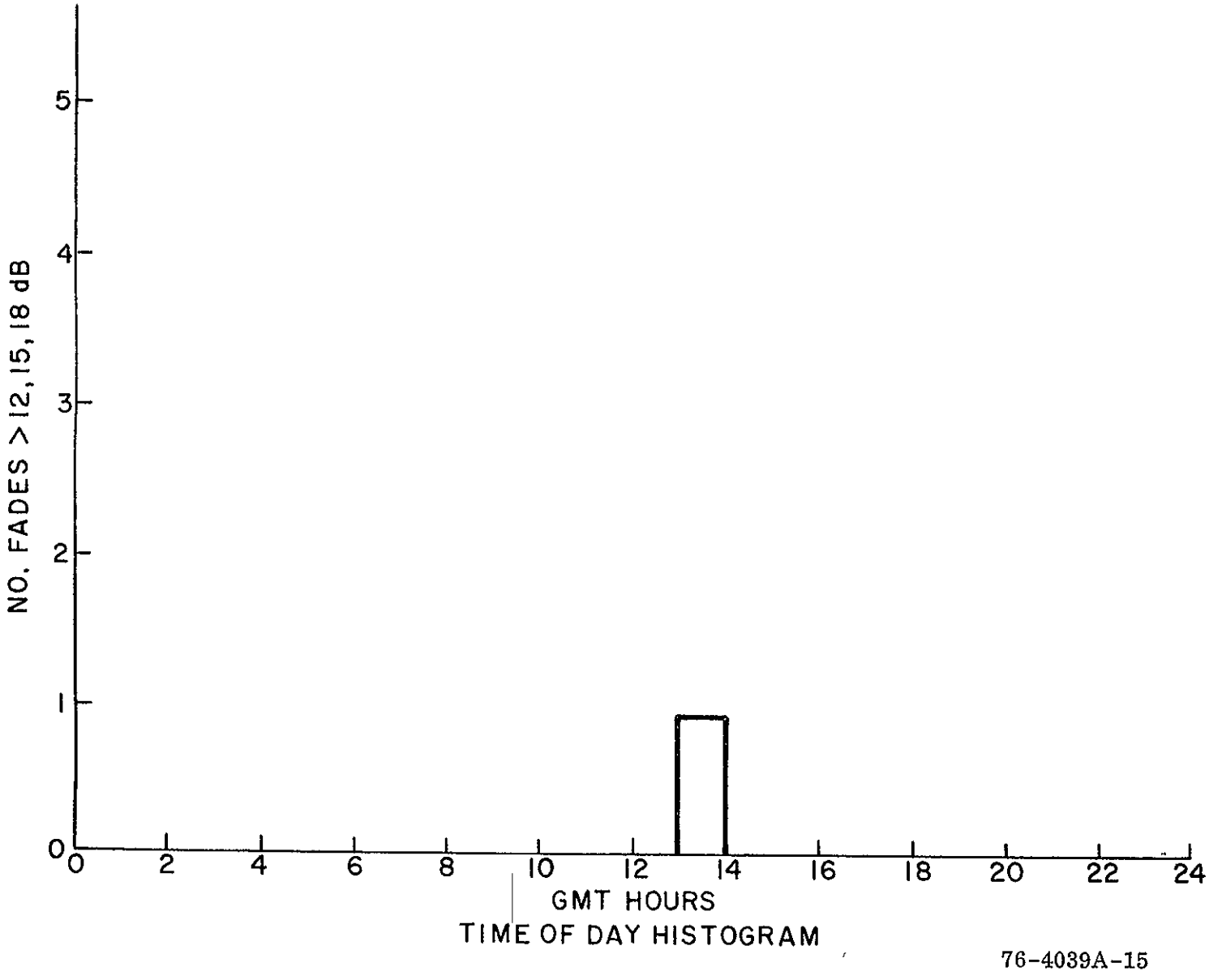

Figure 2-15. NASA Goddard CTS Station, Fades > 12, 15, 18 dB, 11.7 GHz, June, July, August, 1976, Total Test Time = 668 Minutes

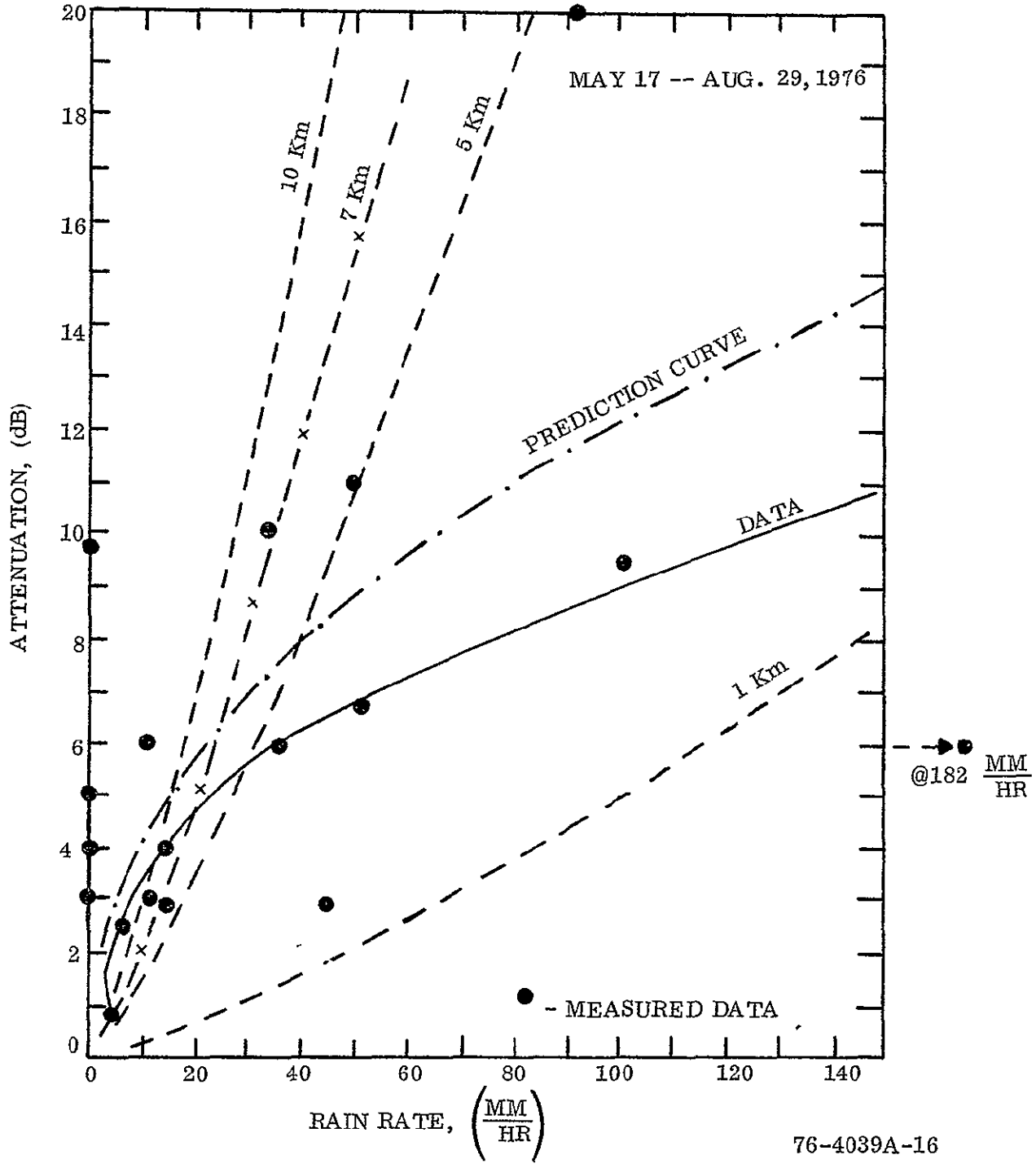

Figure 2-16. CTS 11.7 GHz Beacon, Measurements Summary, Greenbelt, Maryland, Elevation Angle 29.5°

2.4 SIGNAL SCINTILLATION

On numerous occasions marked scintillation activity was in effect. This commonly occurred prior to rainfall. Figure 2-17 shows the most pronounced scintillations recorded so far. This occurred during very dark skies and high winds; some of the signal level fluctuations seen in this figure are due to wind buffeting the antenna. Another example of scintillation activity is seen in figure 2-18. Both these cases occurred during cloudy skies. An example of scintillations occurring without clouds is seen in figure 2-19.

On July 11, 1976 signal level variations shown in figure 2-20 over a 11 minute interval was recorded prior to the occurrence of a thunderstorm. Weather conditions could be described as very windy with heavy dark clouds. In order to keep the received signal within a measurable range an attenuator was inserted or removed at the appropriate times shown on the figure. The signal variation that occurred during these time events were due either to a motion of the receive antenna mount or to atmospheric turbulence.

To differentiate between the two effects an antenna shake test was performed and the resulting time history of the signal variations were analyzed on the Ubiquitous Spectrum Analyzer (USA). No distinct spectral lines were produced from the antenna mount motion as shown in figure 2-21. However, the frequency intervals in which energy was detected were centered at 1 Hz, 2 Hz, 4 Hz, 5 Hz, 6 Hz, 7 Hz, and about 8.5 Hz. The largest amount of energy was measured at 1, 2 and 5 Hz.

Figures 2-22 and 2-23 show the resulting spectrums at the various times shown in figure 2-20. The large amount of energy measured below 3 Hz is mainly due to the antenna mount motion which would completely mask any characteristic frequency due to atmospheric turbulence. It appears that no distinct frequencies are present with the type of weather conditions that characterize a large amount of turbulence for this test run. Figure 2-24 shows the 1.5 Hz spectra for two time periods about 2.5 minutes apart. Over this time period measurable changes in the low frequency spectra are noted. This change could be a measure of the degree of turbulence existing in that time interval.

Figure 2-25 shows the resulting spectra for 3 time values that existed on October 26 in which less atmospheric turbulence was present. The frequencies due to

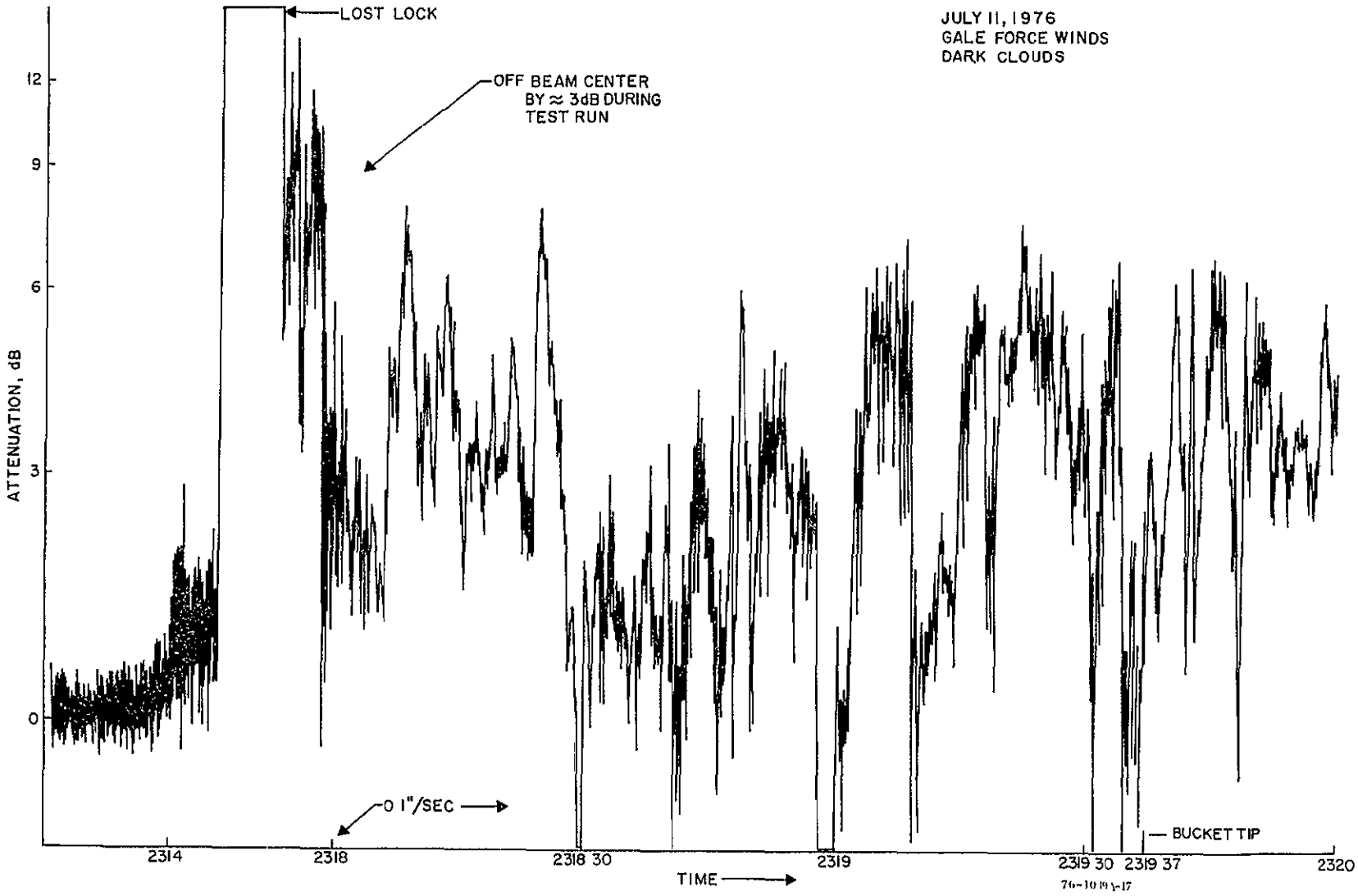

Figure 2-17. Sample of Scintillation

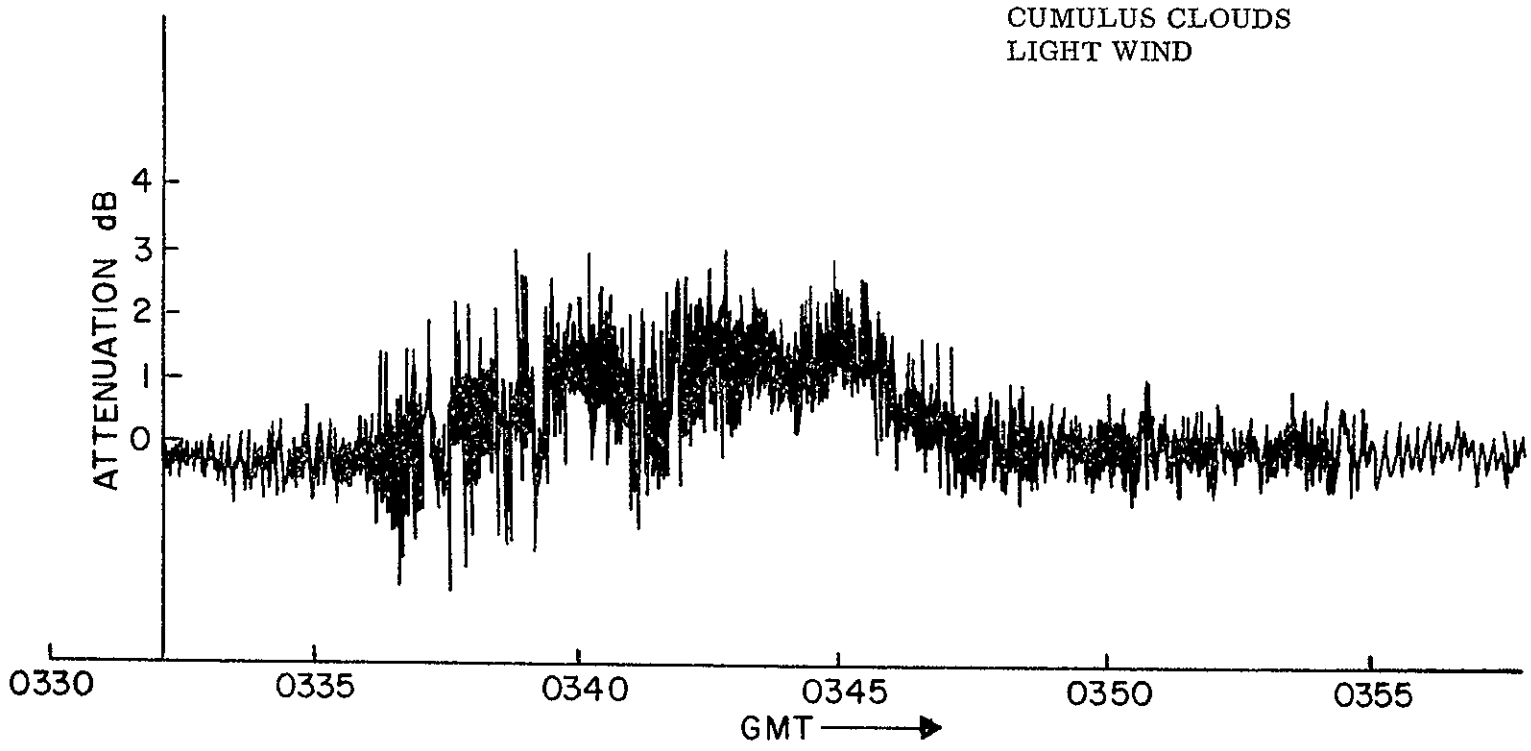

Figure 2-18. Scintillations at 11.7 GHz, Goddard CTS Station, 20 June, 1976

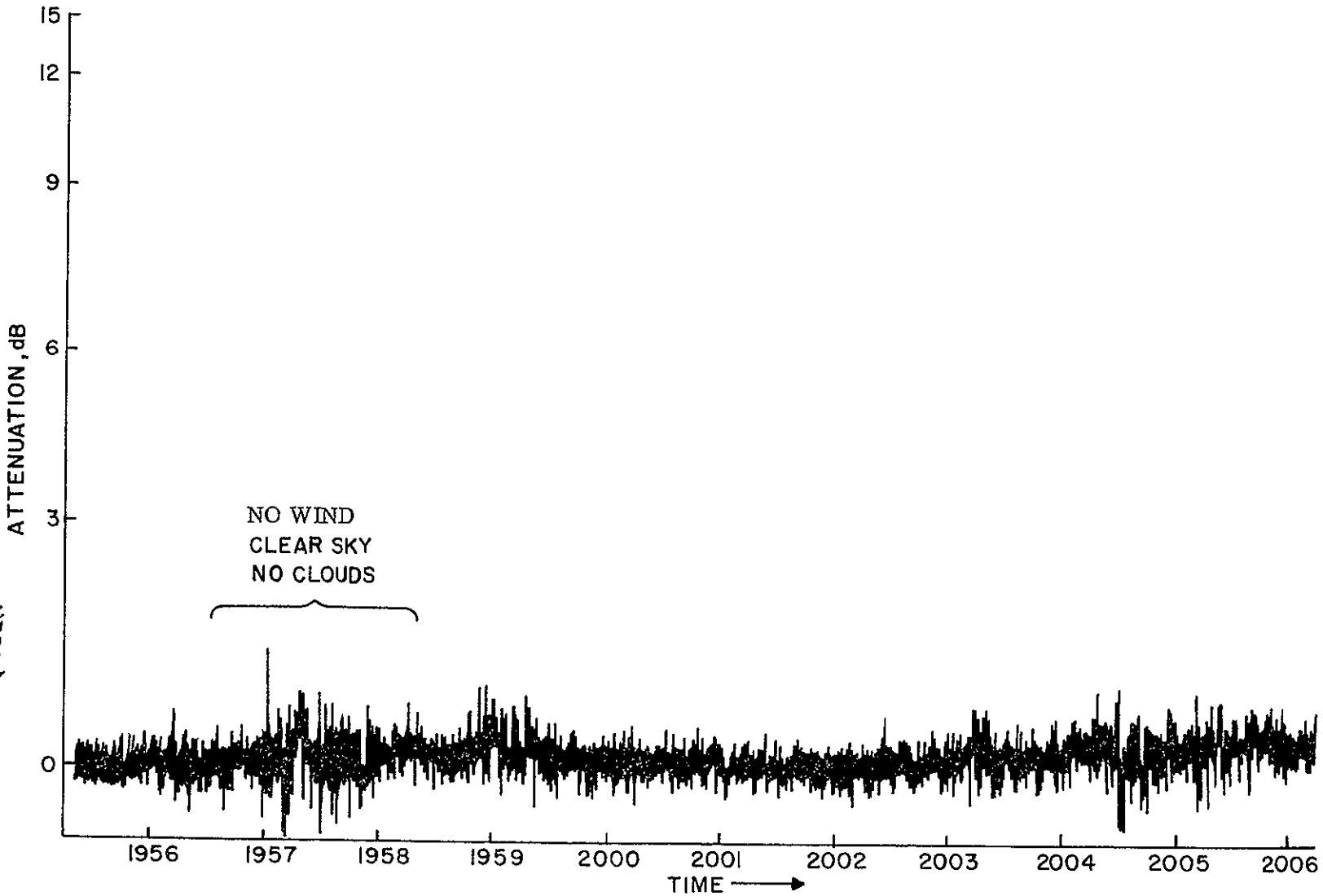

76-4039A-19

Figure 2-19. NASA Goddard CTS Station, Scintillations at 11.7 GHz, 30 June, 1976

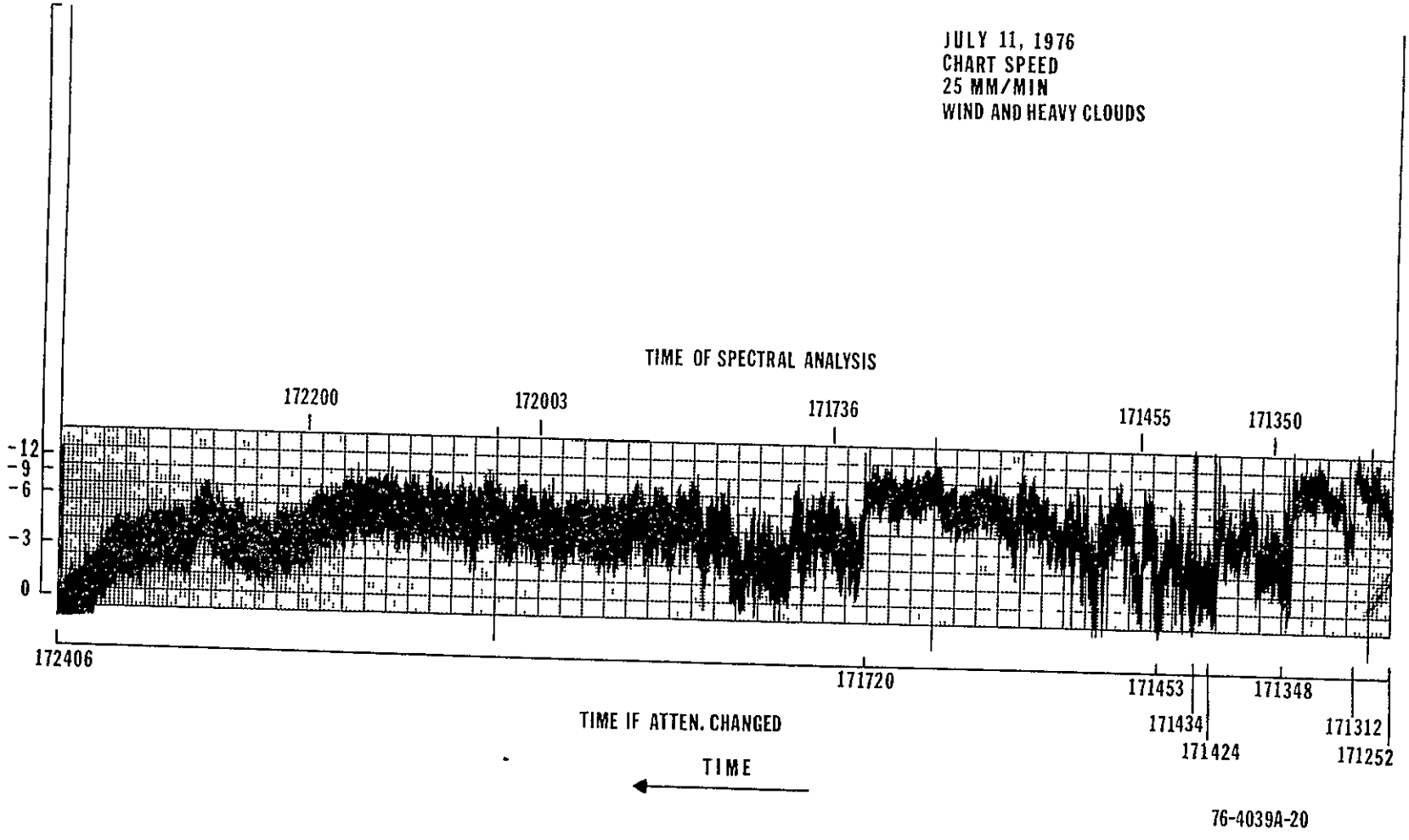

Figure 2-20. Spectrum for Signal Scintillation Test

76-4039A-20

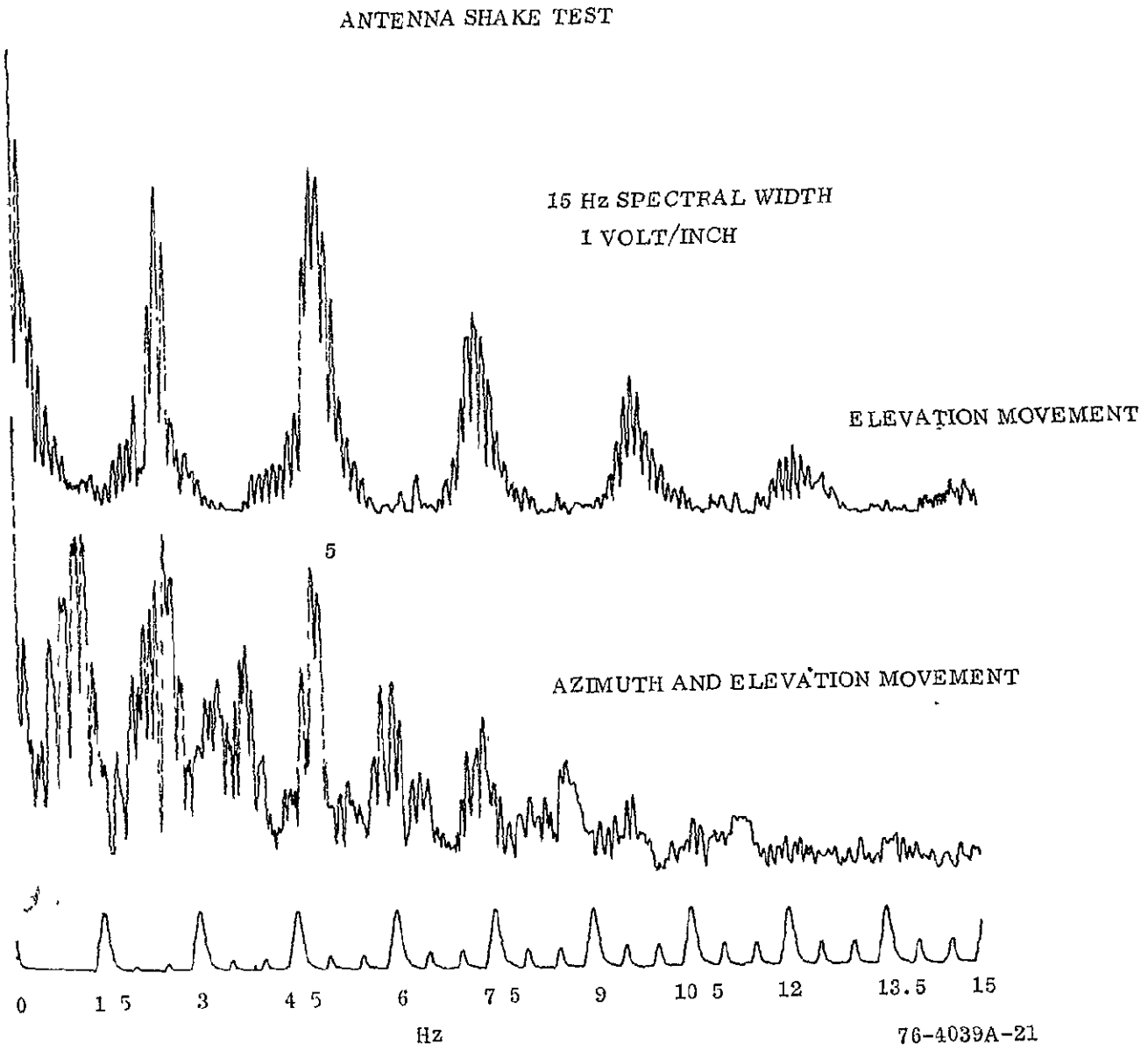

Figure 2-21. Elevation Movement for PTF Receive Antenna

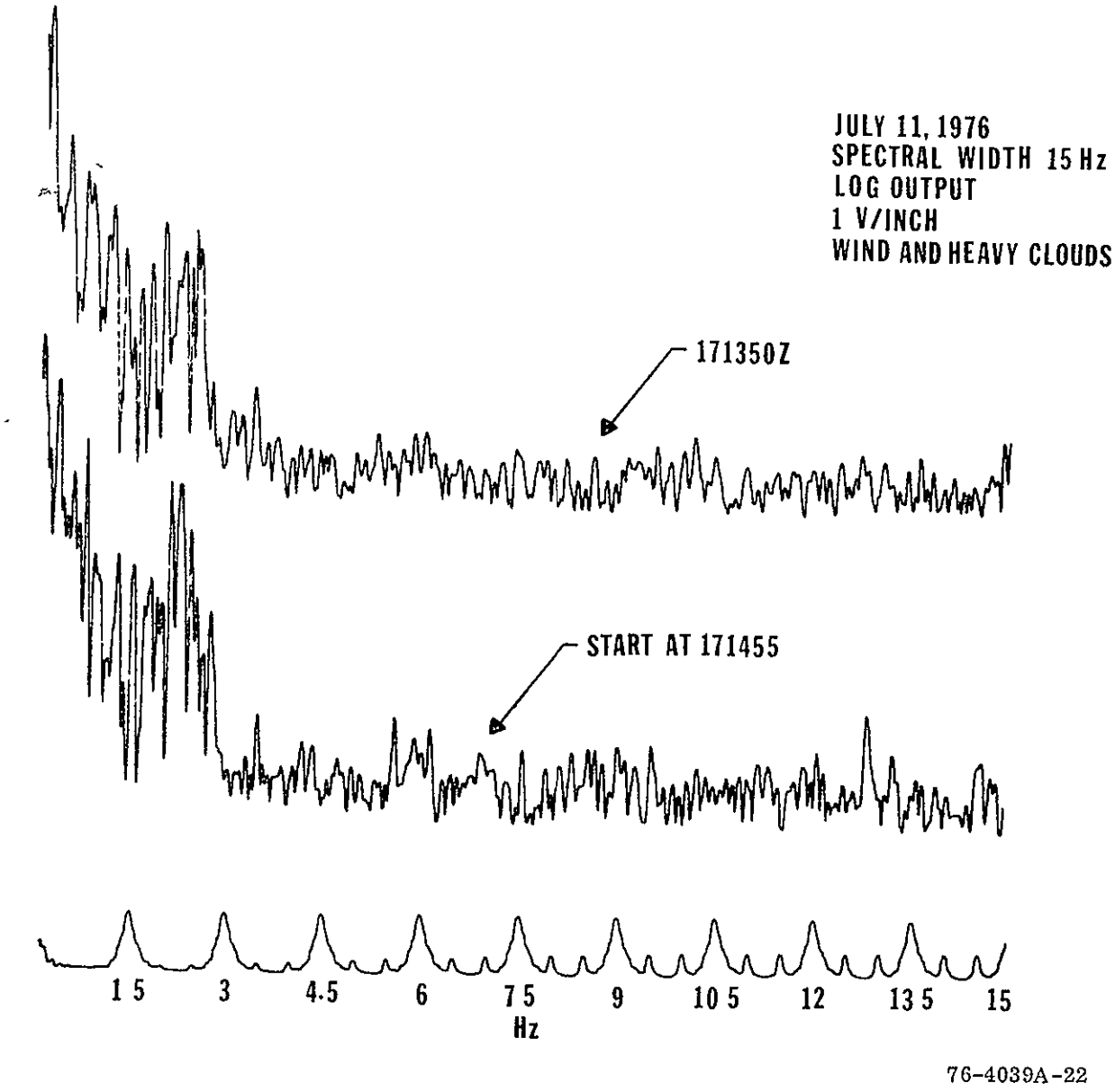

Figure 2-22. Spectrum for Signal Scintillation Test

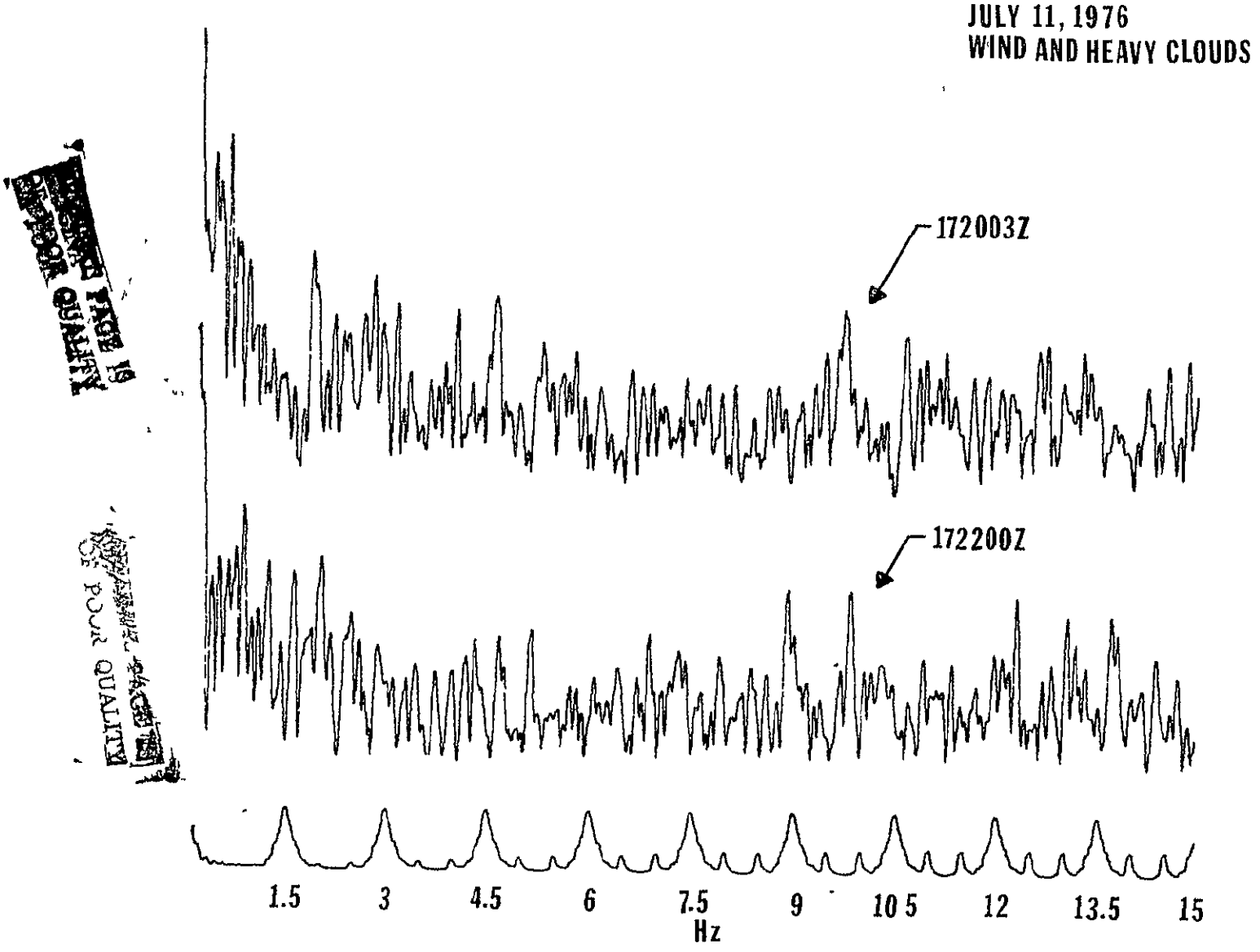

Figure 2-23. Spectrum for Signal Scintillation Test

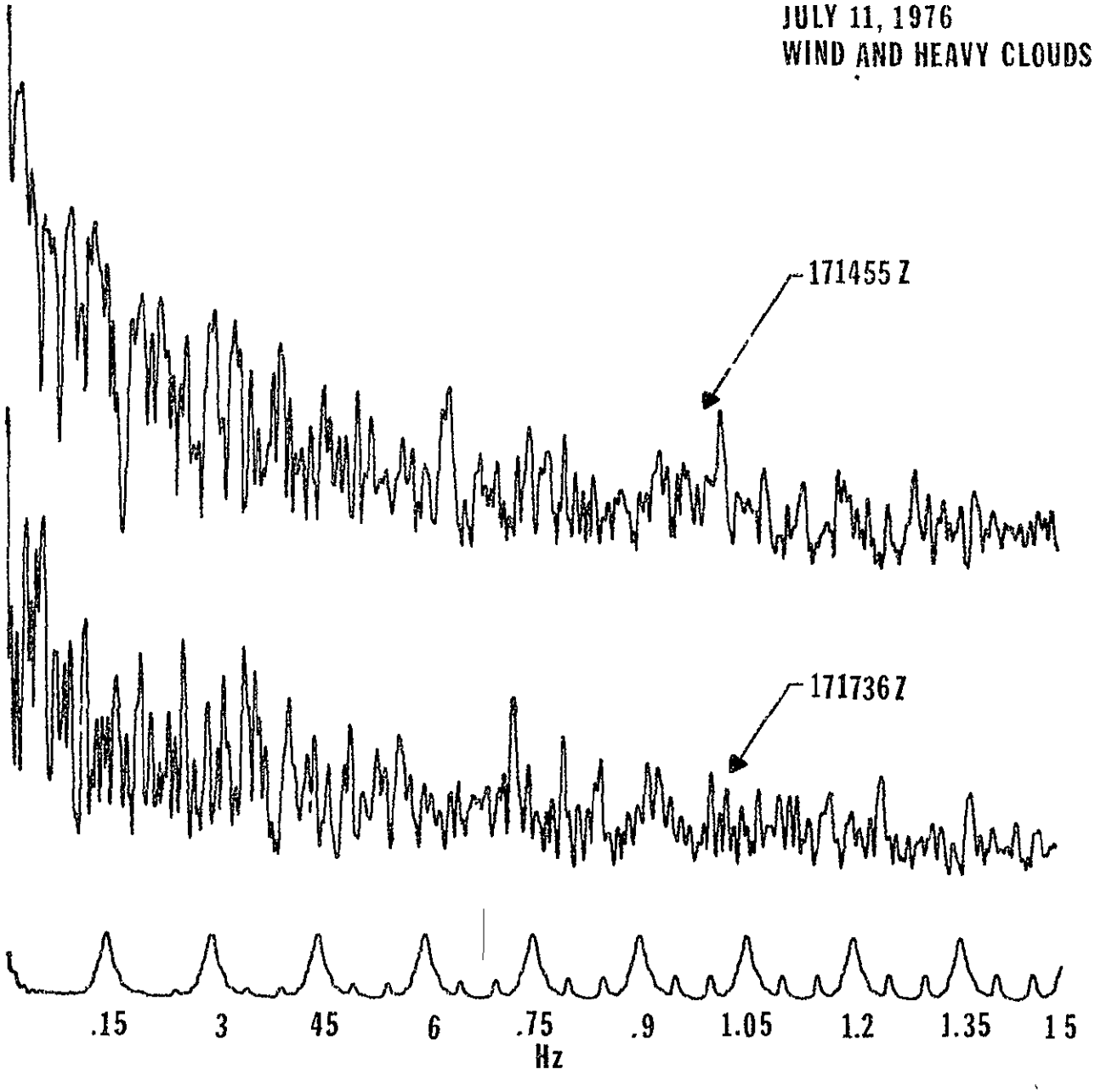

Figure 2-24. Spectrum for Signal Scintillation Test

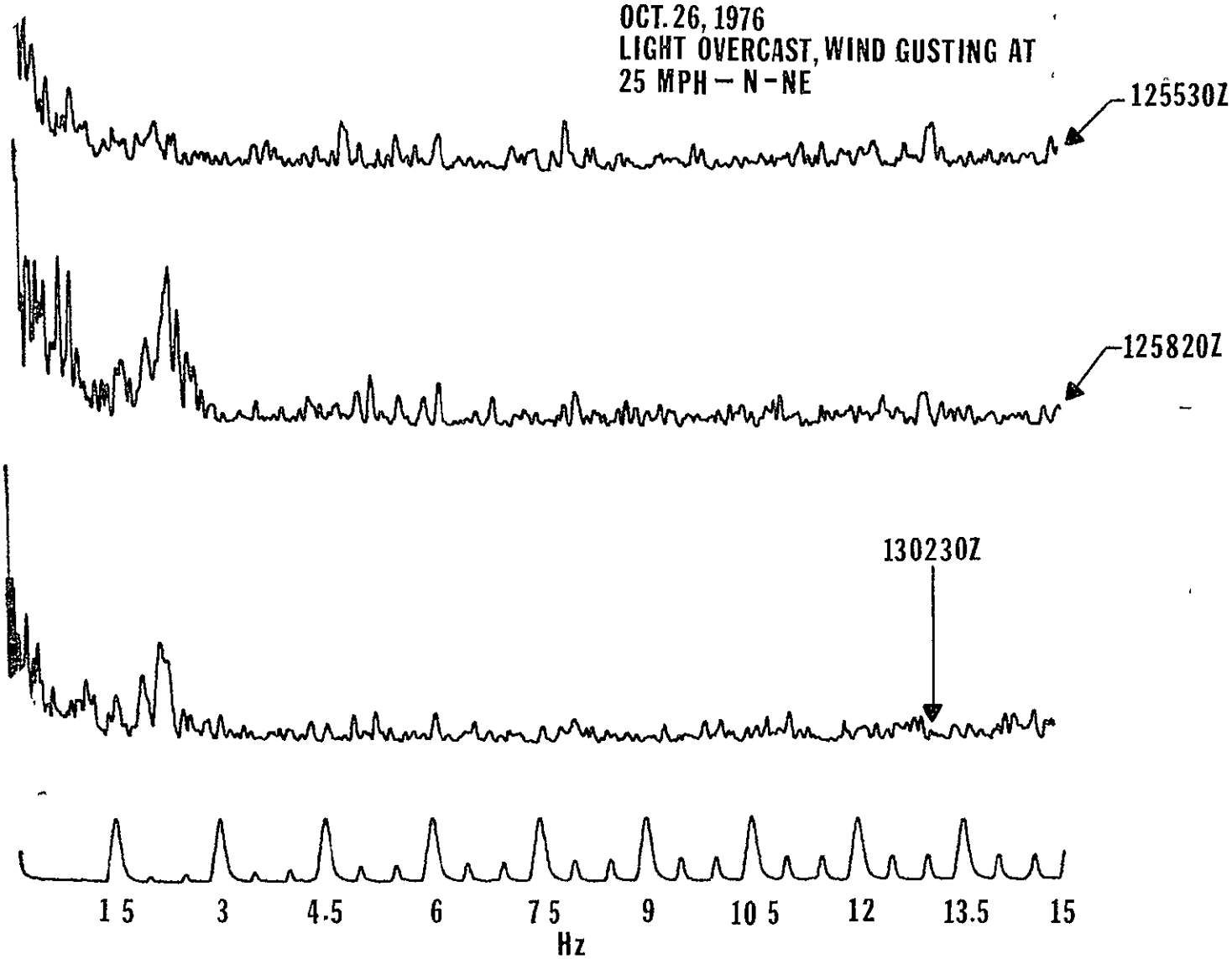

76-4039A-25

Figure 2-25. Spectrum for Signal Scintillation Test

antenna mount motion are clearly shown on the spectrum displays at about 2 Hz. At frequencies above 3 Hz a lower energy content is shown relative to the level measured on the July 11 run. A qualitative measure of the atmospheric turbulence can be obtained by noting the levels of spectra produced during different levels of turbulence.

Scintillation activity was measured during a test run on November 29. The meteorological condition that existed at that time was, little or no wind, heavy dark clouds and a light wet snow falling within the signal path. Various portions of the signal time record is shown in figure 2-26. The corresponding spectral plots are shown in figure 2-27 for two time periods. As shown in figure 2-26 distinct scintillation activity is present on the signal. From figure 2-27 it is shown that this activity has a distinct frequency component at about 9 Hz. Perhaps the meteorological conditions within the elevated beam were of such an intensity that its effect on the signal is measurable by the Ubiquitous Spectrum Analyzer. In most cases it appears that a meteorological effect on the signal is present; however, the measurement apparatus isn't sensitive enough to clearly measure its effect.

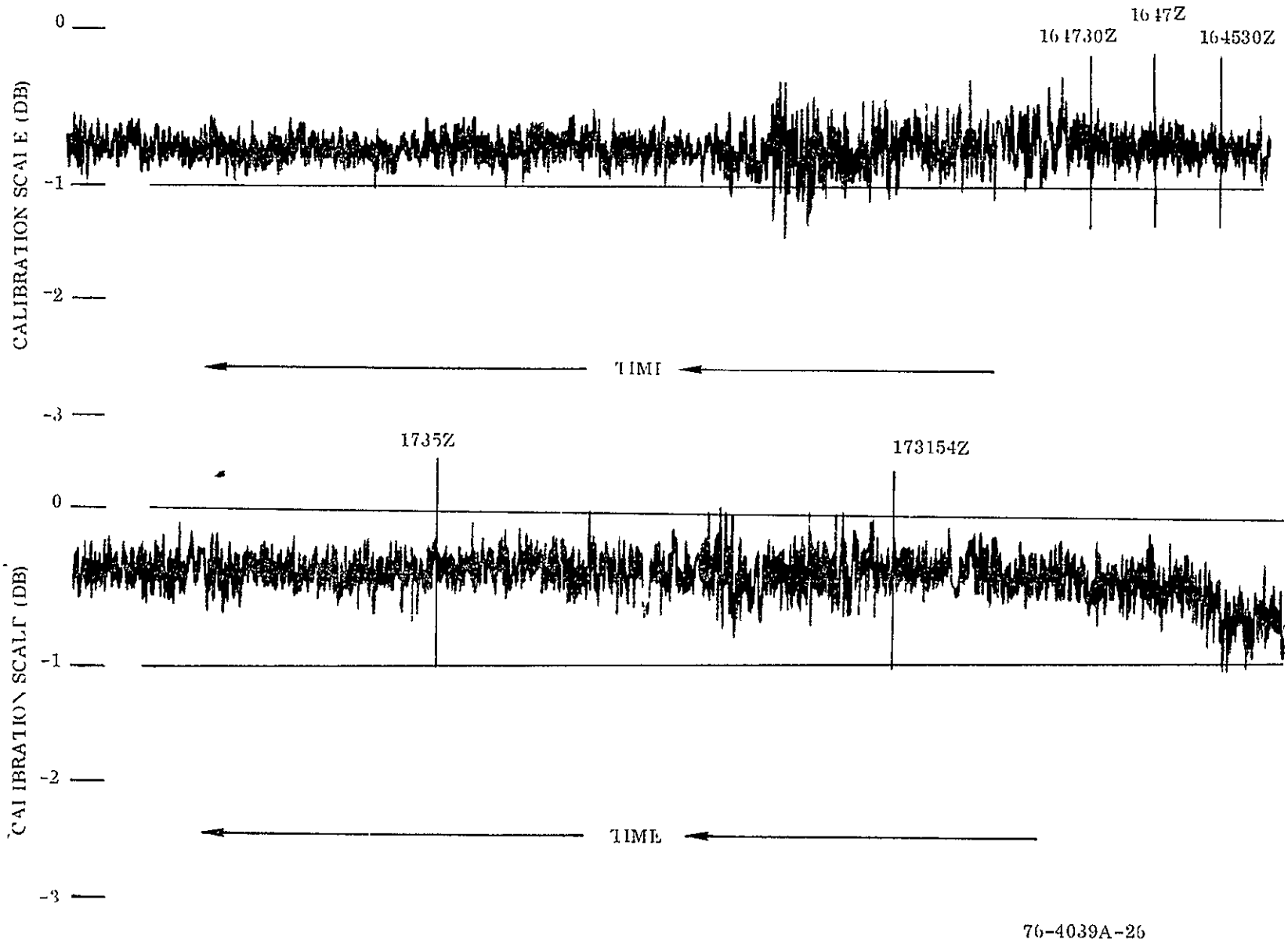

Figure 2-26. Signal Level Record on November 29

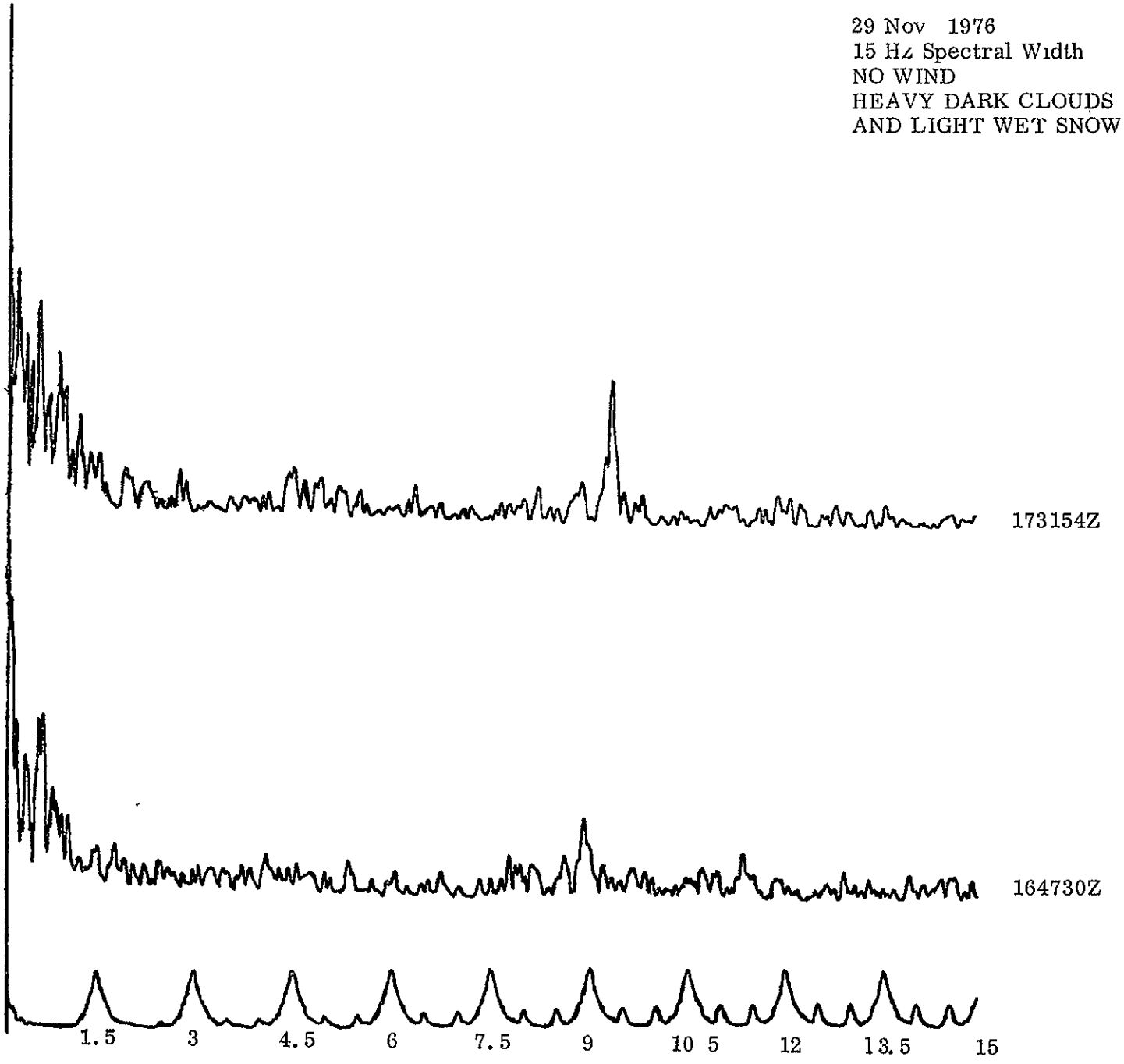

76-4039A-27

Figure 2-27. Scintillation Spectrum for Pronounced Meteorological Condition

SECTION 3
ROSMAN CTS STATION

3.1 STATION DESCRIPTION

The CTS/CLCE system is located within the ATS Facility at the NASA/Rosman STDN Station near Rosman, North Carolina. At present, the system is capable of three modes of operation Propagation data recording, communication testing, and Electro-Magnetic Interference (EMI) measurements. As shown in figure 3-1, the RF signal is received via a 15 foot antenna and amplified by a low-noise amplifier; the amplified spectrum is down-converted to 1.8 GHz-2.4 GHz and applied to the input of a power divider. One of the power divider outputs is applied to the input of the beacon phase-lock loop (PLL); the other output is applied to a second power divider after mixing to and IF of 135 MHz-800 MHz. The second IF is applied to the input of the Upper and Lower PLL Chassis and also to the input of the communications band mixer. The propagation tones are separated and applied to their respective PLL's; the communication carriers are mixed to an IF centered at 70 MHz.

In the propagation mode, the detected tone levels are applied to an A/D converter via a distribution amplifier. The A/D converter also receives meteorological data (wind speed and direction and ambient and dew cell temperatures) and various receiver parameters. The computer receives the A/D converter output as well as radar data, rain bucket data, time-of-year, and system status indicators. The data is formatted by the computer and recorded on magnetic tape. Calibration of the system is accomplished by injecting tones into the system prior to the low-noise amplifier. The level of the calibration signals is established from clear weather measurements on the spacecraft. The expected received levels and signal fade margins are shown in the link calculations in table 3-1. The fade margins are computed on the basis of a closed loop noise bandwidth of 100 Hz for the PLL and a required C/N of 5 dB in this bandwidth to maintain lock. The low noise front end amplifier has a NF of 4.1 dB and additional sky noise and noise generated in the line loss is equal to 290°K. The tone margins greatly exceeds the beacon margin mainly because of the differences in the spacecraft EIRP.

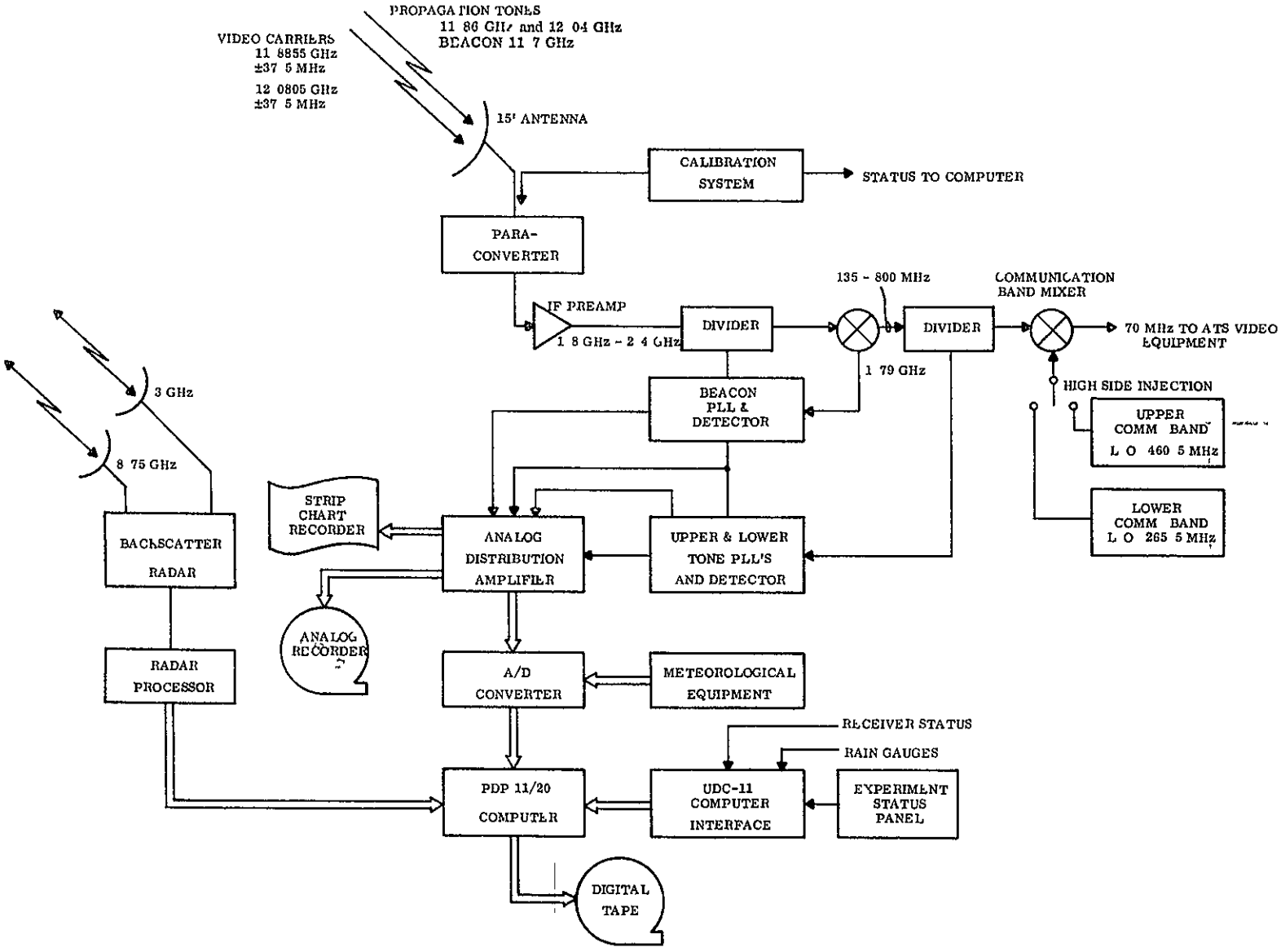

76-4039A-28

Figure 3-1. Receiver and Recording System Functional Diagram

In the communication mode, the band to be tested or monitored is selected by switching the Local Oscillator for the communications band mixer. The 70 MHz IF is interfaced with the ATS video equipment for demodulation.

TABLE 3-1

LINK CALCULATIONS

	BEACON 11.70 GHz	UPPER TONE 12.04 GHz	LOWER TONE 11 86 GHz
EIRP (dBm)	41.5	88.3	78.3
Path Loss	-204.9	-205.2	-205.1
Polarization Loss	-3.0	-.2	-.2
Clear Sky Attn	-.3	-.3	-.3
Receive Ant Gain	52.4	52.4	52.4
Received Sig Strg. (dBm)	-114.3	-65.0	-74.9
Sig Proc. Input (dBm)	-94.3	-45.0	-54.9
Noise (dBm) (100 Hz BW) (4.1 dB N. F.)	-149.9	-149.9	-149.9
C/N in 100 Hz PLL BW (dB)	35.6	84.9	75
Theoretical Fade Margin (dB)	30.6	79.9	70

3.2 TV EXPERIMENT

At the Rosman station preliminary TV tests were performed utilizing the Goddard station as the transmit facility and the Rosman station as the receive facility. The transmitter employed in the tests emitted a power of 67.6 watts. The Martin receiver was employed at Rosman and interfaced at 70 MHz with the standard video processing unit that consists of an IF amplifier, discriminator and video unit. The following tests were performed

a. Overall link C/N tests
b. Audio S/N tests
c. Color vector analysis tests utilizing a vector scope
d. Waveform tests utilizing the waveform monitor.

A ground transmit power of 67.6 watts produced a satellite transmit power of 168 watts, which resulted in a measured overall link C/N_o of 90 dB-Hz. The standard 30 MHz IF filter was employed which has a noise bandwidth of approximately 36 MHz. For this unit a predetection C/N of 14.4 dB was obtained. This value is approaching the threshold of the FM demodulator; hence, any waveform displays were noisy and difficult to interpret.

The audio S/N measurement was made by employing a 1 kHz tone modulation on a 4.5 MHz subcarrier. Without a video signal the audio S/N value was measured to be 38.6 dB. With a video signal in the form of color bars the S/N decreased to 36.2 dB. A distinct video-to-audio crosstalk was noted during this test and the tests utilizing the vector scope display.

Preliminary waveform tests consisting of a video transient response, differential gain and phase and a frequency response tests were performed. In addition, a color vector amplitude and distortion test utilizing a vector scope was also performed. Because of the preliminary nature of the tests no quantitative results were obtained. The overall system gain was below the desired amount and an intermediate transmitter was employed at Goddard for the initial purpose of obtaining some qualitative measure of the system's ability to handle color video signals.

3.3 PROPAGATION MEASUREMENTS

The rain rate and propagation data that has been processed to date for the June to October period is listed in Table 3-2. From day 258 only meteorological test data consisting of rain rate and radar returns was available. The maximum recorded attenuation (δ) value was 12.5 dB which occurred on day 208. A minutely mean time plot of the 11.7 GHz attenuation for days 208 and 209 is shown in figure 3-2. On the plot the minutely mean δ values are jointed together by a straight line in order to show the trend of the δ values as a function of time. For each δ value the corresponding standard deviation (σ) which is computed using the secondly values in each minute is also plotted directly above the δ values. The magnitude of the σ value is a measure of the precision of the δ measurement. The magnitude of the σ value varies inversely with the precision. As expected, the highest σ value occurs at the deepest fade because the relative level of the noise increases; therefore, the deep fade measurements are the most imprecise.

Point rain rate and ground average rain rate are employed as a measure of the precipitation within the elevated beam. The data from the former is taken from the rain bucket nearest to the CTS antenna; hence, it is defined as the near bucket. The ground average is computed from the ten rain buckets located under the beam. For the time period June 10 to October 7 a total of 878 minutes of rain data was computed for the ground average (GA) value. For the near bucket (NB) a total of 691 minutes were computed. Both rain rate parameters are computed on the basis of 4 second means. The disadvantage of employing a point rain rate is evident since the NB did not measure any precipitation when, in fact, it did exist for 187 minutes. The statistics for both rain rate measures are shown in figure 3-3. The smoothing effect of taking an average and destroying the information at peak rain rates is evident from the curves. As a result curve divergence should increase as the rain rate increases. The rapid decrease of the NB curve at the high rain rate shows that the NB did not record the intense rain rate that was recorded by one of the other nine buckets. Since the extent of the intense storm cells are on the order of 100 to 300 meters this result is not surprising. For the 691 minute test period the GA values exceeded 80 MM/HR for 0.1% of the time and the NB values exceeded 91 MM/HR for the same percentage.

TABLE 3-2

BEACON DATA PROCESSING RECORD

TAPE NO.	DAY/TIME	W.C.	PEAK RR	ATTEN	RADARS	LEVEL ONE PROGRAM	LEVEL TWO PROGRAM
001	162:1800-1833	7	57	3	-	X	
002	163·1850-1930	7	182	8	-	X	X
003	191:1719-1730	7	152	2	-	X	
003	191·1839-1900	7	18	2	-	X	
003	208:2252-0001	5	114	12.5	-	X	X
003	209·0012-0330	5	45	6	-	X	X
004	212:1832-1850	7	26	2	-	X	
004	226 1800-1930	5	48	2	-	X	
005	239:1350-1624	5	42	2	8	X	
008	258.1830-2000	5	4	-	3, 8	X	
009	273:1330-	5	21	-	8	X	
010	281·1202-1950	5	101	-	8	X	

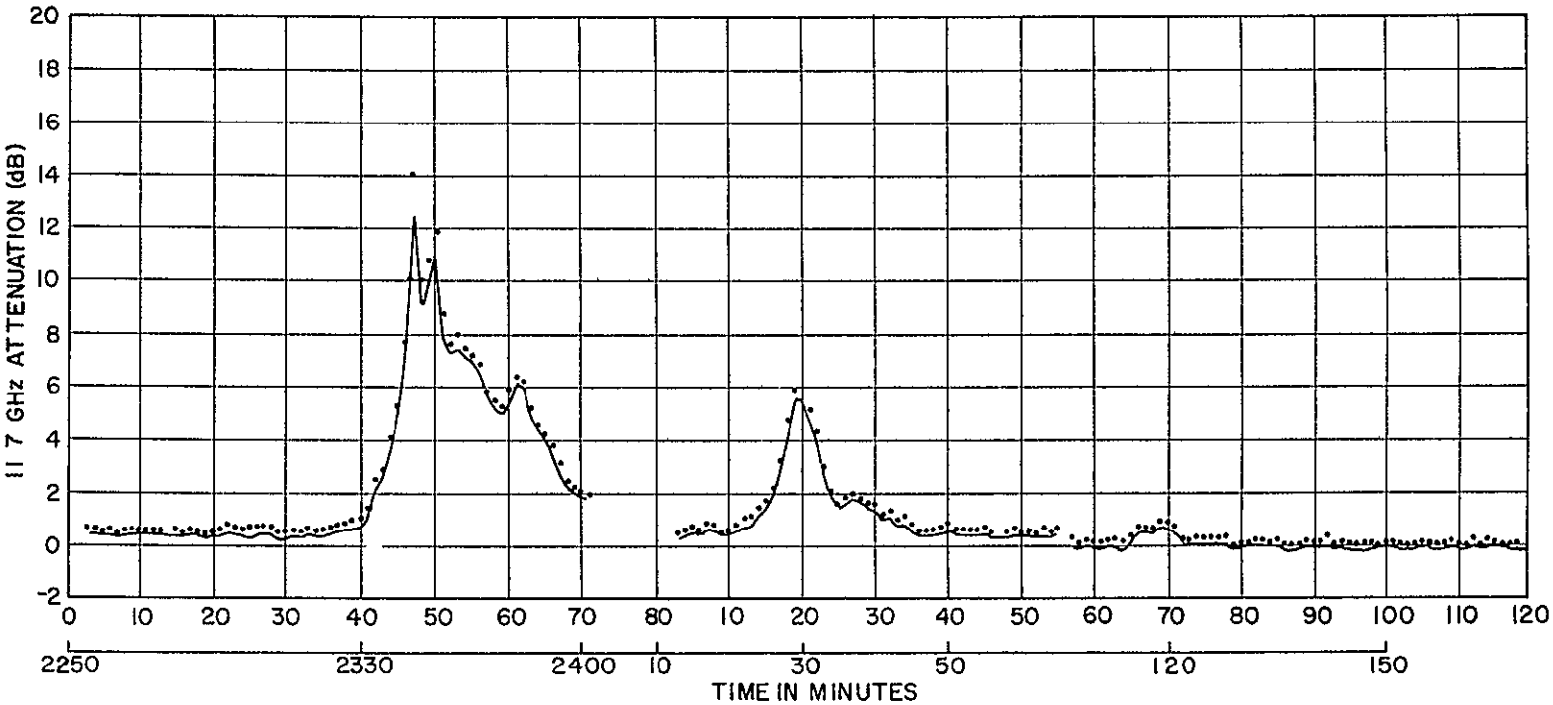

Figure 3-2. Minutely Mean Time Plot of 11.7 GHz Attenuation (dB)

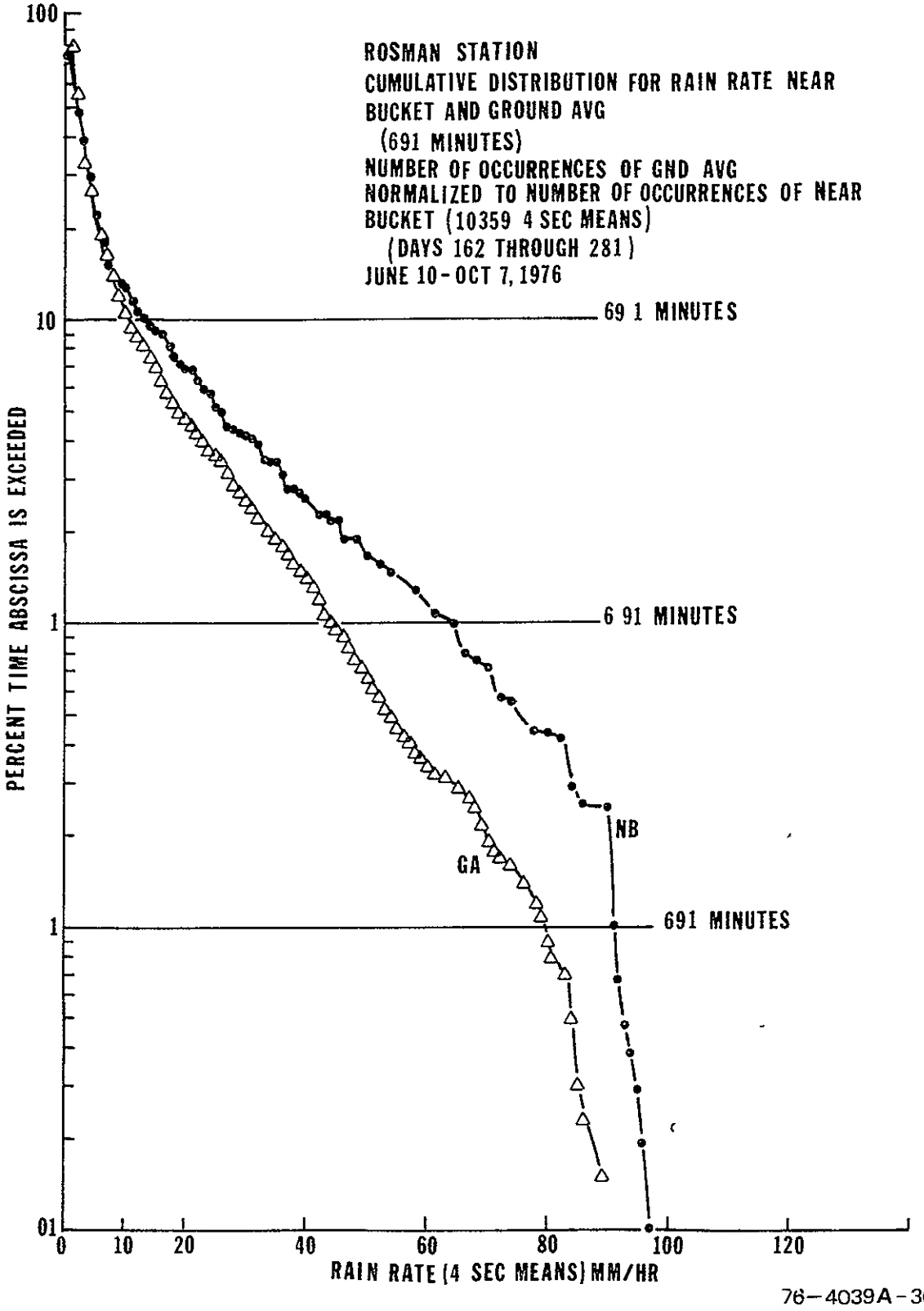

Figure 3-3. Cumulative Distribution For Rain Rate Near Bucket and Ground Average

Figure 3-4 shows the attenuation statistics and the corresponding NB statistics for the June to August test period. Since these plots only pertain to 342 minute time interval, errors in obtaining representative rain rate and attenuation pairs at constant percentage value will result. This is due to the fact that the NB statistics are only representative of the rain environment for only long term statistics. This can be concluded when comparing the NB and GA statistics over a relatively short test time of 691 minutes. For the 0.1% percentage value the NB corresponds to 84 MM/HR and the attenuation to 12 dB.

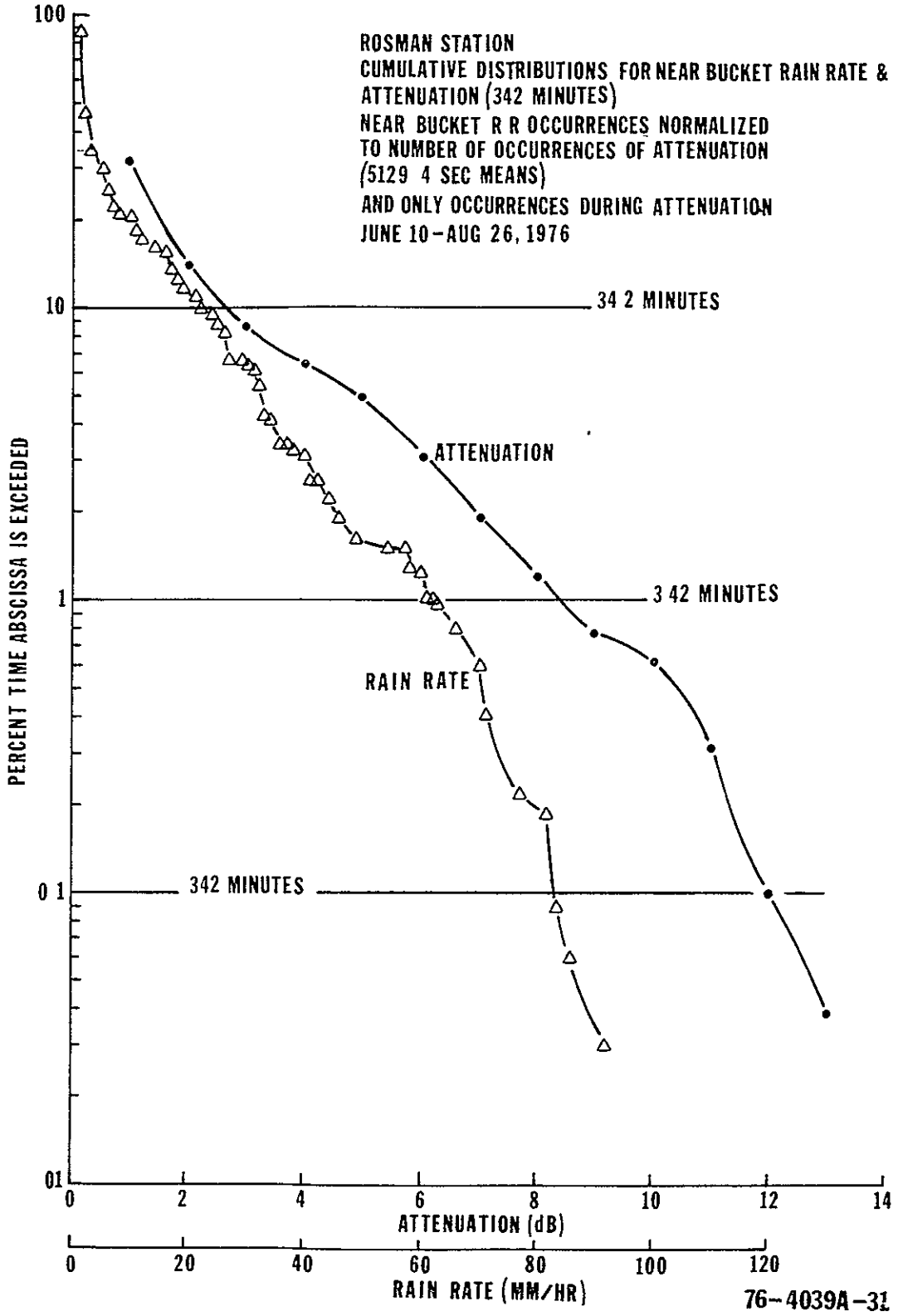

Figure 3-4. Cumulative Distribution For Near Bucket Rain Rate and Attenuation

3.4 METEOROLOGICAL PARAMETERS

During a test run the meteorological parameters that are measured are rain rate and radar return. These parameters can be employed as a measure of the type and extent of the precipitation causing the attenuation. Because the radar return can be resolved within 100 meter range bins and is a direct measure of the precipitation existing within the elevated beam, it follows that it is a more sensitive indicator of the beam precipitation than the ground measured rain rate. This is easily seen in the 4 secondly mean scatter plots for test days 258 and 281 shown in figures 3-5 and 3-6. The integrated reflectivity (η) is plotted against the near bucket rain rate. For day 258, average rain rate values of 2 to 3 MM/HR were recorded. Precipitation in the beam that caused these values resulted in a reflectivity spread of almost 1 to 10. For day 281 rain rates up to 30 MM/HR were measured. In this case the spread in the integrated reflectivity tends to decrease as the rain rate increases. In interpreting these integrated η versus rain rate (R) plots it is necessary to understand the method that is employed for computing R. This involves determining the time between bucket tips. For example, in the case of an R of 2 MM/HR the time between tips would be 7.62 minutes. Therefore, for this period of time all 4 second mean values of the integrated η factor are plotted against the 2 MM/HR value of R. While the average rain rate was measured at 2 MM/HR the instantaneous value (4 second means) can vary over a relatively wide range.

Figures 3-7 and 3-8 show the plots of η versus the ground average rain rate. This is the average of the ten rain buckets placed under the elevated beam. As expected, a better trend is exhibited in these plots due to the smoothing characteristics of the averaging process. Part of the reflectivity spread is due to the natural randomness that exists in the magnitude of the received backscatter power when averaged only over 4 seconds. As expected the ground average rain rate gives a better indication of the amount of precipitation within the beam relative to the near bucket measurement. This is generally true for the low and medium values of rain rate. However, this should not generally hold for high values of rain rate because they exist over a very limited region. The averaging process could destroy the high rain rate information by combining it with low values.

For second scatter plots of the integrated reflectivity versus the 11.7 GHz attenuation for days 239 and 212 are shown in figure 3-9 and 3-10 respectively. As

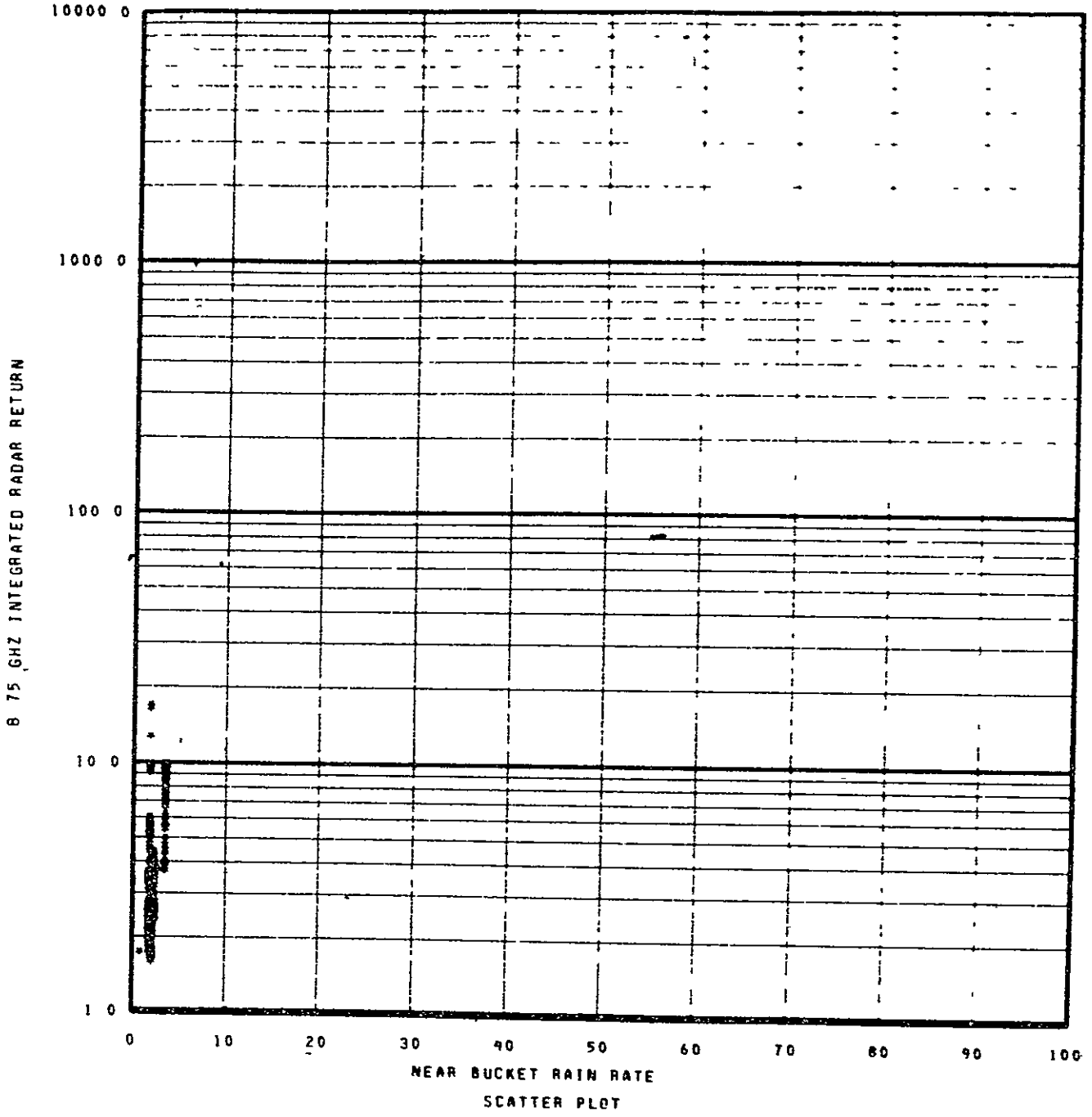

START TIME STOP TIME

OUTER INTERVAL

YEAR	= 1976	YEAR	= 1976
DAY	= 258	DAY	= 258
GMT	= 1830	GMT	= 2000

INNER INTERVAL

DAY	= 258	DAY	= 258
GMT	= 1840	GMT	= 1909

76-4039A-32

Figure 3-5. Integrated Reflectivity η vs Near Bucket Rain Rate

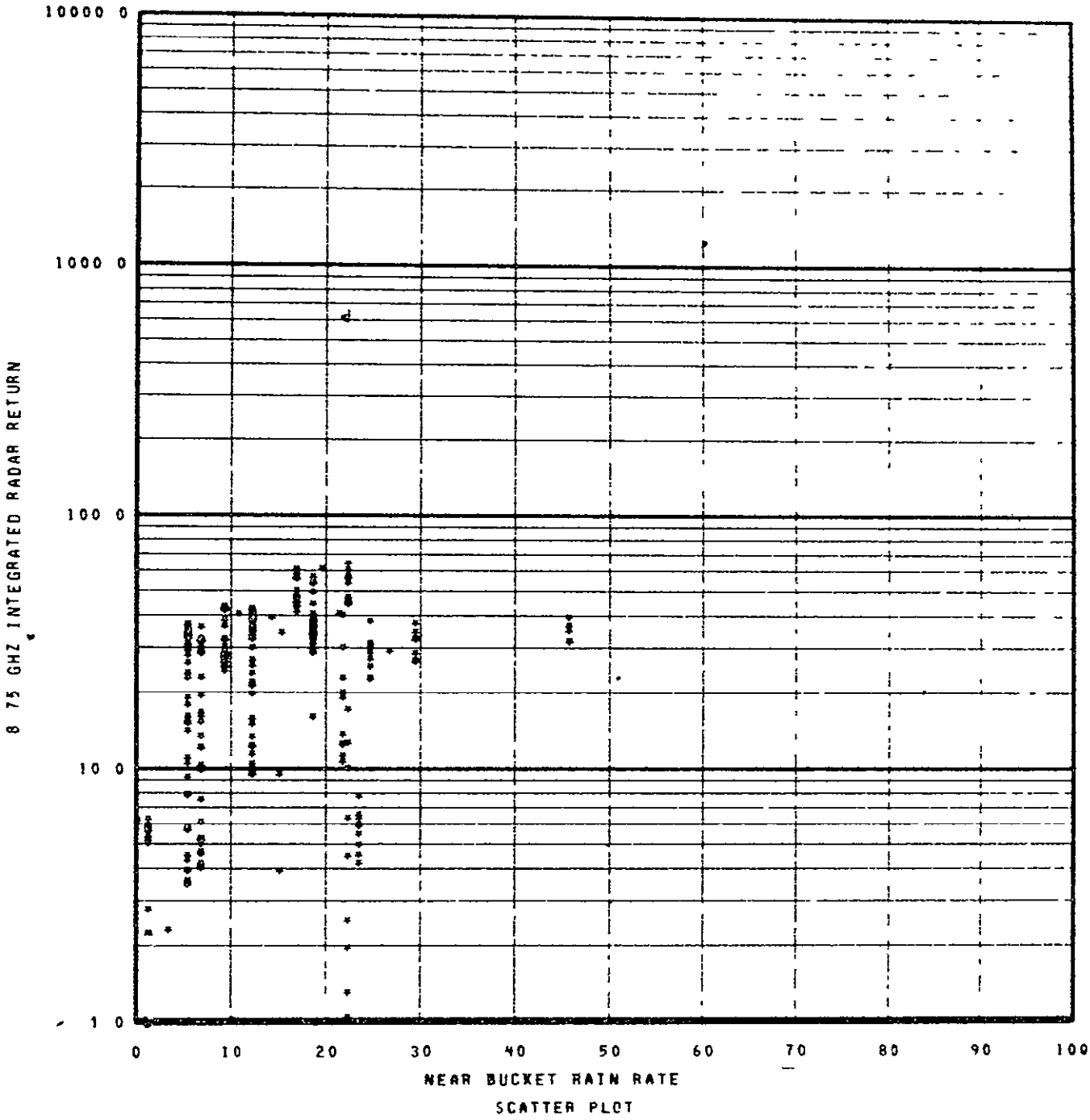

START TIME STOP TIME

OUTER INTERVAL

YEAR	= 1976	YEAR	= 1976
DAY	= 281	DAY	= 281
GMT	= 1600	GMT	= 1759

INNER INTERVAL

DAY	= 281	DAY	= 281
GMT	= 1630	GMT	= 1659

76-4039A-33

Figure 3-6. Integrated Reflectivity η vs Near Bucket Rain Rate

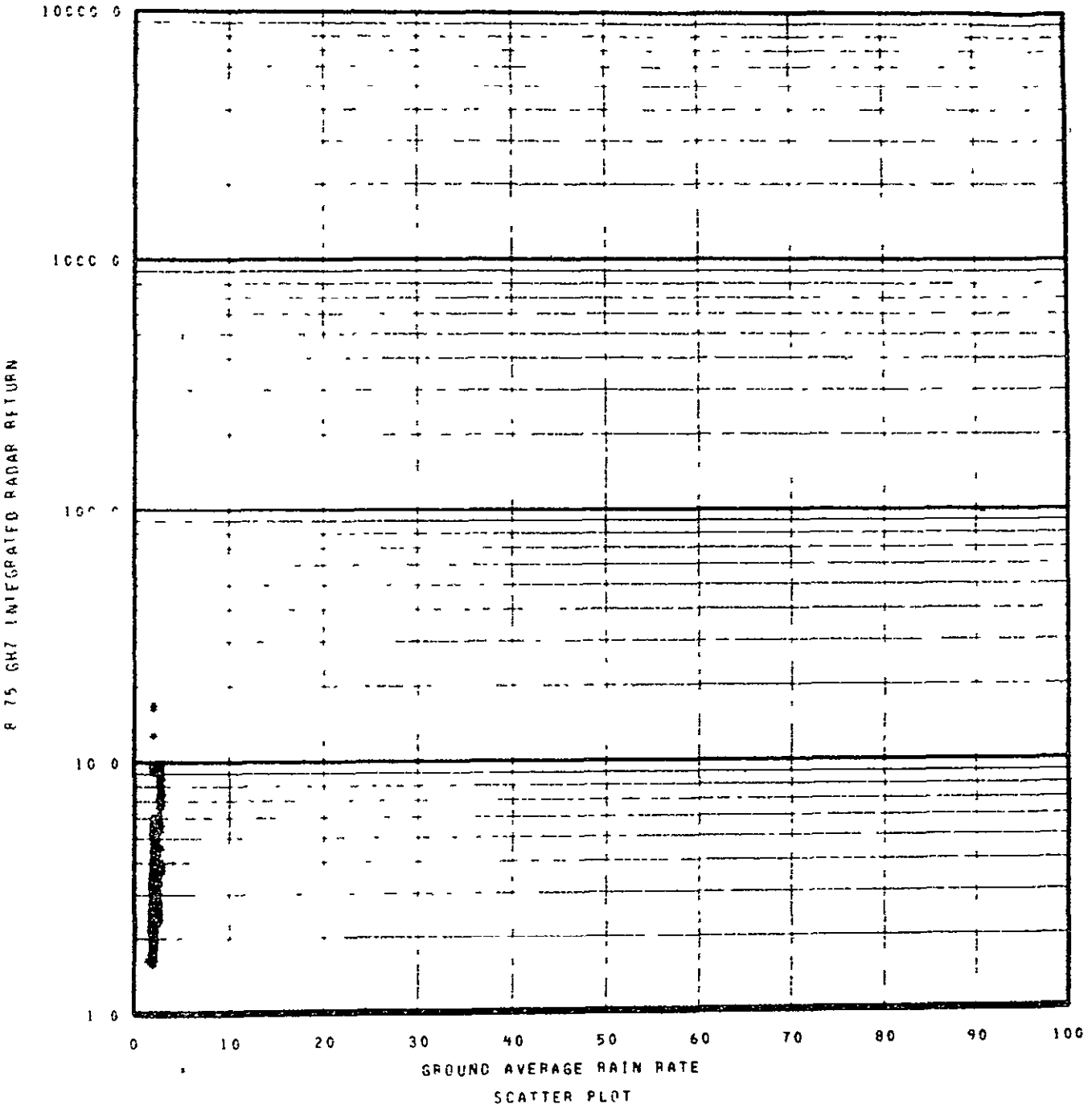

76-4039A-34

Figure 3-7. Integrated Radar Reflectivity versus Ground Average Rain Rate

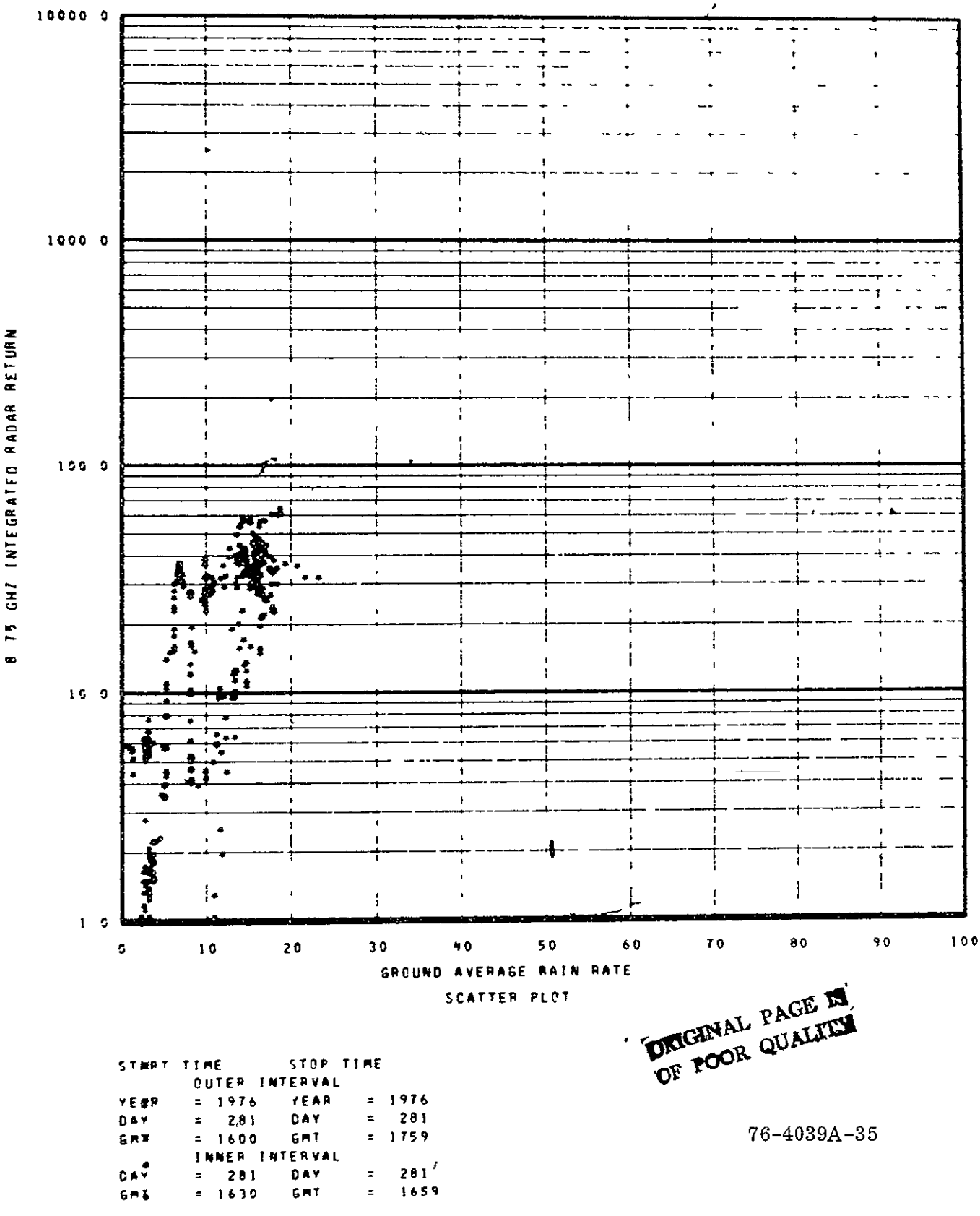

76-4039A-35

Figure 3-8. Integrated Radar Reflectivity versus Ground Average Rain Rate

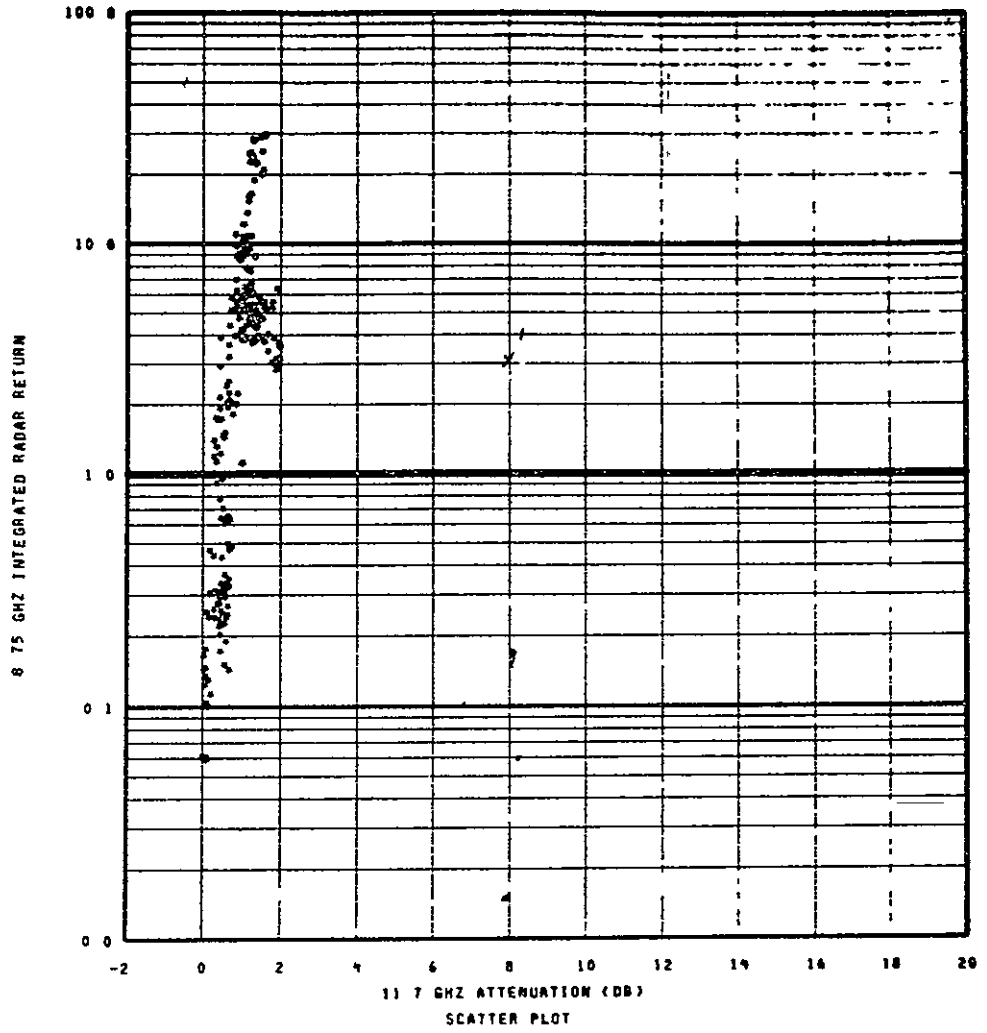

Figure 3-9. Integrated Radar Reflectivity versus 11.7 GHz Attenuation

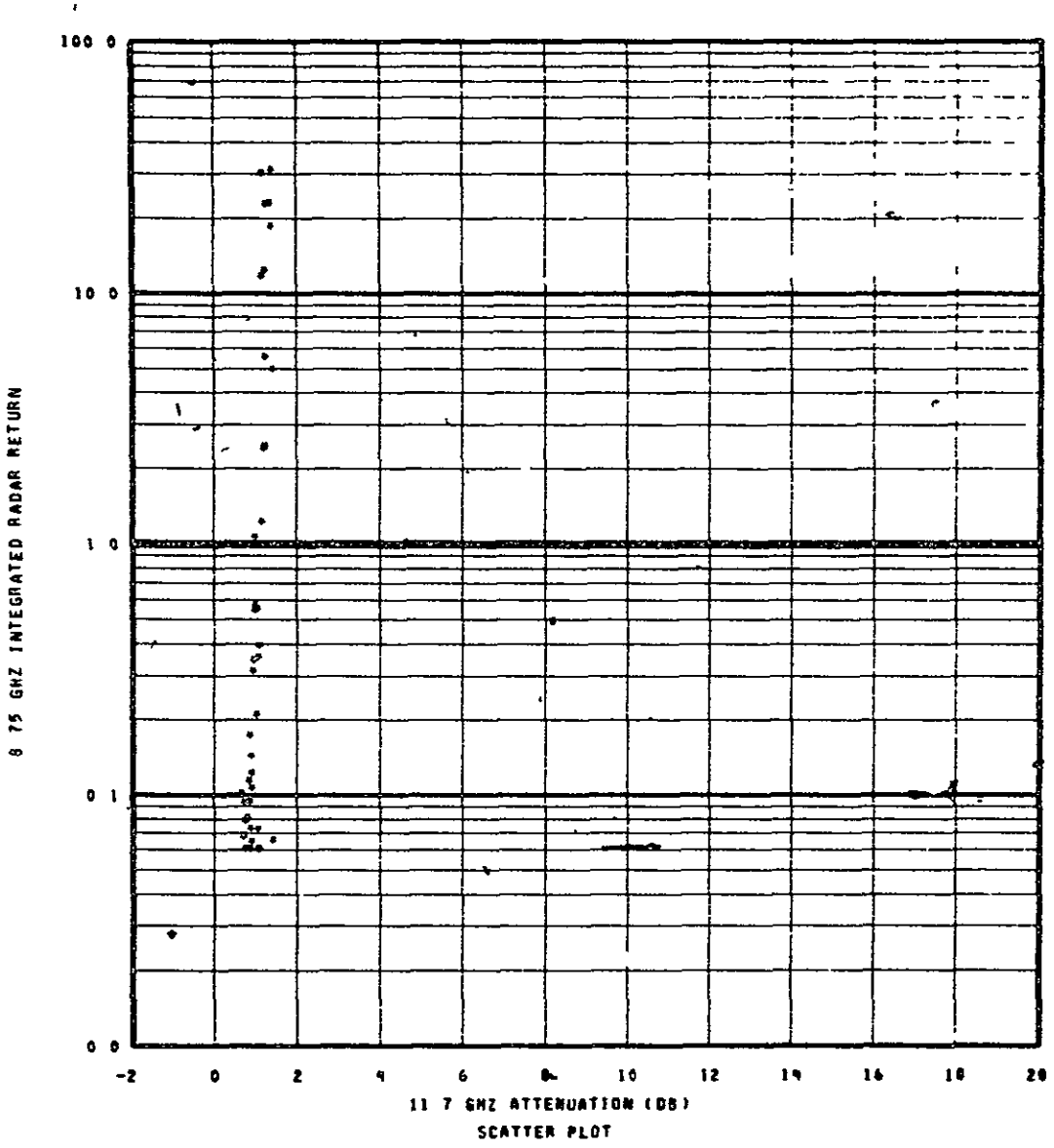

Figure 3-10. Integrated Radar Reflectivity versus 11.7 GHz Attenuation

shown, the integrated η factor is a sensitive indicator of attenuation (δ) at low values of δ. This implies that good accuracy can be obtained in the use of the radar technique for attenuation prediction at low values of δ.

The next sequence of figures show the relationship between rain rate and attenuation. The functional relationship between these two parameters will be considered. For the 11.7 GHz frequency, Ippolito[2] developed a best fit estimate of the coefficients that relate rain rate, R, to attenuation coefficient A in dB/km. It can be shown that,

$$A\ (dB/km) = .0168\ R^{1.25} \qquad (1)$$

Assuming a uniform rain rate over a given path length, L, the total attenuation, δ, can be computed as shown in figure 3-11 for L values between 1 to 10 km. Also shown is a predicted curve generated from measured 15.3 GHz attenuation data and rain rate pairs obtained from the propagation experiment conducted on the ATS-5 satellite. The attenuation data was translated to the 11.7 GHz test frequency by the method developed in section 2.2. With actual measured values, it appears that L should be a function of R, decreasing as R increases.

During a widespread rain, the rain rate should be constant with height up to a distinct melting layer. This is the only rain type that would satisfy condition of a uniform rain rate over a given path length. For the months of June, July and August the height of the melting layer relative to sea level is 3.5 km. Since Rosman is 0.89 km above sea level the effective height is 2.61 km. For an elevation angle of 36° the range to the zero degree isotherm level is 4.44 km. Referring to figure 3-11 for this path length the required R value for a δ of 6 dB is 35 MM/HR. This is a relatively high value of R that is necessary to produce a nominal attenuation of 6 dB. From long term rain rate statistics the percentage of time that R exceeds 35 MM/HR (4 second means) is on the order of 3%. Therefore, it follows that high δ values in excess of say 10 dB will be a rare event at the 11.7 GHz frequency. Hence, during a test run, a low δ value will exist for a large percentage of the time at a magnitude such that it will be difficult to determine if a fade actually exists.

For the test data obtained from Rosman, rain rate and δ pairs can be generated by choosing the peak δ and rain rate (near bucket) values that occurred during a test run. Six pair values from the test data was obtained and are plotted in figure 3-11. As shown, no general trend is noted due to the limited number of points obtained over

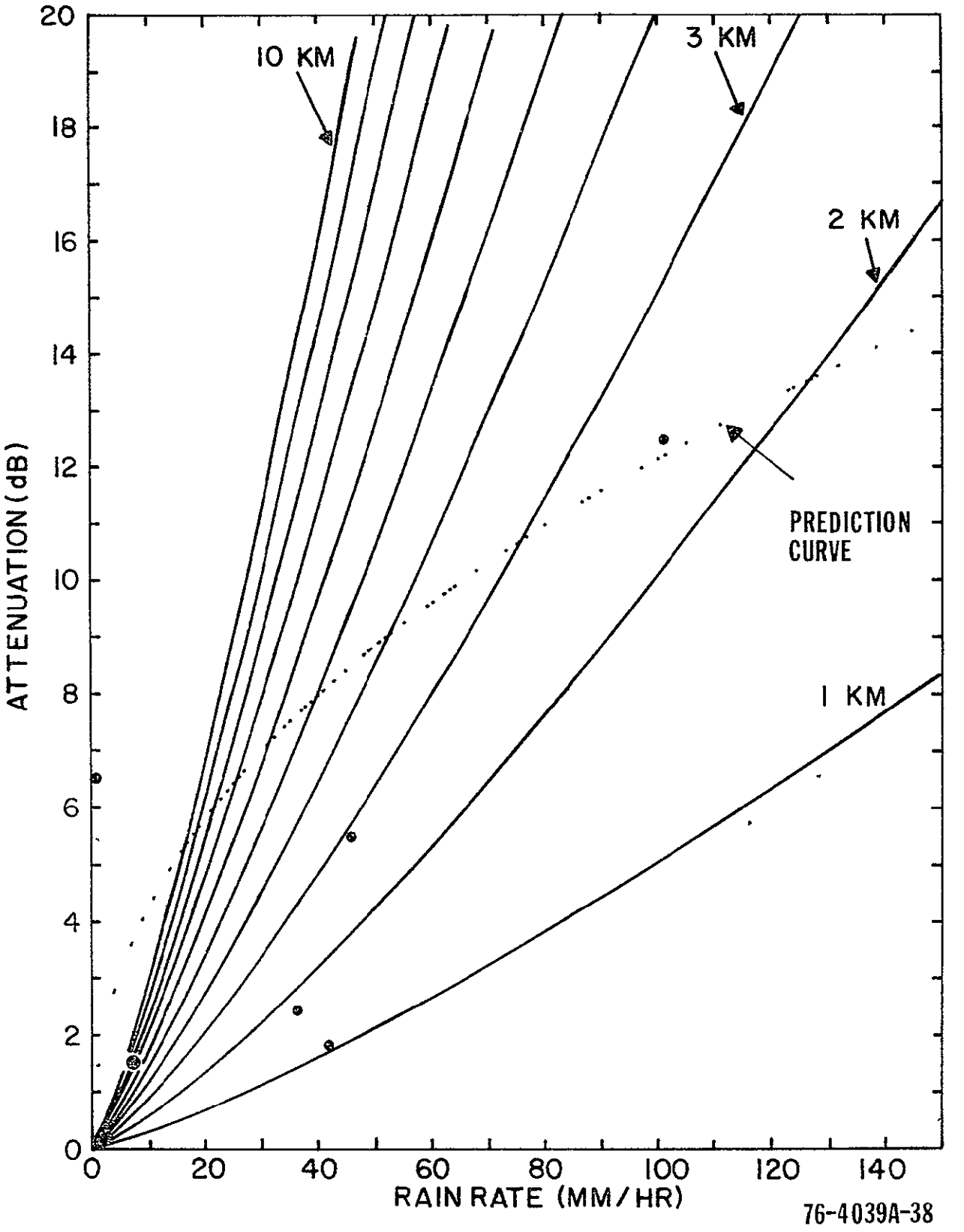

Figure 3-11. 11.7 GHz Attenuation Versus Rain Rate, Rosman North Carolina, Elevation Angle 36°

the test period. The peak δ and rain rate value for the maximum value obtained lies very close to the empirically derived curve. It has been noted from past test data that a strong coorelation exists between rain rate and δ for high values of δ. In the high δ region, the dependence of δ on path length tends to be small since the chief contributor to the high values are intense rain cells of limited extent.

Four secondly mean scatter plots of near bucket rain rate and ground average rain rate for day 162 are shown in figures 3-12 and 3-13. For the 33 minute test period, a definite functional relationship is shown between δ and R. Corresponding plots of δ vs R for test days 208 and 209 are shown in figures 3-14 through 3-17. A more definite functional relationship between R and δ has been realized at the 11.7 GHz frequency than for corresponding plots for 20 GHz and 30 GHz test frequencies. Part of the explanation for these results could be due to the fact that a higher value of R is required to produce a given amount of δ for the 11.7 GHz frequency. For example a R value about 4 times higher is required at 11.7 GHz to produce a comparable δ value at 20 GHz.

The degree of homogeneity of the rain causing the attenuation can be seen by comparing the near bucket R values with the ground average R values. For days 208 and 209 the two R values differ to a large extent with the near bucket R value containing larger peak values. Therefore the δ values produced on these test days were caused by an inhomogeneous rain environment where the most intense cells past through the elevated radio beam close to the main CTS antenna. For test day 162, figures 3-12 and 3-13 the near bucket R and ground average R tend to be similar thus indicating a homogeneous rain environment. It has been generally found that low values of δ are caused by uniform precipitation that extends over a relatively large area. Large values of δ are mainly caused by intense rain cells of limited extent. The above figures tend to agree with that conclusions since low δ values signifies a homogeneous rain environment and high δ values signify an inhomogeneous rain environment. Also for the latter case, it should be expected that lower correlation should exist between the R and δ parameters except for the case when the intense rain cell is recorded by the rain bucket under consideration.

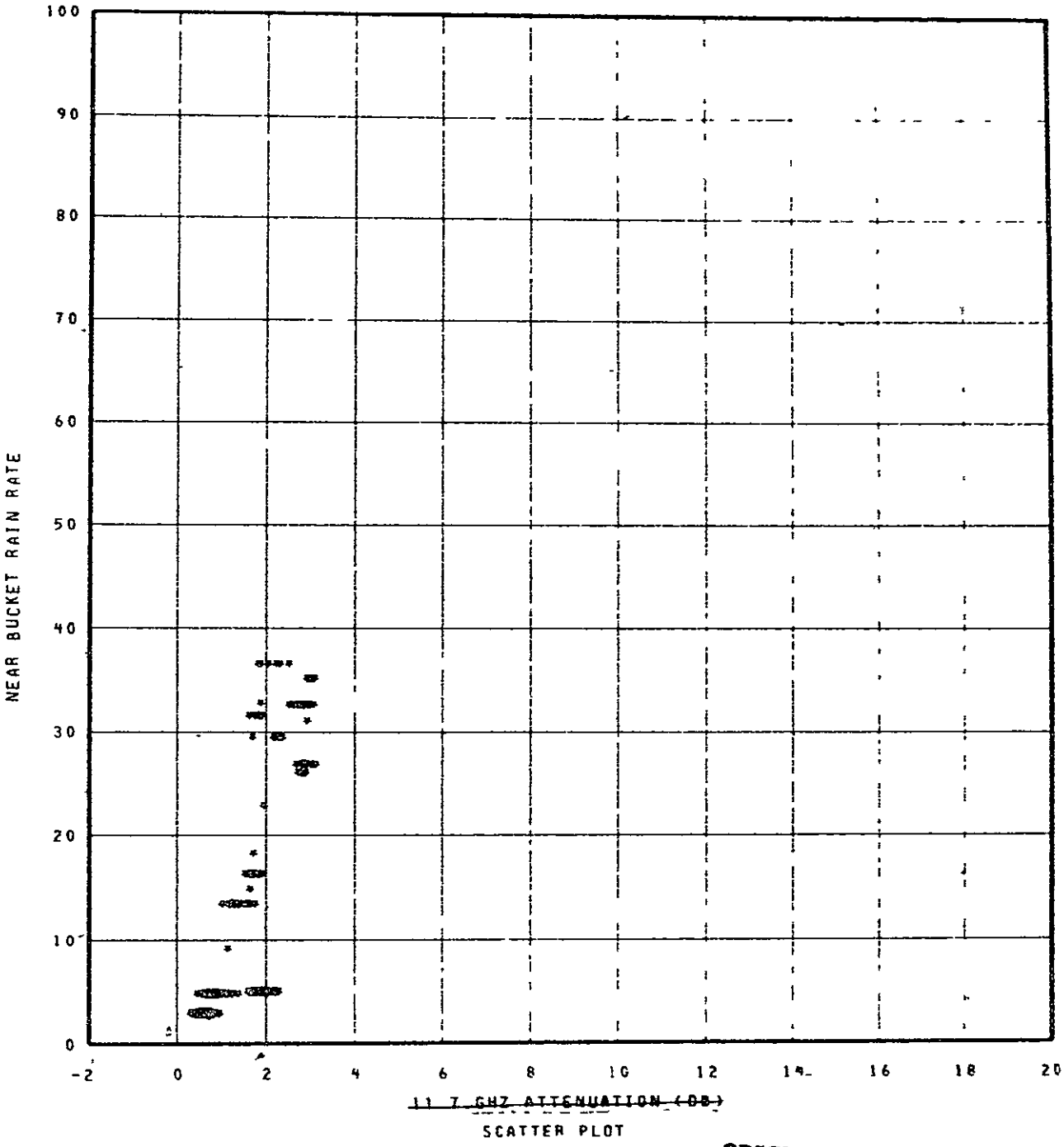

ORIGINAL PAGE IS
OF POOR QUALITY

START TIME		STOP TIME	
OUTER INTERVAL			
YEAR	= 1976	YEAR	= 1976
DAY	= 162	DAY	= 162
GMT	= 1800	GMT	= 1833
INNER INTERVAL			
DAY	= 162	DAY	= 162
GMT	= 1800	GMT	= 1829

76-4039A-39

Figure 3-12. Near Bucket Rain Rate versus 11.7 GHz Attenuation

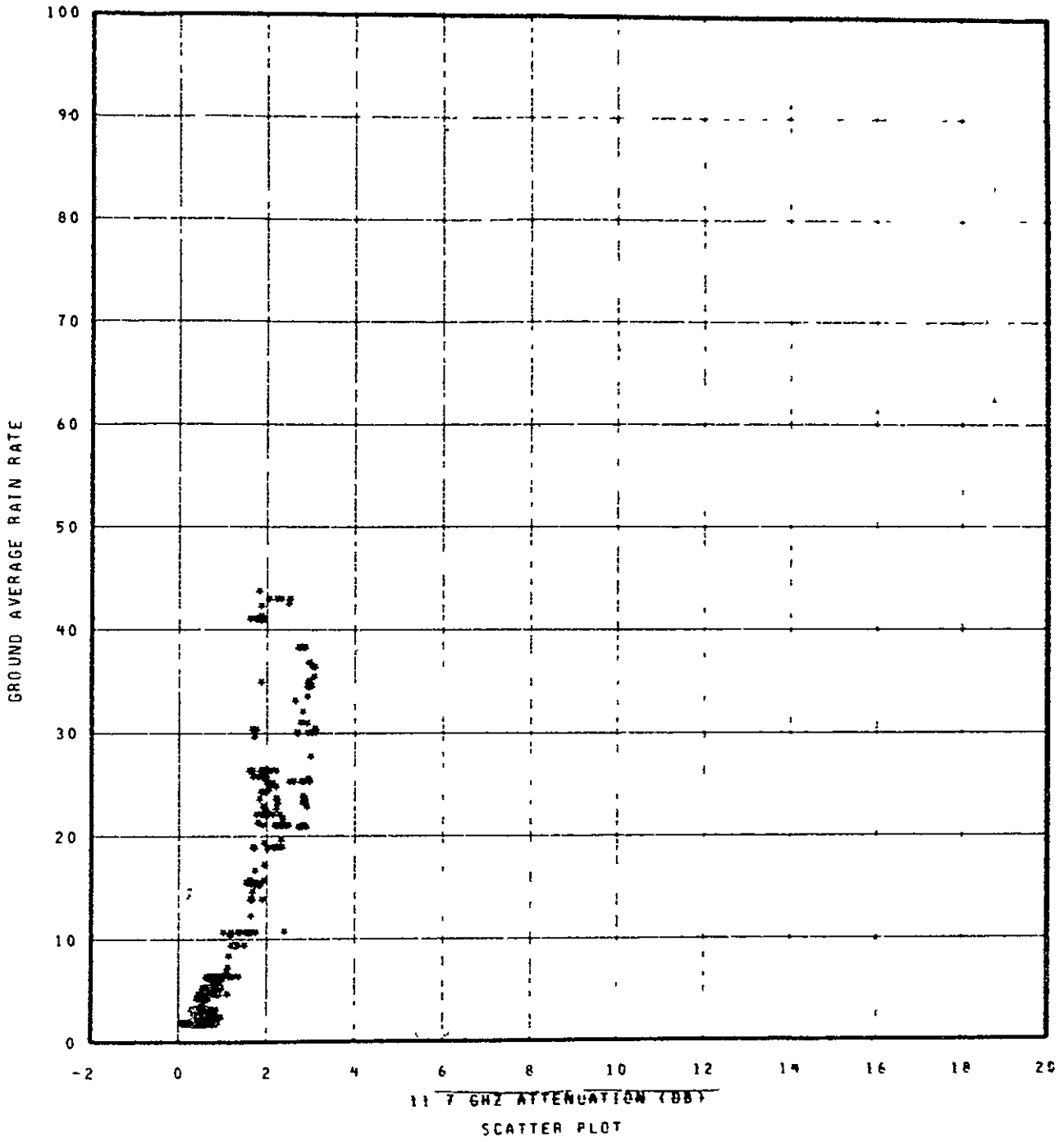

START TIME STOP TIME

OUTER INTERVAL

YEAR	= 1976	YEAR	= 1976
DAY	= 162	DAY	= 162
GMT	= 1800	GMT	= 1833

INNER INTERVAL

DAY	= 162	DAY	= 162
GMT	= 1800	GMT	= 1829

76-4039A-40

Figure 3-13. Ground Average Rain Rate versus 11.7 GHz Attenuation

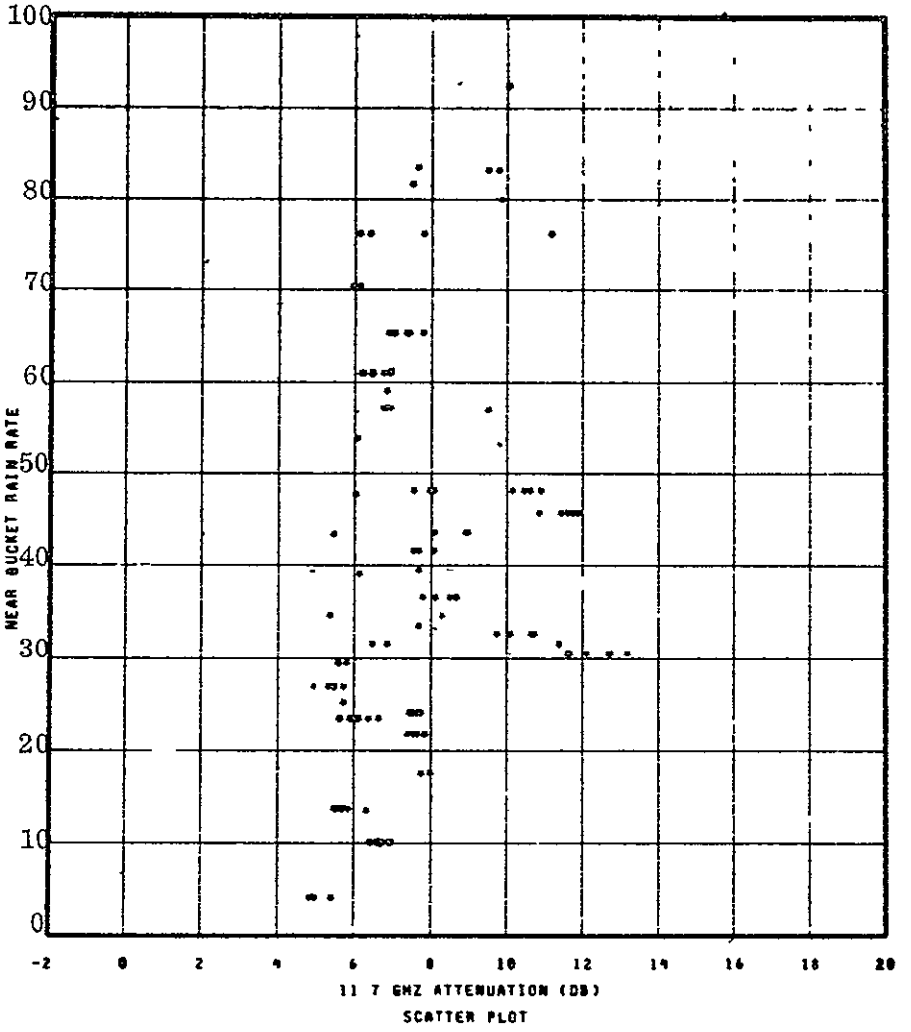

START TIME STOP TIME
OUTER INTERVAL
YEAR = 1976 YEAR = 1976
DAY = 208 DAY = 208
GMT = 2325 GMT = 2359
INNER INTERVAL
DAY = 208 DAY = 208
GMT = 2330 GMT = 2350

76-4039A-41

Figure 3-14. Near Bucket Rain Rate versus 11.7 GHz Attenuation

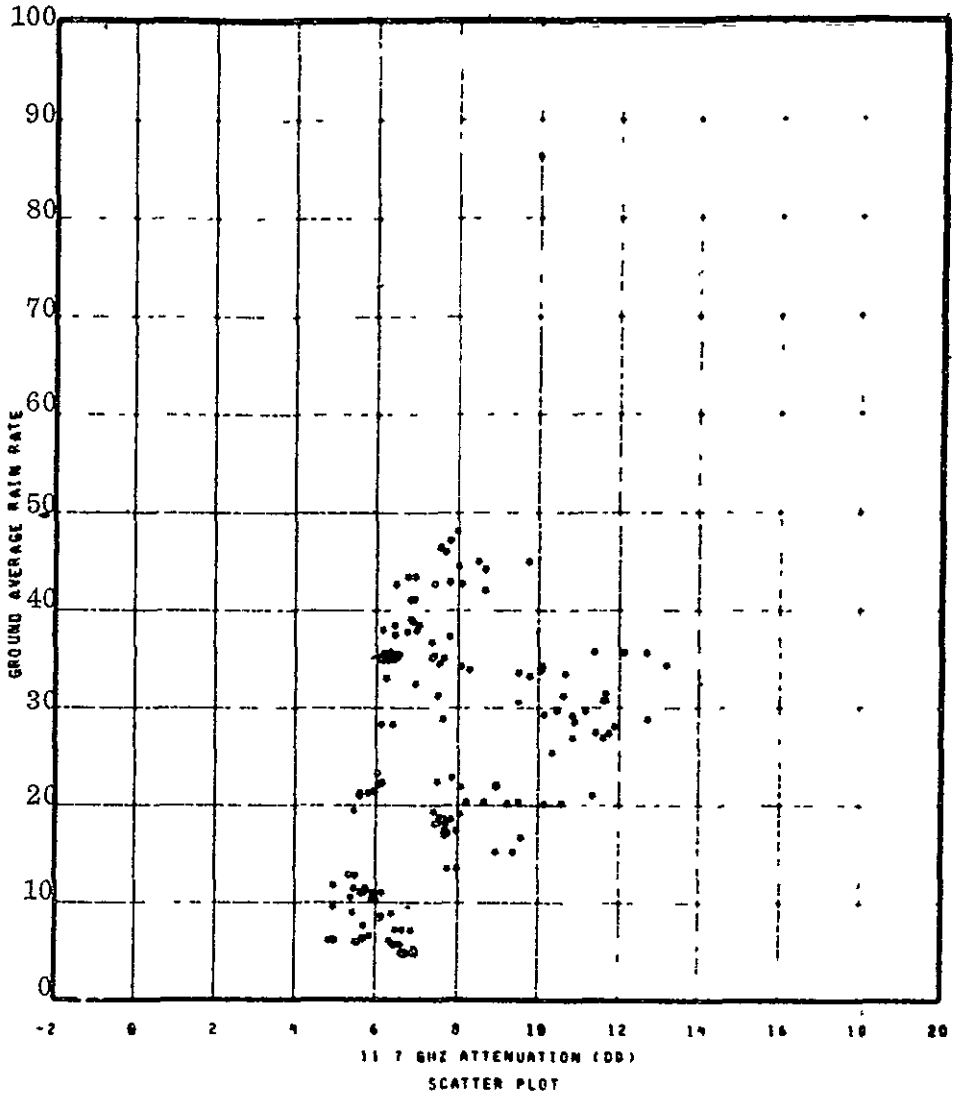

76-4039A-42

Figure 3-15. Ground Average Rain Rate versus 11.7 GHz Attenuation

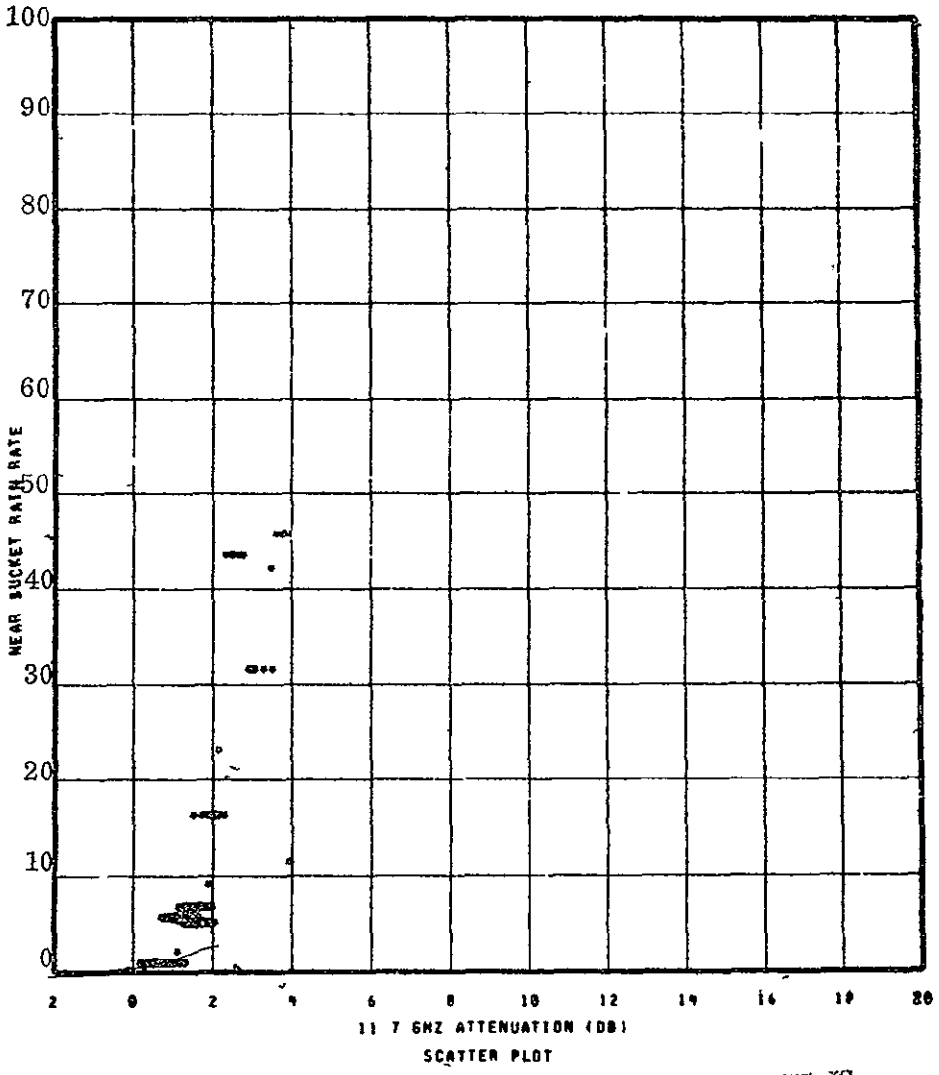

START TIME		STOP TIME	
OUTER INTERVAL			
YEAR	= 1976	YEAR	= 1976
DAY	= 209	DAY	= 209
GMT	= 15	GMT	= 210
INNER INTERVAL			
DAY	= 209	DAY	= 209
GMT	= 15	GMT	= 44

76-4039A-43

Figure 3-16. Near Bucket Rain Rate versus 11.7 GHz Attenuation

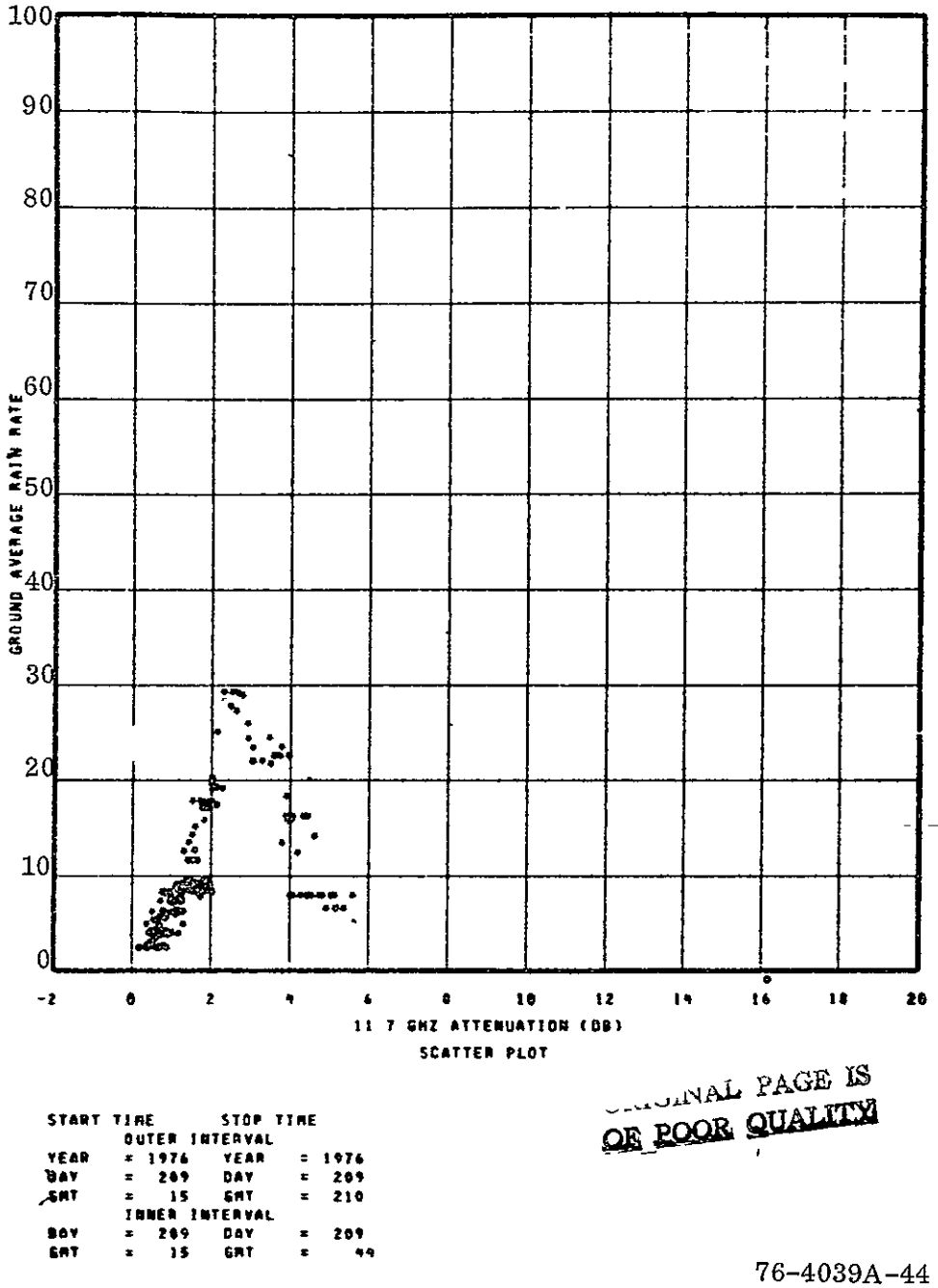

76-4039A-44

Figure 3-17. Ground Average Rain Rate versus 11.7 GHz Attenuation

3 5 ELECTRO-MAGNETIC INTERFERENCE (EMI) EXPERIMENT

The objective of this experiment is two-fold:

a. To develop a data base in order to characterize man-made sources radiating in the uplink bands of CTS.

b. Develop a method of "on demand" analysis of possible interference signals for CTS users.

The overall system consists of four major components, as shown in figure 3-18. The receiver, computer, programmable synthesizer and spectrum analyzer. The output of the receiver, which is either the upper or lower communication band, (upper centered at 2 1805 GHz and lower centered at 1 9805 GHz), is applied to the input of the spectrum analyzer at 70 MHz $\pm$42.5 MHz. The local oscillator for the spectrum analyzer is generated by the synthesizer which is remotely programmed by the computer. The vertical output or detected signal from the spectrum analyzer is applied to the computer via an amplifier and A/D converter; the computer performs a signal-to-noise computation which is then correlated to the uplink frequency. The data is printed out by the Decwriter if it meets criteria established by the operator.

The transmitter shown in figure 3-18 will be installed at the Rosman station in the January to April period of 1977. For the EMI experiment it will be employed for calibration purposes. To date, transmitters located mainly at GSFC and COMSAT have been employed.

To date, the primary purpose of the EMI tests has been to evaluate the system, and operating techniques. Several attempts were made to achieve a transmit power calibration, a number of problems were encountered in trying to accomplish this The major problem has been that the transmitters at GSFC and Westinghouse could not be reduced in power enough (below 40 dBw) to allow linear operation of the system. Test conducted with COMSAT indicated that to maintain linear operation the EIRP of the source had to be below 40 dBw and the output of the spectrum analyzer had to be between 0 and -1.3 volts. The tests with COMSAT also indicated that a signal of 30 dBw EIRP was easily detectable; the signal to noise ratio was 23.76 dB in a 1 KHz bandwidth. This would imply that signals of 10 dBw to 20 dBw EIRP could be detected, it may be necessary, however, to reduce the bandwidth below 1 KHz. The problem this creates is that narrower spectrum widths are required with longer dwell times. The longer dwell times would compensate for longer filter response times.

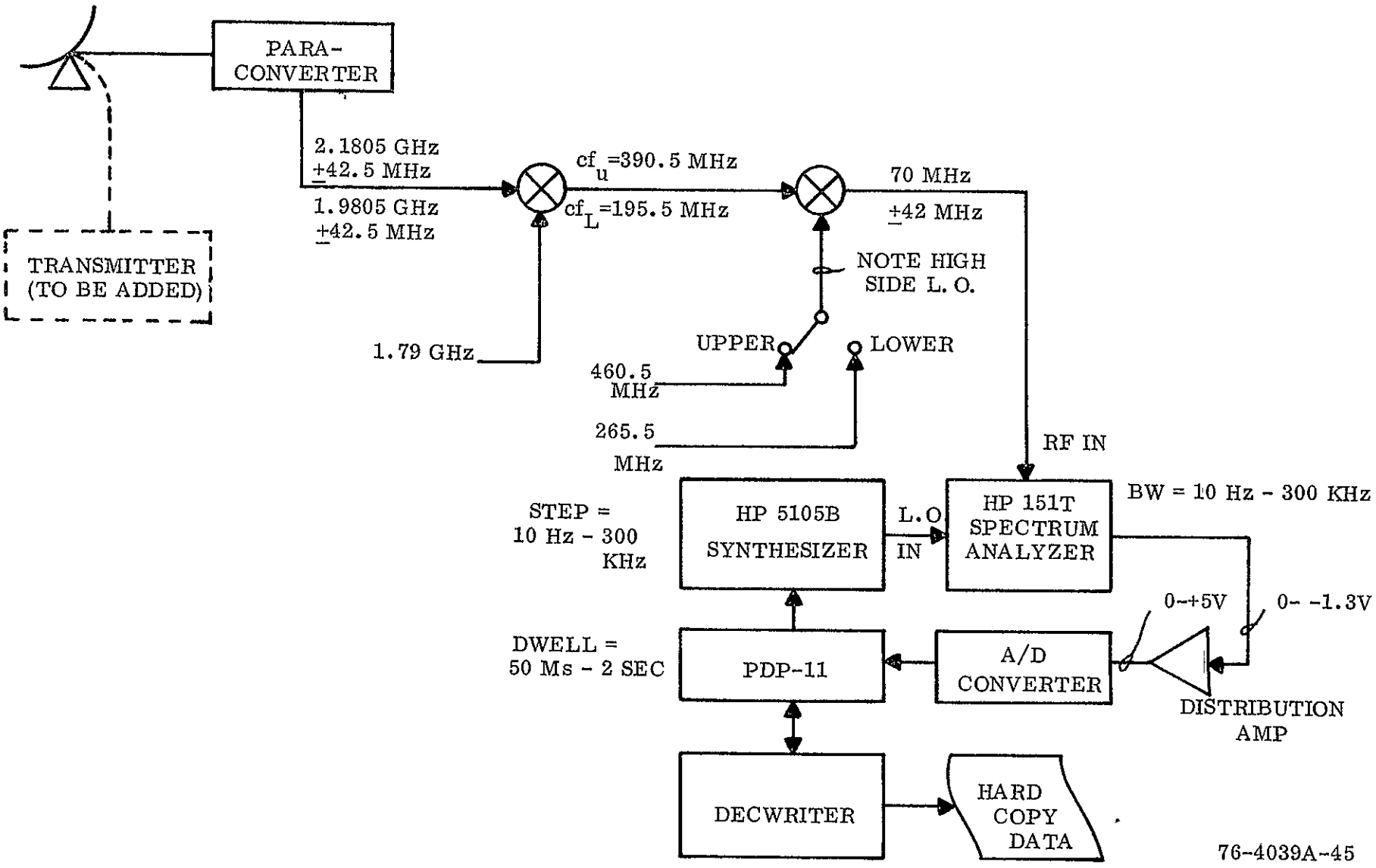

Figure 3-18. EMI System Description

For system checkout and calibration, 17.5 hours of test time was required. This included a deliberate interference test that was arranged with the FAA to utilize their air-traffic control radar at the Los Angeles Airport as an interference source. The radar transmitted at a frequency of 14.175 GHz which is about 30 MHz below the bottom edge of the search band. The radar signal was not detected within the CTS receive bands. The minimum detectable interference EIRP was determined by utilizing an internal test loop. The results show that a signal level of -138 dBm can be detected by the system when a test bandwidth of 100 Hz and 1000 A/D samples per step are utilized for the measurement. The corresponding minimum signal level for a 10 kHz bandwidth and 20 A/D samples per step is -120 dBm. For the former signal level, it was determined that the minimum detectable EIRP interference source is -6.8 dBw. Because of the relatively high antenna gains that exist at the 14 GHz frequency values, even with nominal antenna sizes it was not possible to obtain a direct measurement of the threshold value.

3.6 MULTIFREQUENCY RADAR TEST RESULTS

Part of the ATS-6 Millimeter Wave Propagation Experiment involved the use of a multifrequency weather radar (3 GHz and 8.75 GHz) to measure the meteorological conditions that exist in an elevated path at the time attenuation (δ) measurements are being performed. The radar is also being employed for the CLCE to make the same type of measurements. A detailed description of the radar is given in reference 3.

For the test period covered by this report, different types of radar tests were conducted which include:

a. the radar clutter test
b. calibration tests
c. a continuation of the drop size distribution investigation

The radar clutter test involved varying the elevation angle of the antenna from zenith to as low as 5° during clear weather. The existence of clutter within the range bins was measured by utilizing the signal levels that were present when the antenna was at zenith as a reference. It was assumed that no clutter would be present when the antenna is in the zenith position. No measurable clutter was noted beyond the 300 meter minimum operational range. A calibration test was then performed during a period of precipitation when the antenna elevation angle was set at the 5° value. However, it was noted that no rain return could be detected beyond the 300 meter range. By increasing the elevation angle to 11° a return was measured. Evidently, signal blockage due to the terrain factors within the minimum 300 meter range occurs when the elevation angle is set at 5°. Hence, the minimum operational elevation angle should be on the order of 10°.

From the results of the clutter test, it was decided to set the antenna elevation angle at 11° for the calibration test. This test involved comparing the ground measured rain rate with the radar computed rain rate and then adjusting the radar constant until the latter rain rate agrees with the former. The equations utilized for the test are as follows.

3 GHz

$$R^d = \left[\frac{C_3}{\frac{3.0\ 4 \times 10^{10} L}{P_t(\text{mw})}} \right] \quad \frac{P_r(\text{mw})\ r^2\ (\text{meters})}{B} \qquad (2)$$

8.75 GHz

$$R^d = \left[\frac{C_{8.75}}{\frac{2.62 \times 10^3 L}{P_t(mw)}} \right] \frac{P_r(mw)\ r^2\ (meters)}{B} \qquad (3)$$

where:

R - Rain rate in MM/HR

P_t - Transmit power in milliwatts (mw)

P_r - Receive power in mw

L - Two way transmission line loss

r - Range to 100 meter range bin in meters

B, d - Constant that related the reflectivity factor Z to R e.g. $Z=200\ R^{1.6}$,

$B = 200 \quad d = 1.6$

The terms within the brackets in the above equations define the radar constants, C_3 and $C_{8.75}$. For a given range bin, the C factors will vary with P_r and the ground measured rain rate (R). It can be shown[4] that the respective constants are related to their parameters by the equations

$$db\ C_3 = db\ P_3\ (r_J) + 2\ db\ r_J + \left(\frac{db(1/B) - db\ R(r_J)}{1/d} \right) \qquad (4)$$

$$db\ C_{8.75} = db\ P_8(r_J) + 2\ db\ r_J + \left(\frac{db(1/B') - db\ R(r_J)}{1/d'} \right) \qquad (5)$$

$$+2 \sum_{i=1}^{J} K(r_i)$$

where

$K(r_i)$ is the one way attenuation of the signal within a range bin r_I, the attenuation in db is summed over all range bins between the radar antenna and the range bin of interest r_J.

$R(r_J)$ is the ground measured rain rate that is measured directly below the r_J range bin.

As shown in equations (4) and (5) the value of C_3 and $C_{8.75}$ not only depend on the received backscatter power P_3 but also on the derived constants (B and d) which are a function of rain type and frequency.

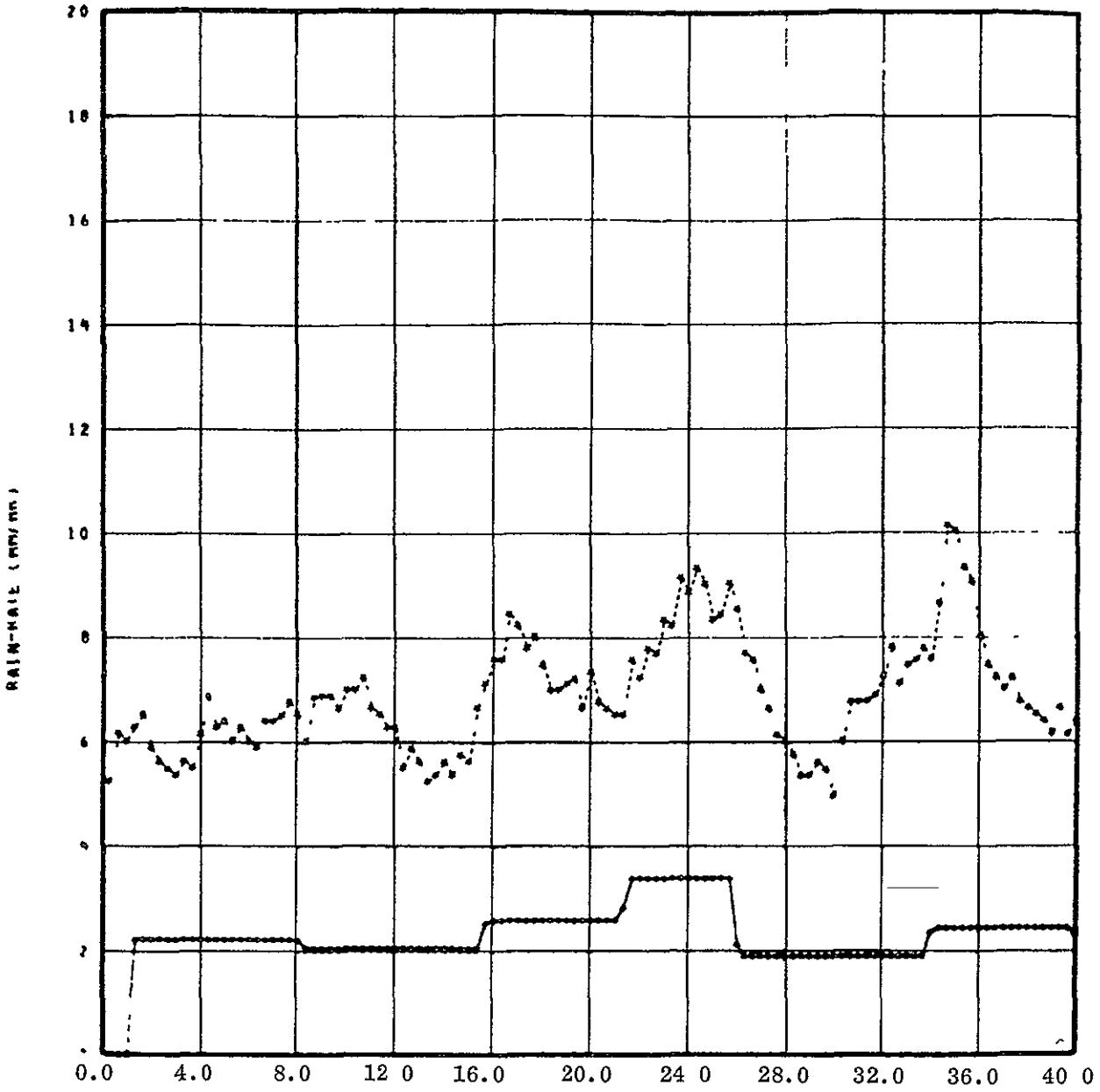

Figure 3-19. Measured and Computed Rain Rate versus Time

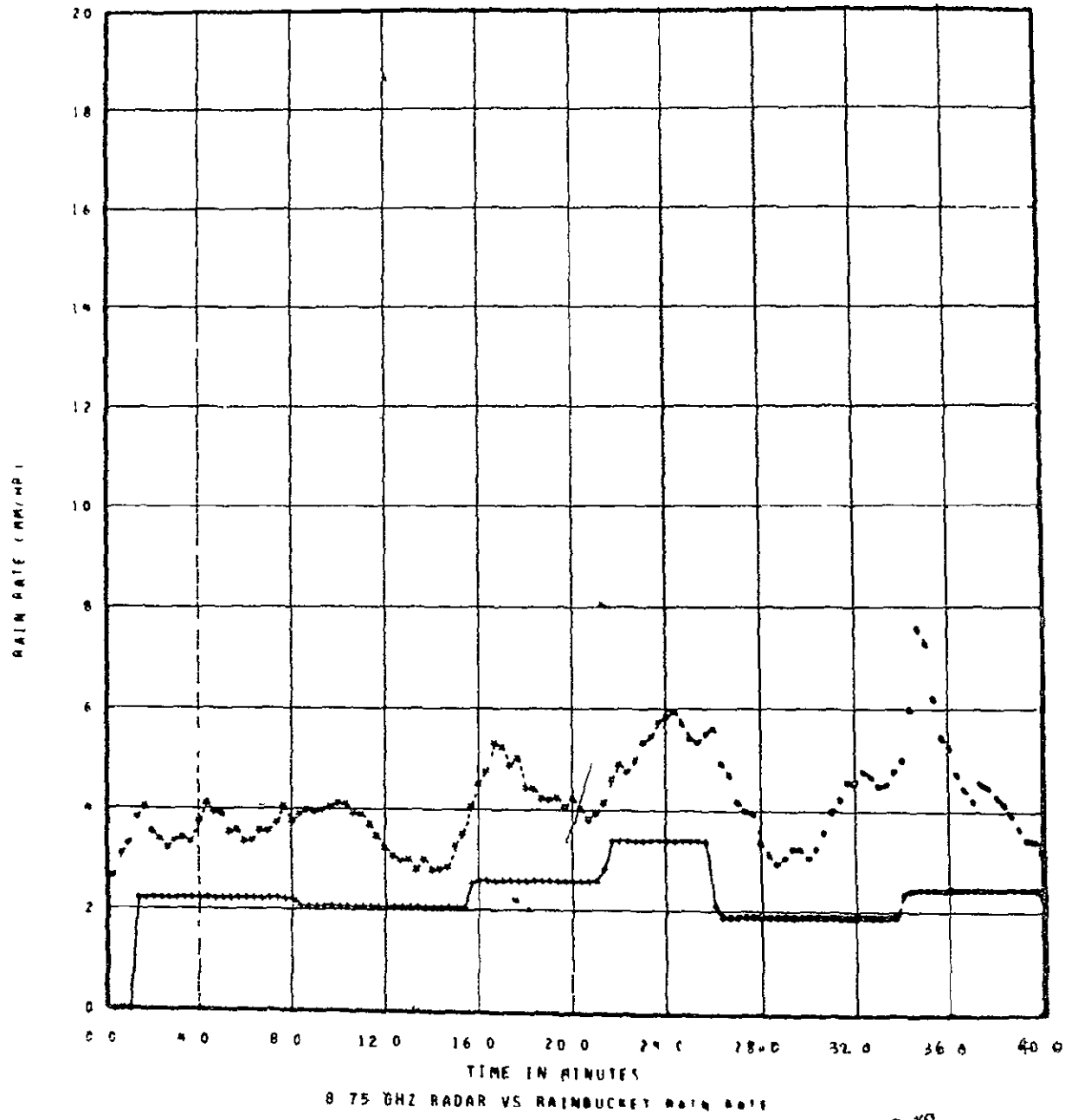

76-4039A-47

Figure 3-20. Measured and Computed Rain Rate versus Time

Time plots of the 20 second averages of radar computed rain rate (range bin 1, range = 300 meters) ground measured rain rate (rain bucket 2) are given in figures 3-19 and 3-20 for the 3 GHz and 8.75 GHz radars. The radar computed rain rate values fluctuates more rapidly relative to the ground measured rain rate. The 8.75 GHz values fluctuates less rapidly because the correlation time of the 8.75 GHz signal is only 10 milliseconds relative to the 30 millisecond value for the 3 GHz signal. This means that 3 times as many independent samples are available for the 8.75 GHz signal in the averaging process.

The radar constants defined in equations (2) and (3) were computed for a $P_{t8.75}$ of 16.9 dBm and an L of 5.2 dB For the 3 GHz radar, P_{t3} was 16.4 dBm and the L value was 5 dB. A B of 200 and a d of 1.6 was employed for equations (4) and (5). Also the K value was set equal to zero for these computations. The following statistical results were obtained:

Mean of Ground Measured Rain Rate	Mean of Radar Computed Rain Rate		Standard Deviation σ_3	Standard Deviation $\sigma_{8\ 75}$
1.93	3 GHz	8.75 GHz		
(σ = 0.657 MM/HR	6.06	2.7	1.77	3.88

In order to obtain correspondence between the above mean values C_3 must be decreased by a factor of 3.1 dB and $C_{8.75}$ by a factor of 0.9 dB for a B of 200 and a d of 1.6. The mean and σ values were computed from a sample approximately 76 minutes in length. The data shown in figures (3-19) and (3-20) are the values for the first 40 minutes of the sample. The mean values may not be the best parameter to employ for the best estimate of the sample. This is true in the 8.75 GHz case because of the high σ value. The technique to be investigated will be to generate a least mean square fit of equations (4) and (5) to a horizontal line. The y intercept of the resulting line would be the best estimate of the C factors for the measured samples.

As detailed in reference 3, a measure of the drop size distribution can be obtained by utilizing the computed reflectivity factor Z determined within a range bin and the ground measured rain rate, R. The technique was designated as the Z/R method. In assuming a Marshall-Palmer drop size distribution the technique determined the value of the Λ factor and the N_o factor as defined in the following equations:

$$n(D)\ dD = N_o e^{-\Lambda D}\ dD$$

where.

n(d) dD is the number of rain drops of diameter between D and D+dD, and N_o and Λ are parameters that define the distribution. N_o is the zero drop size population and Λ is defined by the expression:

$$R = \left(\frac{41}{\Lambda}\right)^{4.76}$$

The main point in the continuing investigation was determined if the Λ and N_o factors are sensitive to changes in rain rate and rain type. Utilizing a disdromoter Joss (5) found that these changes were measurable. The results are as follows

Type of Precipitation	No ($mm^{-1} m^{-3}$)	Λ-R Λ in mm^{-1} R in MM/HR
Drizzle	30,000	$\Lambda = 5.7\ R^{-0.21}$
Wide Spread Rain	8,000	$\Lambda = 4.1\ R^{-0.21}$
Thunderstorm	1,400	$\Lambda = 3.0\ R^{-0.21}$

The largest change in value due to rain type is in the N_o value. Therefore, this parameter is a good measure of the effectiveness of the radar method to note changes in the drop size distribution as the rain types vary. For the test runs to be presented the N_o factor will be plotted along with the Z factor. This latter factor is the most sensitive measure of the drop size since its magnitude varies as a function of the sixth power of the rain drop diameter. Since Λ is a function of rain rate it will be plotted along with the ground measured value of the rain rate. As the drop size distribution changes both Z and rain rate will change thus causing changes in N_o and Λ. If these latter factors do not change because of the various limitations of the radar method then the use of the S-X band radar at a low peak power for drop size determination will be questionable.

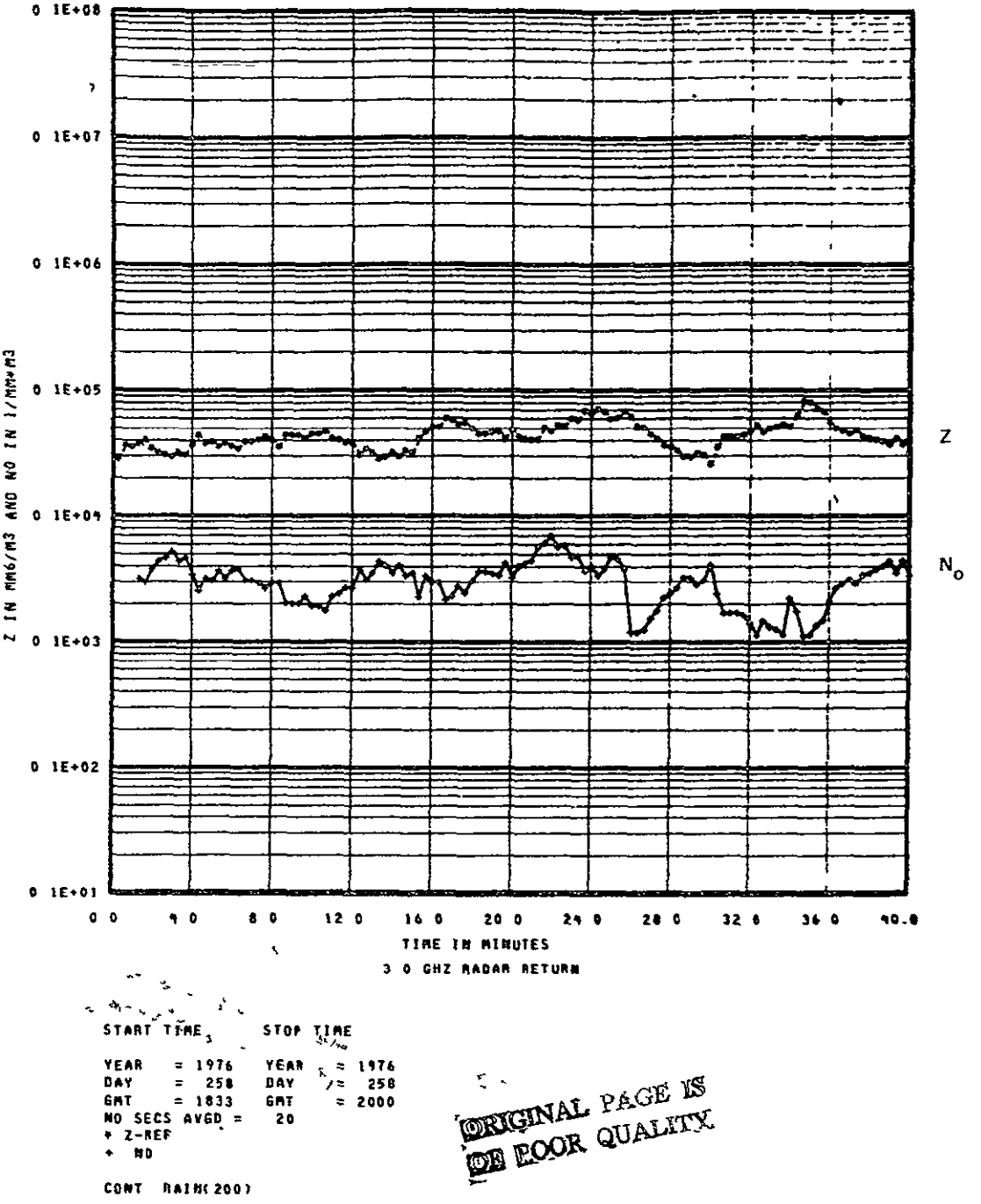

76-4039A-48

Figure 3-21. Drop Size Distribution Factors (Z and N_o) versus Time-3GHz Radar

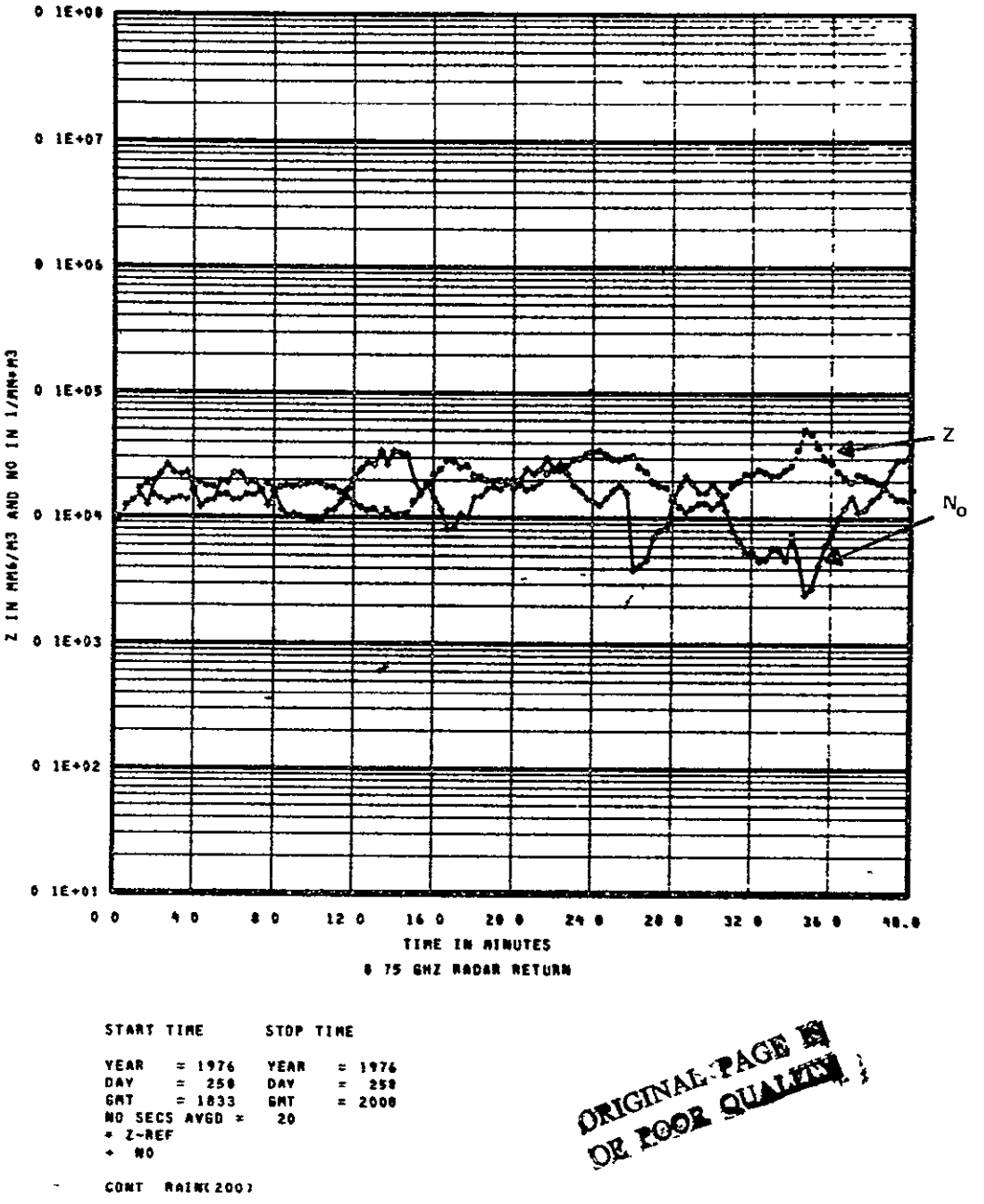

76-4039A-49

Figure 3-22. Drop Size Distribution Factors (Z and N_o) versus Time - 8.75 GHz Radar

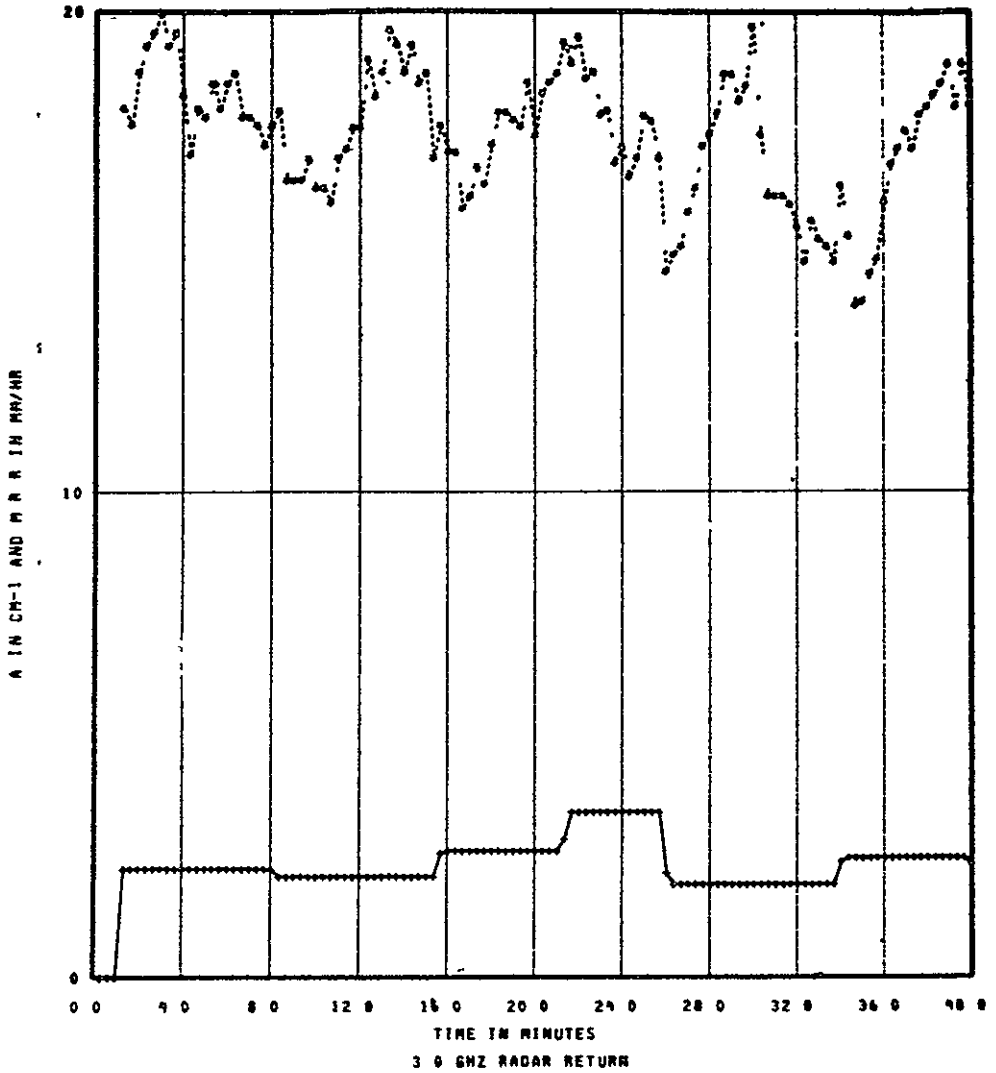

76-4039A-50

Figure 3-23. Drop Size Distribution Factor Λ and Rain Rate versus Time - 3 GHz Radar

For the test run under consideration (day 258) the mean measured rain rate was only about 2 MM/HR. For this value of R, it would be expected that N_o should fall somewhere between 8000 and 30,000, probably closer to 8000, Z should be on the order of 600 mm^6/m^3 and Λ should approximate 35.4, this corresponds to a measured R of 2 MM/HR.

Time plots of Z and N_o for the 3 GHz and 8.75 GHz radars are shown in figures 3-21 and 3-22 for day 258. To a first approximation, Z is not a function of frequency; hence the Z values for both radars should be approximately equal. The average value of Z_3 is approximately 5000 mm^6/m^3 and the corresponding value of $Z_{8.75}$ is approximately 1000 mm^6/m^3. Utilizing the corrected radar constants in the computation of Z results in a corrected value of 2450 for Z_3 and 813 for $Z_{8.75}$.

Because of the errors involved in computing Z, the determination of Λ and also N_o are also in error to a greater extent than the resulting errors in the radar constant. This can be seen in the computed values of N_o in figures 3-21 and 3-22 and for Λ in figure 3-23 for the 3 GHz radar. For an adjusted radar constant, Λ would increase thus causing an increase in N_o to a more realistic value for the low rain rate condition. From the above discussion, it appears that utilizing the ground measured rain rate as a standard in calibrating the weather radars has merit. Also a check on the corrected radar constant by computing the approximate values of Λ and N_o for a given rain rate condition also appears to produce reasonable results. The effects on the radar constants of varying the B and d factors according to frequency and rain type must also be considered in future investigations.

3.7 BEST FIT ANALYSIS

One of the objectives of the CLCE is to determine the best fit probability density distribution for the measured attenuation (δ) data. From the results of a similar investigation involving measured 20 GHz and 30 GHz δ data utilizing ATS-6, it appears that the most promising density functions to investigate are the Log Normal function and a particular case of the generalized Gamma function called the Weibull function. Details of these functions and procedures for utilizing the chi-square criterion for the "Goodness of Fit" tests are given in Appendix B.

Details for fitting the Weibull function to the δ data will be given in this report. In a future report the Log Normal function will be discussed. The Weibull density function in general can be expressed as follows:

$$f(x) = \beta \alpha (x - \gamma)^{\beta - 1} e^{-\alpha(x-\gamma)^{\beta}} \qquad (6)$$

The α parameter is a scale factor, the β parameter is a shape factor and the γ parameter is a location factor. Utilizing the origin of the coordinate system as a reference, the γ parameter can be set equal to zero. Equation (6) reduces to,

$$f(x) = \beta \alpha x^{\beta-1} e^{-\alpha x^{\beta}} \qquad (7)$$

The mean for the Weibull function can be shown[6] to be,

$$\text{Mean } (x) = \left(\frac{1}{\alpha}\right)^{1/\beta} \Gamma\left(\frac{1+\beta}{\beta}\right) \qquad (8)$$

Also the corresponding variance is.

$$\text{Variance } (x) = \Gamma\left(\frac{\beta+2}{\beta}\right) - \Gamma^2\left(\frac{\beta+1}{\beta}\right) \qquad (9)$$

The "Goodness of Fit" test involves comparing the expected frequency (e_i) that should exist within a given δ bin with the actual measured frequency (m_i) that was found from the data. After the above frequencies have been determined, a "chi-square" statistic (X^2) is computed for N attenuation bins,

$$X^2 = \sum_{i=1}^{N} \frac{(m_i - e_i)^2}{e_i} \qquad (10)$$

The X^2 factor is a measure of the discrepancy that exists between m_1 and e_1 The above test involves determining whether the discrepancy is significant or can be reasonably attributed to chance. Hence, the hypothesis to be tested is that the measured distribution constitutes a sample from a population having a Weibull distribution. The criterion involves determining a value of X^2 at a generally accepted level of significance of .05. If the computed value of X^2 exceeds the $X^2_{.05}$ then the hypothesis is rejected, if it is less than the computed value it is accepted at the .05 level of significance. The $X^2_{.05}$ factor is determined from the theoretical chi-square distribution and it is the value of X^2 at which the probability of exceeding it due to chance is .05. The magnitude is a function of the number of degrees of freedom (DEF) involved with the data. DEF is equal to N-1. The assumption of a particular theoretical distribution and a specific number of δ bins results in the loss of 1 degree of freedom. An additional DEF is lost for each parameter estimated from the data The level of significance is defined as the probability of committing a Type I error which is usually taken as 0.05. A Type I error is defined as an error that results from rejecting a hypothesis when it is, in fact, true. A Type II error is accepting a hypothesis when it is, in fact, false.

To determine f(x) in equation (7) both β and α must be defined. The α factor is determined from the data as shown in Appendix A, and equation (8).

$$\alpha = \left[\frac{\Gamma\left(\frac{1+\beta}{\beta}\right)}{\text{Mean (x)}} \right]^{\beta} \qquad (11)$$

Since the α factor is determined from the data, another DEF is lost, resulting in an overall DEF of N-2. The β factor is chosen so that the actual shape of the distribution closely approximates the measured data. If β is chosen as unity an exponential distribution is obtained, for a β of 2 a Rayleigh distribution results. From a previous analysis of the ATS-6 data it was shown that a β of about 0.9 minimized the X^2 factor.

For this report the δ data compiled from the Goddard station will be employed for determining the goodness-of-fit of the data to a Weibull distribution utilizing the chi-square statistic. The minutely mean δ values of the sample is shown in Table 3-2. The total sample involves 2830 minutes with the δ bins being 2 dB wide. Because of the limited time sample and the use of the minutely average values, a very small

amount of data exists at δ values greater than 12 dB. For the Rosman data, 4 second averages are employed; hence, less smoothing of the high δ values occurs. This small number of samples within the higher δ bins makes it necessary to combine the ranges bins until the sum of the expected frequencies at least equals 5. This is necessary since the sampling distribution of X^2, as defined by equation (10), only approximates the theoretical distribution on which the $X^2_{.05}$ values are based, the criterion stated for the acceptance or rejection of the hypothesis should not be used when the expected frequencies are small. This is unfortunate since the smaller number of δ bins results in a smaller DEF which in turn requires a more stringent fit before the hypothesis can be accepted.

As shown in Table 3-3, the effective number of δ bins is 6. Since the mean of 1.34 dB was computed from the sample the corresponding DEF value is 4. It can be shown for this DEF value, the X^2 value is 9.5. This means that the X^2 value as computed from equation (10) must be ≤ 9.5 in order for the hypothesis to be accepted at the .05 level of significance. Since the computed X^2 is a large 283.6 mainly due to the high measured frequency in the first two δ bins the hypothesis must be rejected. A smaller value of β will be required in order to decrease the computed X^2 value. From this analysis it appears that minutely mean averages tend to smooth the data to a point that reduces the information in the high δ bins thus causing a large percentage of the data to fall in the lower δ bins. This reduced data causes the conditions for an acceptance of the hypothesis to be more stringent.

Figure (3-24) shows plots of the measured attenuation values and the Weibull distribution computed for a β of 0.9 and a mean of 1.34 dB. It is obvious that the distribution results in a poor fit to the data especially in the $\delta > 10$ dB region. Part of the problem lies in the value of β chosen and the fact that not enough data was obtained in the high δ region to realize a statistically significant sample.

In future work on this best fit problem emphasis will be placed in obtaining an optimum fit in the $\delta > 6$ dB region. Lack of a fit at lower δ values is not important since system margins are usually high enough to compensate for these values. The important factor that must be determined is the percentage of time the δ value is greater than say 8 dB in a given time period of interest. This will define the outtage time for a given system margin.

TABLE 3-3

ATTENUATION DATA

FROM NASA GODDARD STATION

Two DB Cells	Number of Minutes	Attn. Value (DB)	$\eta_1 x_1^{\beta}$	Measured Freq. (m_1) (Minutes)	Expected Freq. (e_1) (Minutes)	$\frac{(m_1 - e_1)^2}{e_1}$
1	2495	1	2495	2495	2134	61
2	184	3	493.1	184	487	188.5
3	92	5	392	92	141 5	17.3
4	29	7	167	29	46.4	6.5
5	14	9	101.1	14	14.2	.003
6	9	11	77.9	9	4.8	
7	3	13	30.2	3	1.64	
8	1	15	11.4	1	.59	10.3
9	2	17	12.8	2	2	
10	0	19	0	0	.07	
11	1	21	15.5	1	.02	
	2830		3796	16	7.32	283.6

$\beta = 0.9$

Total = 2830 Minutes

(Mean) = 1.34 dB

$\alpha = 0.8$ $\quad 1.34 = \left(\frac{1}{\alpha}\right)^{1/.9} \Gamma\left(\frac{1.9}{.9}\right)$

$X^2 = 283.6$

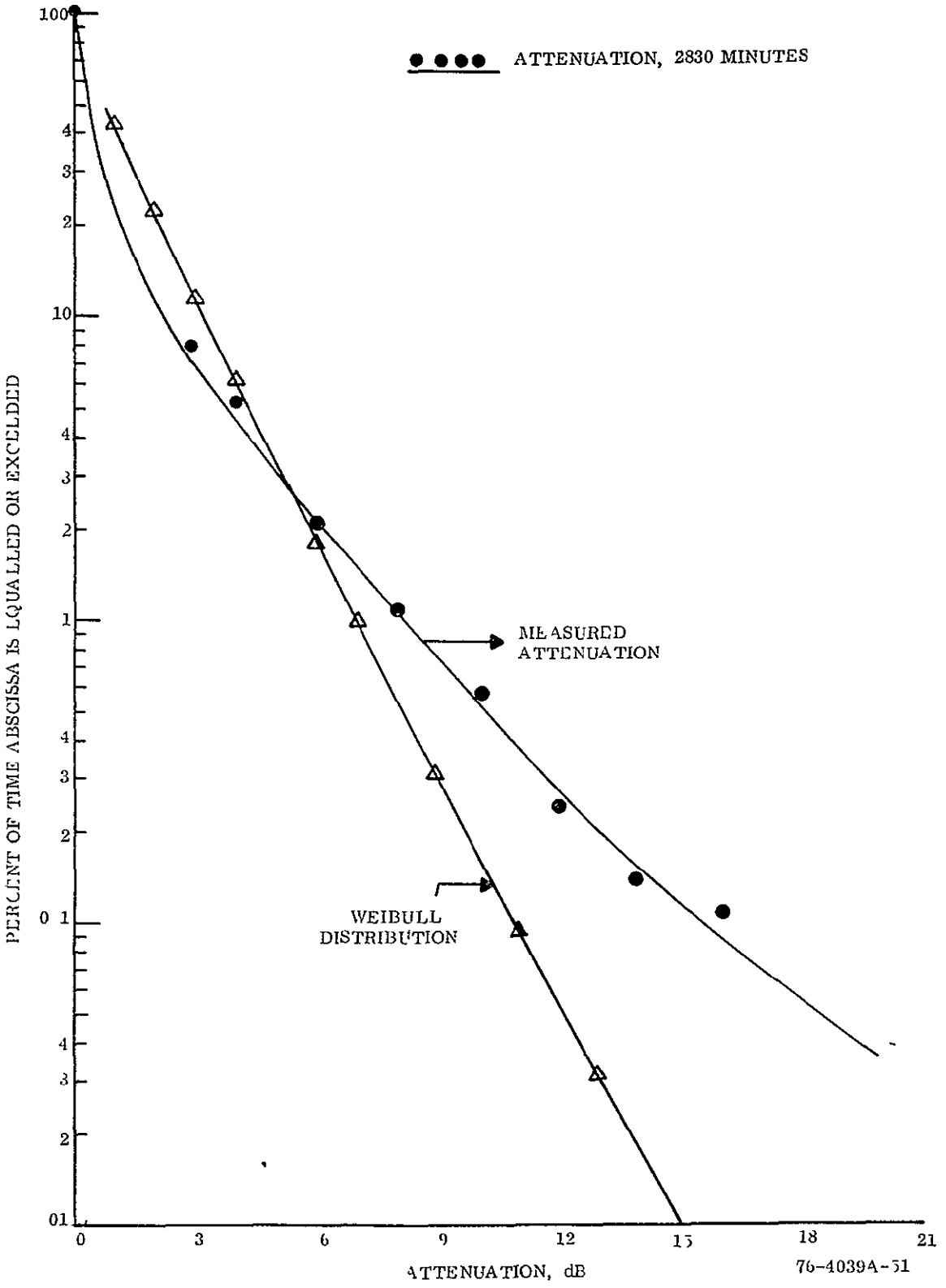

Figure 3-24. NASA Goddard CTS Station
Minutely Average Measured Attn.
June - August Oct 17 - Oct 31, 1976
2830 Minutes

SECTION 4
SUMMARY AND CONCLUSIONS

4.1 GODDARD STATION SYSTEM PERFORMANCE

Link performance calculations for the downlink beacon link predict a margin of 30.7 dB. This defines the maximum measurable fade level for the system. It was assumed that a minimum C/N of 5 dB is required to maintain lock in a closed loop noise bandwidth of 100 Hz.

4.1.1 TV EXPERIMENT (GODDARD)

For the video link an overall link C/N of 15 dB was measured during the initial test period. This includes 95.4 dB noise contribution due to earth noise relayed through the satellite. In the temporary system configuration, a 4.4 dB degradation was also measured from transmitter to - receiver leakage. Also a post detection test tone to noise ratio of 35 dB was measured in a 4.2 MHz filter bandwidth.

A total of 65 hours of test time was utilized in various system performance tests. During this time no precipitation was encountered to determine the possible picture degradation due to rain attenuation. As a result, this attenuation condition was simulated by antenna movement. Preliminary waveform test results show a 4% differential gain value and 0.5° differential phase value.

For the simulated fade condition test it was determined that the color fidelity of the color bars started to degrade at an uplink (14 GHz) fade value of 8 dB. This corresponds to a 6.2 dB fade at 11.7 GHz. From the long term attenuation statistics that corresponds to 2830 minutes at 11.7 GHz the fade level percentage was 2%. Therefore, for a total test time of 2830 minutes, fidelity of the color picture will be effected by rain for 56.6 minutes of that period, for the system under consideration over an overall time period of June through October.

4.1.2 PROPAGATION MEASUREMENTS (GODDARD)

At the Goddard station, rain rate measurements were started in January of 1976. From January to October, 18,700 minutes of precipitation was measured. From June through October 6,271 minutes of precipitation was measured. Measure-

ments of clear weather scintillations and rain attenuation were recorded for 35,947 minutes. Attenuation measurements were attempted for 2830 minutes. The beacon level measurements cover the period June - August, and October 17 to October 31. The highest measured minutely average rain rate during the above test period was 77 MM/HR. The highest minutely average attenuation that was measured was nearly 21 dB. The highest instantaneous rain rate that was measured was 182 MM/HR. For the 2830 minute test period the following parameters were exceeded for 0.1% of the time Minutely average rain rate - 70 MM/HR, instantaneous rain rate - 80 MM/HR, minutely mean attenuation - 15.5 dB.

In utilizing point rain rate, R, to predict attenuation, δ, some method of determining the path length through the precipitation must be developed. For low values of δ, utilizing the long term seasonal measurements of the melting layer height to determine path length seems to produce reasonable estimates of δ for a measured value of R.

4.2 SIGNAL SCINTILLATION

Signal scintillation effects were measured during the test period for a range of atmospheric conditions that included no visible clouds in the radio path to very dark clouds and high winds. Wind buffetting the antenna caused pronounced signal level variations whose major frequency values occurred in bands centered at 1, 2 and 5 Hz. It appears that all frequencies less than about 3 Hz present due to signal scintillation caused by atmospheric turbulence will be completely masked by antenna mount motion if high winds are present. For the meteorological conditions defined by heavy dark clouds and light wet snow and no wind a distinct frequency component at bout 9 Hz was measured. In this one case the meteorological conditions within the elevated beam were of such an intensity that its effect on the signal was measurable by the Ubiquitous Spectrum Analyzer.

4.3 ROSMAN STATION SYSTEM PERFORMANCE

Link calculations were performed for the downlink signals of the beacon and upper and lower tones. The theoretical fade margin for the beacon was computed to be 30.6 dB and for the upper and lower tones 79.9 dB and 70 dB, respectively. The tone margins greatly exceed the beacon margin mainly because of the differences in the spacecraft EIRP.

4.3.1 TV EXPERIMENT (ROSMAN)

Various television tests were performed at Rosman utilizing Goddard as the transmit terminal. C/N_o, audio S/N, color vector analysis and various waveform tests were performed. The overall link C/N_o was 90 dB-Hz which corresponds to a C/N of 14.4 dB. With no video signal the resulting audio S/N value was 38.6 dB. With a video signal applied, the resulting crosstalk caused a decrease of 2.4 dB in the audio S/N. No quantitative results were obtained from the waveform and color vector analysis tests. For both stations a total of 65 hours on the spacecraft was employed for TV performance tests. During these test hours no precipitation was encountered at either station to determine the effects of rain attenuation on system performance.

4.3.2 PROPAGATION MEASUREMENTS

For the Rosman station over the time period between June 10 to October 7 a total of 878 minutes of data was computed for the ground average rain rate. Only 691 minutes of data was obtained for the near bucket point rain rate. In some test runs the latter rain rate factor did not measure precipitation due to the spatial variation of the rain environment. For the 691 minute test period the ground average values exceeded 80 MM/HR for 0.1% of the time and the near bucket values exceeded 91 MM/HR for the same percentage. Attenuation statistics were computed for a 342 minute time period. For the 0.1% value the near bucket rain rate corresponds to 84 MM/HR and the attenuation to 12 dB. These values were computed from 4 second mean values. The maximum minutely mean attenuation value measured at Rosman is 12.5 dB. The limited amount of test data obtained at Rosman was mainly due to the fact that operation of the station was only performed during an eight hour period each day.

4.4 METEOROLOGICAL PARAMETERS

Rain rate and radar reflectivity are the two meteorological parameters that were employed as a measure of the extent and degree of precipitation causing the attenuation. The reflectivity parameter gave a much better description of the beam precipitation since it measures these factors directly in the elevated radar beam and it can differentiate different degrees of precipitation within 100 meter range increments. Also it has the ability of measuring a closer estimate of the instantaneous value of rain rate within the elevated beam.

At values of attenuation less than 2 dB it was shown that the integrated reflectivity was a sensitive indicator of attenuation. This implies that good accuracy can be obtained in the use of the radar technique for attenuation prediction at low values of attenuation.

Point rain rate defined as the near bucket (NB) and the ground average rain rate (GA), which is the average of the ten rain buckets placed under the beam, are the two rain rate factors that were employed Of the two, the GA factor shows a better functional relationship with attenuation. This is not surprising since the average value would give a better indication of the degree of precipitation for light and medium rainfall rates. This would not be true for cases involving large attenuation values. These values are mainly caused by intense cells of limited extent which would signify a heterogeneous rain environment. Point rain rates measured in the proper location should show better correlation. In comparing the NB and GA factors some measure of the degree of homogeneity of the precipitation can be obtained. For uniform rains good correspondence should be obtained between the factors.

4.5 MULTIFREQUENCY RADAR TEST RESULTS

In attempting to obtain data for calibration purposes of the multifrequency weather radar, an antenna elevation angle of 5° was employed. At this angle signal blockage from the terrain occurs for the useable range values greater than 300 meters. As a result an elevation angle of 11° was employed for the calibration test. In employing the ground measured rain rate as a calibration source, it was found that correspondence between measured and radar computed rain rate can be obtained by decreasing the 3 GHz radar constant by 3.1 dB and the 8.75 GHz radar constant by 0.9 dB. From the above results it appears that utilizing the ground measured rain rate as a standard for calibrating the weather radars has merit. Also a check on the corrected radar constant by computing drop size distribution parameters that involve the reflectivity factor Z and the ground measured rain rate R also appears to produce reasonable results.

4.6 BEST FIT ANALYSIS

A best fit analysis of the Goddard attenuation data to a Weibull distribution was attempted. The criterion for the goodness of fit was the Chi-Square Test. A very poor fit to the minutely mean attenuation values was obtained. It appears that the

above values tend to smooth the data to a point that reduces the information at the high attenuation values that causing a large percentage of the data to fall in the lower attenuation bins. This reduced data causes the conditions for an acceptance of the Weibull distribution to be very stringent.

4.7 FUTURE TESTS AND ANALYSIS

In subsequent test periods measurements of rain rate, attenuation and radar returns will continue in order to provide a more meaningful statistical sample over a longer period of time. Emphasis will be placed on evaluating the use of the radar return as a method of attenuation prediction. Lack of radar data at moderately high attenuation values prevented the evaluation in this report. Also additional work will be performed on the calibration of the radars.

For the "Best Fit Analysis", future work will involve fitting the attenuation data to the Weibull and Log Normal distributions mainly for attenuation values greater than 6 dB. The main problem in this area is obtaining a statistically significant sample at high attenuation values.

Work in evaluating rain attenuation on TV picture fidelity will continue. A video tape of an actual photograph of a suitable subject will be used as a standard rather than a color bar pattern It is hoped that data resulting from actual rain attenuation can be obtained in future tests.

APPENDIX A

WEATHER CLASS DESIGNATION

During any given test run, a general weather classification parameter is recorded on a continuous basis by ground station personnel. While a parameter of this nature is admittedly subjective, it is easy to acquire and can provide a convenient basis for categorizing data. It should be noted that this weather description is strictly qualitative and can only be employed as a general indicator.

The classification employed in the millimeter wave experiment are listed below with their corresponding definitions. These classifications are taken partly from U.S Weather Bureau practice and partly from previous used codes.

WEATHER CLASS DESIGNATIONS

Weather Class	Category	Definition
1	Clear Skies	
2	Partly Cloudy	0-20% cloud cover
3	Broken Skies	20-80% cloud cover
4	Overcast	80-100% cloud cover
5	Showers	Moderate to high intensity rainfall characterized by short durations and rapid fluctuations of intensity, as well as considerable variation in space Rain of this type normally falls from clouds which extend to much higher altitudes than those causing drizzle.
6	Continuous Rain	A uniform, light to moderate intensity rain which covers a relatively large geographical area, and which lasts for extended periods of time with a fairly constant rainfall rate. The drop sizes are larger than those associated with drizzle, and the associated cloud systems generally cover a large geographical area than those associated with showers and thunderstorms.
7	Thunderstorm	A localized storm produced by clouds having great vertical development and always accompanied by thunder and lightning. Usually strong gusts of surface winds, heavy, and variable rain, and sometimes hail are observed with thunderstorms. The duration is normally longer than that of showers, but shorter than that of continuous rain. Temperatures often fall sharply, and the rainfall rate typically reaches peak intensity very quickly and then decreases at a slower rate.
8	Sleet or Wet Snow	A uniform heavy snow which usually occurs in temperatures near the freezing point.
9	Hail or Dry Snow	Smaller flakes than wet snow, usually occurs at much lower temperature, and will accumulate on the ground.

APPENDIX B

The best fit analysis for the attenuation data will utilize the various factors presented below. The analysis will involve comparing the probability density function obtained with the measured data with the Log Normal and Weibull functions assuming the same mean and standard deviation values.

The probability that a random variable will lie in an interval Δx is equal to

$$\int_{X}^{X+\Delta} f(x)dx$$

where f(x) is the probability density function of the random variable x, X is the lower boundary of the interval.

Gaussian or Normal

$$F(X+\Delta x) - F(X) = \int_{X}^{X+\Delta x} \frac{1}{\sigma\sqrt{2\pi}} e^{-(x-m)^2/2\sigma^2} dx$$

$$= \int_{\frac{(X-m)}{\sigma}}^{\frac{X+\Delta x-m}{\sigma}} \frac{1}{\sqrt{2\pi}} e^{-y^2/2} dy$$

$$= Q\left(\frac{X+\Delta x-m}{\sigma}\right) - Q\left(\frac{X-m}{\sigma}\right)$$

where Q ( ) is a tabulated value.

Log Normal

$$F(\bar{X}+\Delta x) - F(\bar{X}) = \int_{\bar{X}}^{\bar{X}+\Delta x} \frac{1}{x\sigma\sqrt{2\pi}} e^{-(\mathrm{LOG}_e x - m)^2 / 2\sigma^2} dx$$

$$= \int_{\frac{\mathrm{LOG}_e \bar{X} - m}{\sigma}}^{\frac{\mathrm{LOG}_e (\bar{X}+\Delta x) - m}{\sigma}} \frac{1}{\sqrt{2\pi}} e^{-y^2/2} dy$$

$$= Q\left(\frac{\mathrm{LOG}_e(\bar{X}+\Delta x) - m}{\sigma}\right) - Q\left(\frac{\mathrm{LOG}_e \bar{X} - m}{\sigma}\right)$$

where Q ( ) indicates the normal distribution function.

Weibull (includes exponential ($\beta = 1$) and Rayleigh ($\beta = 2$))

$$F(\bar{X}+\Delta x) - F(\bar{X}) = \int_{\bar{X}}^{\bar{X}+\Delta x} \beta\alpha\, x^{\beta-1} e^{-\alpha x^{\beta}} dx$$

$$= e^{-\alpha \bar{X}^{\beta}} - e^{-\alpha(\bar{X}+\Delta x)^{\beta}}$$

Gamma

$$F(\bar{X}+\Delta x) - F(\bar{X}) = \int_{\bar{X}}^{\bar{X}+\Delta x} \frac{\lambda^{\alpha}}{\Gamma(\alpha)} e^{-\lambda x} x^{\alpha-1} dx$$

$$= \int_{\lambda(\bar{X})}^{\lambda(\bar{X}+\Delta x)} \frac{1}{\Gamma(\alpha)} y^{\alpha-1} e^{-y} dy$$

This is the incomplete Gamma function which is tabulated.

As an example, the log normal distribution is under consideration with

$$m = 1 \quad \sigma^2 = 4$$

and it is desired to find the percentage of the distribution between x = 3 and x = 3.5 i.e.

$$\int_3^{3.5} \frac{1}{x\sigma\sqrt{2\pi}} e^{-(\text{LOG}_e x - m)^2/2^2} dx$$

$$= \int_{.0493}^{.1264} \frac{1}{\sqrt{2\pi}} e^{-y^2/2} dy$$

$\cong .55 - .52 = 3\%$ from normal curve

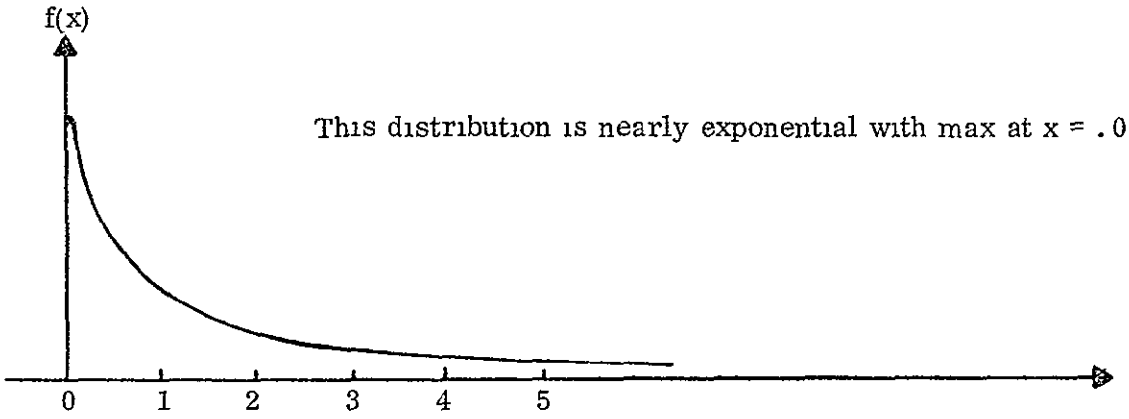

This distribution is nearly exponential with max at x = .05

(The highly skewed log-normal is very difficult to differentiate from an exponential. Given α for the exponential, the corresponding log-normal would be.

$$\alpha e^{-\alpha x} \cong \frac{1}{\sqrt{2}\, x\, \sqrt{2\pi}} e^{-(\text{LOG}_e x - 1 + \text{LOG}_e \alpha)^2 / 4}$$

Chi-Square (χ^2) Goodness-Of-Fit Test

For the Weibull

Choose a value of β

Find Mean = $\frac{\sum_{x_i} \beta_{n_i}}{n}$ where n = Total number of data points

x_i = Midpoint of cell (or bin)

n_i = Number in cell.

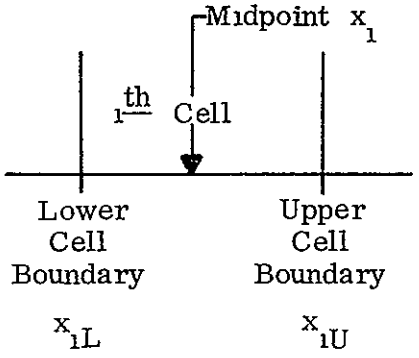

There should be $(e^{-\alpha x_{iL}^{\beta}} - e^{-\alpha x_{iU}^{\beta}})$ n data points in that cell if the distribution is Weibull with those α and β.

Form

CELL #	ACTUAL NUMBER IN CELL	EXPECTED NUMBER IN CELL	$\frac{(\text{ACTUAL-EXPECTED})^2}{\text{EXPECTED}}$
1	-	$n(e^{-\alpha x_{iL}^{\beta}} - e^{-\alpha x_{iU}^{\beta}})$	-
2	-	-	-
3	-	-	-
4	-	-	-
5	-	-	-

The sum of $\frac{(\text{Actual-Expected})^2}{\text{Expected}}$ is χ^2 which has degrees of freedom equal to one less than the number of cells (bins).

Repeat with different β to yield minimum χ^2. This would be the best fitting Weibull.

For the Log Normal

$$\text{Find} \qquad \bar{x} = \frac{\Sigma x_i n_i}{n} \qquad \text{and} \qquad \frac{\Sigma n_i x_i^2}{n}$$

$$e^{m + \sigma^2/2} = \frac{\Sigma n_i x_i}{n} \qquad \text{call this M}$$

$$e^{2m + 2\sigma^2} = \frac{n_i x_i^2}{n} \qquad \text{call this N}$$

$$\text{Then} \qquad m = 2 \text{ LOG}_e \text{ M} - \frac{\text{LOG}_e \text{ N}}{2}$$

$$\sigma^2 = \text{LOG}_e \text{ N} - 2 \text{ LOG}_e \text{ M}.$$

$$\text{Find} \qquad \left[Q\left(\frac{\text{LOG}_e x_{iU} - m}{\sigma} \right) - Q\left(\frac{\text{LOG}_e x_{iL} - m}{\sigma} \right) \right] n$$

for each cell. This is the expected number for the cell.

$$\text{Find} \qquad \sum \frac{(\text{Actual} - \text{Expected})^2}{\text{Expected}} = \chi^2_c$$

C = no. of cells minus 1

There should be no reason to repeat this with other values of m and σ^2. The first calculation should result in the best fit.

REFERENCES

(1) Fredendall, C.L., and Behrend, W.L. Procedure for Evaluating Subjective Effects of Interference-Proceedings IRE (June 1960)

(2) Ippolito, L.J. 20 and 30 GHz Millimeter Wave Experiments With the ATS-6 Satellite NASA Technical Note NASATND-8197 April 1976

(3) National Aeronautics and Space Administration-ATS-6 Millimeter Wave Propagation Experiment Final Data Analysis Report September 1975 Contract No. NAS 5-20904

(4) Meneghini, Robert Review of Data Analysis Procedures for the ATS-6 Millimeter Wave Experiment Telecommunications Systems Branch Communications and Navigations Division Applications Directorate Goddard Space Flight Center August 1975 X-951-75-235

(5) Joss, J., Thomas J.C., Waldvagel A. (1968) The Variations of Raindrop Size Distributions at Lorcano, Proceedings of the International Conference on Cloud Physics, August 26-30, Toronto, Canada, Pg. 369-372

(6) Shoaman, Martin L. Probabilistic Reliability An Engineering Approach 1968 McGraw Hill Book Company